

EUROPEAN ORGANISATION FOR NUCLEAR RESEARCH (CERN)



Phys. Lett. B 789 (2019) 167
 DOI: [10.1016/j.physletb.2018.12.023](https://doi.org/10.1016/j.physletb.2018.12.023)



CERN-EP-2018-196
 17th January 2019

Measurement of photon–jet transverse momentum correlations in 5.02 TeV Pb+Pb and $p p$ collisions with ATLAS

The ATLAS Collaboration

Jets created in association with a photon can be used as a calibrated probe to study energy loss in the medium created in nuclear collisions. Measurements of the transverse momentum balance between isolated photons and inclusive jets are presented using integrated luminosities of 0.49 nb^{-1} of Pb+Pb collision data at $\sqrt{s_{\text{NN}}} = 5.02 \text{ TeV}$ and 25 pb^{-1} of $p p$ collision data at $\sqrt{s} = 5.02 \text{ TeV}$ recorded with the ATLAS detector at the LHC. Photons with transverse momentum $63.1 < p_T^\gamma < 200 \text{ GeV}$ and $|\eta^\gamma| < 2.37$ are paired with all jets in the event that have $p_T^{\text{jet}} > 31.6 \text{ GeV}$ and pseudorapidity $|\eta^{\text{jet}}| < 2.8$. The transverse momentum balance given by the jet-to-photon p_T ratio, $x_{J\gamma}$, is measured for pairs with azimuthal opening angle $\Delta\phi > 7\pi/8$. Distributions of the per-photon jet yield as a function of $x_{J\gamma}$, $(1/N_\gamma)(dN/dx_{J\gamma})$, are corrected for detector effects via a two-dimensional unfolding procedure and reported at the particle level. In $p p$ collisions, the distributions are well described by Monte Carlo event generators. In Pb+Pb collisions, the $x_{J\gamma}$ distribution is modified from that observed in $p p$ collisions with increasing centrality, consistent with the picture of parton energy loss in the hot nuclear medium. The data are compared with a suite of energy-loss models and calculations.

1 Introduction

The energy loss of fast partons traversing the hot, deconfined medium created in nucleus–nucleus collisions can be studied in a controlled and systematic way through the analysis of jets produced in association with a high transverse momentum (p_T) prompt photon [1–7]. At leading order in quantum chromodynamics, the photon and leading jet are produced back-to-back in the azimuthal plane, with equal transverse momenta. Measurements of prompt photon production in Au+Au collisions at the Relativistic Heavy Ion Collider (RHIC) [8] and Pb+Pb collisions at the Large Hadron Collider (LHC) [9] have confirmed that, since photons do not participate in the strong interaction, their production rates are not modified by the medium [10]. Thus, photons provide an estimate of the p_T and direction of the parton produced in the initial hard-scattering before it has lost energy through interactions with the medium. Measurements of jet production with different requirements on the photon kinematics can therefore shed light on how the absolute amount of parton energy loss depends on the initial parton p_T .

Furthermore, photon–jet events offer a particularly useful way to probe the distribution of energy lost by jets in individual events, and are complementary to measurements such as the dijet p_T balance [11–13]. Whereas those measurements report the ratio of the transverse momenta of two final-state jets, both of which may have lost energy, photon–jet events provide an alternative system in which one high- p_T object is certain to remain unaffected by the hot nuclear medium. Finally, jets produced in association with a photon are more likely to originate from quarks than those produced in dijet events at the same p_T . Thus, when considered together with measurements of dijets or of inclusive jet [14–16] and hadron [17–19] production rates in Pb+Pb collisions, analysis of photon–jet events can help to further constrain the flavour (i.e. quark versus gluon) dependence of parton energy loss.

Studies of photon–hadron correlations, in which high- p_T hadrons are used as a proxy for the jet, were first performed at RHIC [20–22], and measurements using fully reconstructed jets have since begun at the LHC [23, 24]. In the LHC studies, the distribution of the photon–jet azimuthal separation, $\Delta\phi$, was found to be consistent with that in simulated photon–jet events embedded into a heavy-ion background, and the jet-to-photon transverse momentum ratio, $x_{J\gamma} = p_T^{\text{jet}}/p_T^\gamma$, was studied for inclusive photon–jet pairs. The per-photon jet yield $(1/N_\gamma)(dN/dx_{J\gamma})$ distribution was shifted to significantly smaller values in Pb+Pb data.

In these previous measurements, the $x_{J\gamma}$ distributions in Pb+Pb events were not corrected for detector resolution effects, which led to a substantial broadening of the reported distributions in data. As a result, qualitative comparisons with models or even with the analogous distributions in proton–proton (pp) data could only be accomplished by applying an additional smearing to the comparison distributions to introduce detector effects. Recent measurements of dijet p_T correlations [12] and inclusive jet fragmentation functions at large longitudinal momentum fraction [25] in Pb+Pb collisions used unfolding procedures to correct for bin-migration effects and return the distributions to the particle level, i.e. free from detector effects.

This Letter reports a study of photon–jet correlations in Pb+Pb collisions at a nucleon–nucleon centre-of-mass energy $\sqrt{s_{\text{NN}}} = 5.02$ TeV and pp collisions at the same centre-of-mass energy $\sqrt{s} = 5.02$ TeV. The data were recorded in 2015 with the ATLAS detector at the LHC and correspond to integrated luminosities of 0.49 nb^{-1} and 25 pb^{-1} , respectively. Events containing a prompt photon with $63.1 < p_T^\gamma < 200$ GeV and pseudorapidity $|\eta^\gamma| < 2.37$ (excluding the region $1.37 < |\eta^\gamma| < 1.52$) are studied. The p_T balance of photon–jet pairs for jets with $p_T^{\text{jet}} > 31.6$ GeV and $|\eta^{\text{jet}}| < 2.8$ which are approximately back-to-back with the photon in the transverse plane, $\Delta\phi > 7\pi/8$, is analysed through the per-photon yield of jets as

a function of $x_{J\gamma}$, with all jets that meet this selection requirement counted separately. In Monte Carlo simulations, the fraction of photons paired with more than one jet rises from 1% to $\approx 15\%$ over the reported photon p_T ranges. The particular photon and jet p_T ranges used in the measurement are chosen to be evenly spaced on logarithmic scales to facilitate the unfolding procedure described below.

The yields are corrected via data-driven techniques for background arising from combinatoric pairings of each photon with unrelated jets in Pb+Pb events and from the contamination by neutral mesons in the photon sample. The resulting $x_{J\gamma}$ distributions are corrected for the effects of the experimental resolution on the photon and jet p_T via a two-dimensional unfolding procedure similar to that used in Ref. [12]. Due to higher-order effects, photon–jet events do not generally have the back-to-back leading order topology mentioned above. Thus the pp data, which includes these effects, provides the reference distributions against which to interpret the results in Pb+Pb events. This Letter directly compares photon–jet data in Pb+Pb and pp events, and with Monte Carlo event generators and analytic calculations [26–29].

2 Experimental set-up

The ATLAS experiment [30] is a multipurpose particle detector with a forward–backward symmetric cylindrical geometry and nearly 4π coverage.¹ This analysis relies on the inner detector, the calorimeter and the data acquisition and trigger system.

The inner detector comprises three major subsystems: the pixel detector and the silicon microstrip tracker, which extend out to $|\eta| = 2.5$, and the transition radiation tracker which extends to $|\eta| = 2.0$. The inner detector covers the full azimuth and is immersed in a 2 T axial magnetic field. The pixel detector consists of four cylindrical layers in the barrel region and three disks in each endcap region. The silicon microstrip tracker comprises four cylindrical layers (nine disks) of silicon strip detectors in the barrel (endcap) region.

The calorimeter is a large-acceptance, longitudinally-segmented sampling detector covering $|\eta| < 4.9$ with electromagnetic (EM) and hadronic sections. The EM calorimeter is a lead/liquid-argon sampling calorimeter with an accordion-shaped geometry. It is divided into a barrel region, covering $|\eta| < 1.475$, and two endcap regions, covering $1.375 < |\eta| < 3.2$. The EM calorimeter has three primary sections, longitudinal in shower depth, called “layers”, in the barrel region and up to $|\eta| = 2.5$ in the end cap regions. In the barrel and first part of the end cap ($|\eta| < 2.4$), with the exception of the regions $1.4 < |\eta| < 1.5$, the first layer has a fine segmentation in η ($\Delta\eta = 0.003$ – 0.006) to allow the discrimination of photons from the two-photon decays of π^0 and η mesons. Over most of the acceptance, the total material upstream of the EM calorimeter ranges from 2.5 to 6 radiation lengths. In the transition region between the barrel and endcap regions ($1.37 < |\eta| < 1.52$), the amount of material rises to 11.5 radiation lengths, and thus this region is not used for the detection of photons. The hadronic calorimeter is located outside the EM calorimeter. It consists of a steel/scintillator-tile sampling calorimeter covering $|\eta| < 1.7$ and a liquid-argon calorimeter with copper absorber covering $1.5 < |\eta| < 3.2$.

¹ ATLAS uses a right-handed coordinate system with its origin at the nominal interaction point (IP) in the centre of the detector and the z -axis along the beam pipe. The x -axis points from the IP to the centre of the LHC ring, and the y -axis points upward. Cylindrical coordinates (r, ϕ) are used in the transverse plane, ϕ being the azimuthal angle around the z -axis. The pseudorapidity is defined in terms of the polar angle θ as $\eta = -\ln \tan(\theta/2)$. Transverse momentum and transverse energy are defined as $p_T = p \sin \theta$ and $E_T = E \sin \theta$, respectively. ΔR is defined as $\sqrt{(\Delta\eta)^2 + (\Delta\phi)^2}$.

The forward calorimeter (FCal) is a liquid-argon sampling calorimeter located on either side of the interaction point. It covers $3.1 < |\eta| < 4.9$ and each half is composed of one EM and two hadronic sections, with copper and tungsten serving as the absorber material, respectively. The FCal is used to characterise the centrality of Pb+Pb collisions as described below. Finally, zero-degree calorimeters (ZDC) are situated at large pseudorapidity, $|\eta| > 8.3$, and are primarily sensitive to spectator neutrons.

A two-level trigger system is used to select events, with a first-level trigger implemented in hardware followed by a software-based (high-level) trigger. Data for this measurement were acquired using a high-level photon trigger [31] covering the central region ($|\eta| < 2.5$). At the first-level trigger stage, the transverse energy of EM showers is computed within regions of $\Delta\phi \times \Delta\eta = 0.1 \times 0.1$, and those showers which satisfy an E_T threshold are used to seed the high-level trigger stage. At this next stage, reconstruction algorithms similar to those applied in the offline analysis use the full detector granularity to form the final trigger decision. The trigger was configured with an online photon- p_T threshold of 30 GeV (20 GeV) in the pp (Pb+Pb) running period and required the candidate photon to satisfy a set of loose criteria for the electromagnetic shower shape [31]. For the Pb+Pb data-taking, the high-level trigger included a procedure to estimate and subtract the underlying event (UE) contribution to the E_T measured in the calorimeter [9], ensuring high efficiency in high-activity Pb+Pb events.

In addition to the photon trigger, Pb+Pb data were recorded with minimum-bias triggers; these events are used to characterise the centrality of Pb+Pb collisions as described in Section 3. The minimum-bias triggers are based on the presence of a minimum amount of approximately 50 GeV of transverse energy in all sections of the calorimeter system ($|\eta| < 3.2$) or, for events that do not meet this condition, on substantial energy deposits in both ZDC modules and an inner-detector track identified by the high-level trigger system.

3 Data selection and Monte Carlo samples

Photon-jet events in pp and Pb+Pb collisions are initially selected for analysis by the high-level triggers described above. The typical number of interactions per bunch crossing in the pp and Pb+Pb data-taking were one and smaller than 10^{-4} , respectively. Events are required to satisfy detector and data-quality requirements, and to contain a vertex reconstructed from tracks in the inner detector. An additional requirement in Pb+Pb collisions, based on the correlation of the signals in the ZDC and the FCal, is used to reject a small number of recorded events consistent with two Pb+Pb interactions in the same bunch crossing (pile-up) [32]. The pile-up rate is largest in the most central events, where it is at most 0.1% and rejected with an efficiency greater than 98%. No pile-up rejection is applied in pp collisions.

The centrality of Pb+Pb events is defined using the total transverse energy measured in the FCal, evaluated at the electromagnetic scale and denoted by $\sum E_T$. The same observable was used to characterise 2010 and 2011 Pb+Pb data at $\sqrt{s_{NN}} = 2.76$ TeV [33] and a similar procedure, based on Monte Carlo Glauber modeling [34], is followed in 2015 data [35]. In this analysis, Pb+Pb events within five centrality ranges are considered that represent 0–10% (largest $\sum E_T$ values and degree of nuclear overlap), 10–20%, 20–30%, 30–50% and 50–80% (smallest $\sum E_T$ values and degree of nuclear overlap) of the population. The mean number of participating nucleons in minimum-bias Pb+Pb collisions, N_{part} , ranges from 33.3 ± 1.5 in 50–80% events to 358.8 ± 2.3 in 0–10% events.

Monte Carlo simulations of $\sqrt{s} = 5.02$ TeV pp photon-jet events are used to correct the data for bin migration and inefficiency effects, and for comparison with distributions measured in pp collision data. For

all the samples described below, the generated events were passed through a full GEANT 4 simulation [36, 37] of the ATLAS detector under the same conditions present during data-taking and were digitised and reconstructed in the same way as the data.

For the primary simulation samples, the PYTHIA 8.186 [38] generator was used with the NNPDF23LO parton distribution function (PDF) set [39], and generator parameters which were tuned to reproduce a set of minimum-bias data (the “A14” tune) [40]. Both the direct and fragmentation photon contributions are included in the simulation. Six million pp events were generated with a generator-level photon in the p_T range 50 GeV to 280 GeV. Additionally, a sample of 18 million events were produced with the same generator, tune and PDF, and were overlaid at the detector-hit level with minimum-bias Pb+Pb events recorded during the 2015 run. The relative contribution of events in this “data-overlay” sample were reweighted on an event-by-event basis to match the $\sum E_T$ distribution observed in the photon–jet events in Pb+Pb data selected for analysis. Thus the Pb+Pb simulation samples contain underlying-event activity levels and kinematic distributions of jets (used in the combinatoric photon–jet background estimation) identical to those in data.

Additional samples of 0.3 million pp events and 6 million events overlaid with Pb+Pb data were produced with the SHERPA 2.1.1 [41] generator using the CT10 PDF set [42], as were 0.6 million pp HERWIG 7 [43] events with the MMHT UE tune and PDF set [44]. The SHERPA samples were generated with leading-order matrix elements for photon–jet final states with up to three additional partons, which were merged with the SHERPA parton shower. The HERWIG events were generated in a way that includes the direct and fragmentation photon contributions. Both the SHERPA and HERWIG samples were filtered for the presence of a photon in the required kinematic region, and are used because they contain different photon+multijet topological distributions and jet-flavour compositions.

At generator level, photons are required to be isolated by requiring the sum of the transverse energy carried by primary particles² in a cone of size $\Delta R = 0.3$ around the photon, E_T^{iso} , to be smaller than 3 GeV. In the analysis, the background subtraction, described below, removes photons which pass the isolation cut in data but fail this isolation requirement at the particle level. Jets are defined by applying the anti- k_t algorithm [45, 46] with radius parameter $R = 0.4$ to primary particles within $|\eta| < 4.9$. In simulation, the jet flavour, i.e. whether it is quark- or gluon-initiated, is defined as the flavour of the highest- p_T parton that points to the generator-level jet [47].

4 Event reconstruction

4.1 Photon reconstruction

Photon candidates are reconstructed from clusters of energy deposited in EM calorimeter cells, following a procedure used for previous measurements of isolated prompt photon production in Pb+Pb collisions [9]. The procedure is similar to that used extensively in pp collisions [48, 49], but is applied to the calorimeter cells after an event-by-event estimation and subtraction of the pile-up and UE contribution to the deposited energy in each cell [14]. In Pb+Pb collisions, all photon candidates are treated as if they were unconverted photons. Photon identification is based primarily on shower shapes in the calorimeter [50], selecting those candidates which are compatible with originating from a single photon impacting the calorimeter.

² Primary particles are defined as those with a proper mean lifetime, τ , exceeding $c\tau = 10$ mm. For the jet and isolation E_T measurements, muons and neutrinos are excluded from the definition.

The measurement of the photon energy is based on the energy collected in a small region of calorimeter cells centred on the photon ($\Delta\eta \times \Delta\phi = 0.075 \times 0.175$ in the barrel and $\Delta\eta \times \Delta\phi = 0.125 \times 0.125$ in the endcaps), and is corrected via a dedicated calibration [51], which accounts for upstream losses and both lateral and longitudinal leakage. The sum of transverse energy in calorimeter cells inside a cone size of $\Delta R = 0.3$ centred on the photon candidate, excluding a small central area of size $\Delta\eta \times \Delta\phi = 0.125 \times 0.175$, is used to compute the isolation energy E_T^{iso} . It is corrected for the expected leakage of the photon energy into the isolation cone.

Reconstructed photon candidates are required to satisfy identification and isolation criteria. The identification working point (called “tight”) includes requirements on each of several shower-shape variables [50]. These criteria reject two-photon decays of neutral mesons using information in the finely segmented first calorimeter layers, and reject hadrons which began showering in the EM section using information from the hadronic calorimeter. The isolation energy is required to be $E_T^{\text{iso}} < 3 \text{ GeV}$ in pp collisions. In Pb+Pb collisions, where UE fluctuations significantly broaden the distribution of E_T^{iso} values, this requirement is set to approximately one standard deviation of the Gaussian-like part of the distribution centred at zero, $E_T^{\text{iso}} < 8 \text{ GeV}$.

In simulation, prompt photons in pp collisions have a total reconstruction and selection efficiency greater than 90%. At low $p_T \approx 60 \text{ GeV}$ in the most central Pb+Pb collisions, this efficiency is $\approx 60\%$, rising with increasing p_T and in less central collisions. In all events, the p_T scale, defined as the mean ratio of measured photon p_T to the generator-level p_T , for photons which satisfy these criteria is within 0.5% (1%) of unity in the barrel (endcap). The p_T resolution decreases from 3% to 2% over the measured p_T range.

4.2 Jet reconstruction

Jets are reconstructed following the procedure previously used in 2.76 TeV and 5.02 TeV pp and Pb+Pb collisions [14, 15, 52], which is briefly summarised here. The anti- k_t algorithm [46] with $R = 0.4$ is applied to energy deposits in the calorimeter grouped into towers of size $\Delta\eta \times \Delta\phi = 0.1 \times 0.1$. An iterative procedure, based entirely on data, is used to obtain an event-by-event estimate of the average η -dependent UE energy density, including that from pile-up, while excluding from the estimate the contribution from jets arising from a hard scattering. An updated estimate of the jet four-momentum is obtained by subtracting the UE energy from the constituent towers of the jet. This procedure is also applied to pp data. The p_T values of the resulting jets are corrected for the average calorimeter response using an η - and p_T -dependent calibration derived from simulation. An additional correction, derived from *in situ* studies of events with a jet recoiling against a photon or Z boson and from the differences between the heavy-ion reconstruction algorithm and that normally used in the 13 TeV pp data [53], is applied. A final correction at the analysis level is applied to correct for a deficiency in jet calibration due to it being derived from an event sample with a different jet flavour composition.

The distribution of reconstructed jet p_T values was studied in simulation as a function of generator-level jet p_T . In pp and Pb+Pb collisions, the jet p_T scale is within 1% of unity. In pp collisions, the jet p_T resolution decreases from 15% at $p_T \approx 30 \text{ GeV}$ to 10% at $p_T \approx 200 \text{ GeV}$. In Pb+Pb collisions, the resolution at fixed jet p_T becomes worse in more central collisions in a way consistent with the increasing magnitude of UE fluctuations in the jet cone. In the most central events and at the lowest jet- p_T values, the resolution reaches 50%. At high p_T , the resolution asymptotically becomes centrality-independent and,

at 200 GeV, consistent with that in pp collisions. More information about the jet reconstruction and jet performance in this dataset may be found in Ref. [54].

5 Data analysis

5.1 Photon purity and yield

After applying the identification and isolation selection criteria in pp collisions, approximately 19 500, 7800, 4100 and 400 photons are selected with $p_T^\gamma = 63.1\text{--}79.6$ GeV, 79.6–100 GeV, 100–158 GeV and 158–200 GeV, respectively. In Pb+Pb collisions, the analogous yields are 15 400, 6300, 3500 and 300. These raw yields are determined as a function of p_T^γ and are then corrected for background and for the effects of p_T bin migration.

First, the selected photon sample is corrected for the background contribution, primarily from misidentified neutral hadrons. For each p_T^γ and centrality range, the purity of prompt photons within this range is estimated with a double-sideband approach [9, 48, 49], which is summarised in the following.

In addition to the nominal selection, background-enhanced samples of photon candidates are defined by selecting photons failing at least one of four specific shower-shape requirements (referred to as the “non-tight” selection), or by requiring that they are not isolated such that $E_T^{\text{iso}} > 5$ GeV in pp collisions or $E_T^{\text{iso}} > 10$ GeV in Pb+Pb collisions. Regions *A* and *B* are defined as those containing tight photons which are isolated and non-isolated, respectively, with region *A* corresponding to the signal photon selection. Regions *C* and *D* contain non-tight photons which are isolated and non-isolated, respectively. The number of photon candidates in each region is generally a mixture of signal and background photons, i.e. those arising from neutral mesons inside jets. The E_T^{iso} distribution for background photons is expected to be the same for the tight and non-tight selections such that the distribution of background photons “factorises” along isolation and identification axes. Separately, the probability that a prompt photon is found in regions *B*, *C* or *D* is determined from simulation. This information and the background factorisation assumption is then applied to the data to determine the purity of photons in region *A*, defined as the ratio of the number of signal photons to all selected photons. The purity increases systematically with p_T^γ over the measured p_T range. In pp collisions, it rises from $\approx 85\%$ at $p_T^\gamma = 80$ GeV to more than 95% at 100 GeV, while in Pb+Pb collisions it is typically $\approx 75\text{--}90\%$ over the same kinematic range.

The background-corrected prompt photon yields are then corrected for the resolution of the p_T^γ measurement. This is performed by comparing the yields, evaluated separately as a function of reconstructed and generator-level p_T , in simulation. Given the good p_T resolution, these differ by 2% at most, and this small resulting correction is applied to the yields in data.

5.2 Jet background subtraction

The raw jet yields, measured as a function of $x_{J\gamma}$, are corrected for two background components using data-driven methods. The corrections are performed separately for each p_T^γ interval and separately in pp collisions and Pb+Pb collisions of different centrality ranges.

The first background arises from the combination of a high- p_T photon with jets unrelated to the photon-producing hard scattering. These include jets from separate hard parton–parton scatterings and UE

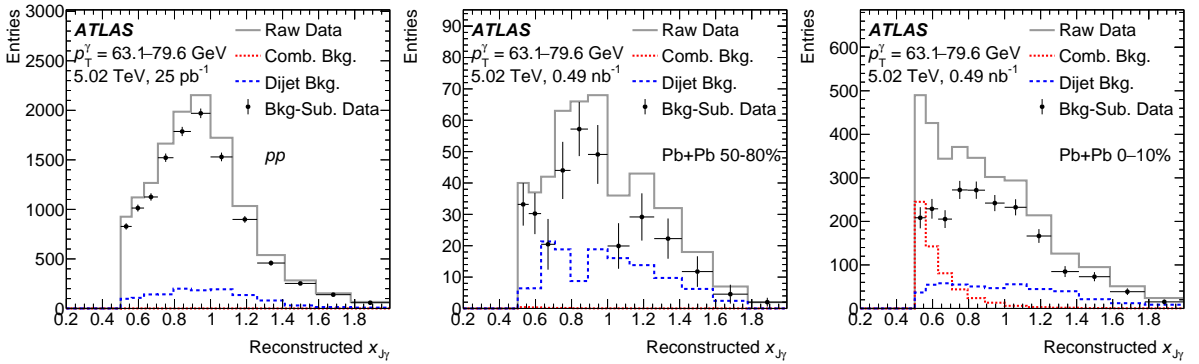


Figure 1: Distributions of the photon–jet p_T -balance $x_{J\gamma}$ for the photon transverse momentum interval $p_T^\gamma = 63.1\text{--}79.6 \text{ GeV}$ for (left) pp , (centre) 50–80% centrality and (right) 0–10% centrality $\text{Pb}+\text{Pb}$ events. Solid grey, dotted red, and dashed blue histograms show the raw jet yields, the estimate of the combinatoric background (non-existent for pp events), and the dijet background, respectively. Black points show the background-subtracted data before unfolding, with the vertical bars representing the combined statistical uncertainty from the data and background subtraction procedure.

fluctuations reconstructed as jets. This background is negligible in pp collisions. Because of the inclusive jet selection in the analysis, the combinatoric background is purely additive and can be statistically subtracted after scaling to the total photon yield. The combinatoric jet yields are determined in the data-overlay simulation, by examining the yield of reconstructed jets separated from a generator-level photon by $\Delta\phi > 7\pi/8$. Reconstructed jets that are not consistent with a generator-level jet, i.e. no generator-level jet with $p_T > 20 \text{ GeV}$ within $\Delta R < 0.4$, are deemed to arise from the original $\text{Pb}+\text{Pb}$ data event and are thus labelled as “combinatoric” jets. The combinatoric jet yields are subtracted from the measured $x_{J\gamma}$ distributions in data.

The second background is related to the estimated purity of the selected photons. The $x_{J\gamma}$ yields for photon candidates in region A contain an admixture of dijets, specifically jets correlated with misidentified neutral mesons. Since these hadrons pass experimental isolation requirements, they may be, for example, the leading fragment inside a jet. The shape of this background in the $x_{J\gamma}$ distribution is determined by repeating the analysis for photon candidates in region C , since this region contains mostly neutral mesons that remain isolated at the detector level. The resulting per-photon $x_{J\gamma}$ distributions are scaled to match the number of background photons, as determined above in Section 5.1, and their yields are statistically subtracted from the jet yields for photons in region A .

Figure 1 shows the size of these backgrounds in the lowest- p_T^γ interval, where they are the largest. The combinatoric jet background for $\text{Pb}+\text{Pb}$ collisions contributes primarily to kinematic regions populated by $p_T^{\text{jet}} < 50 \text{ GeV}$. It also depends strongly on centrality, being largest in 0–10% collisions but nearly negligible already in 30–50% collisions. The dijet background contributes to a broad range of p_T^{jet} values including the region $x_{J\gamma} > 1$, since the p_T ratio of a jet to one of the hadrons in the balancing jet can generally be above unity. This background has a similar shape in all event types. However, since the photon purity is lower in $\text{Pb}+\text{Pb}$ events than in pp events, this correction is larger in the former.

5.3 Unfolding

The background-subtracted $x_{J\gamma}$ yields are corrected for bin-migration effects due to detector resolution via a Bayesian unfolding procedure [55, 56]. To accomplish this, the reconstructed yields are arranged in a two-dimensional ($p_T^\gamma, x_{J\gamma}$) matrix with bin edges that are evenly spaced on logarithmic scales (and with values matching those used in previous jet measurements), and a two-dimensional unfolding is performed similar to that for dijet p_T correlations in Ref. [12]. The unfolding is performed in $x_{J\gamma}$ directly to preserve the fine correlation between p_T^{jet} and p_T^γ which would be washed out if the unfolding were performed in $(p_T^\gamma, p_T^{\text{jet}})$. Although the migration along the p_T^γ axis is small, it is necessary to include it since the degree of bin migration in $x_{J\gamma}$ depends on the p_T of the jets.

To fully account for the effects of bin migration across the analysis selection, the axes of the matrix are extended over a larger range of p_T^γ and $x_{J\gamma}$ than the fiducial region in which the results are reported. A response matrix is determined by matching each pair of $(p_T^\gamma, x_{J\gamma})$ values at the generator level to their counterparts at the reconstruction level, separately for pp events and for each Pb+Pb centrality.

The Bayesian unfolding method requires a choice for the number of iterations, n_{iter} , and an assumption for the prior for the initial particle-level distribution. The PYTHIA simulation does not include the effects of jet energy loss, and thus the underlying particle-level distribution in data is expected to have a shape different from the default prior in the simulation. An initial unfolding using the default PYTHIA prior is performed for each centrality selection, and the ratios of the unfolded distributions to the generator-level priors in PYTHIA are fitted with a smooth function in $x_{J\gamma}$ in each p_T^γ interval. This function is evaluated to give a weight $w = w(x_{J\gamma}, p_T^\gamma)$ that is used to reweight the generator-level distribution in simulation and thus construct a nominal prior. Alternative reweightings, used in evaluating the sensitivity to the choice of prior, are determined by applying \sqrt{w} (the geometric mean of the nominal reweighting and no reweighting) and $w^{3/2}$ to the sample. The reconstruction-level $x_{J\gamma}$ distributions in simulation after each of these reweightings were examined to ensure that they span a reasonable range of values compared to that observed at the reconstruction level in data.

Before applying the unfolding procedure to data, it was tested on simulation. After the nominal reweighting, the Monte Carlo samples were split into two statistically independent subsamples. One subsample was used to populate the response matrix, which was then used to unfold the reconstruction-level distribution in the other subsample. The unfolded result was compared with the original generator-level distribution in the latter sample, which were found to be recovered within the limits of the statistical precision of the samples.

The values of n_{iter} used for the nominal results are chosen following the same procedure as in Ref. [12]. For each centrality selection, the unfolded distributions are examined as a function of n_{iter} . For each value of n_{iter} , a total uncertainty is formed by adding two components in quadrature: (1) the statistical uncertainty of the unfolded data, which grows slowly with n_{iter} , and (2) the sum of square differences between the results and those obtained with an alternative prior, which decreases quickly with n_{iter} . The final values of n_{iter} are chosen to minimise the total uncertainty, and are between two and four.

The unfolded $x_{J\gamma}$ results are corrected for the jet reconstruction efficiency, evaluated in simulation as the p_T^γ -dependent probability that a generated jet at the given $x_{J\gamma}$ is successfully reconstructed within the total $(p_T^\gamma, x_{J\gamma})$ range used in the unfolding. This efficiency is typically $> 99\%$ for all events in the kinematic regions populated by jets with $p_T > 50$ GeV. In pp collisions, this efficiency falls to $\approx 96\%$ in the lowest- $x_{J\gamma}$ region for each p_T^γ interval. In Pb+Pb collisions, the efficiency at fixed $x_{J\gamma}$ decreases

monotonically in increasingly central events, reaching a minimum of $\approx 75\%$ in the lowest- $x_{J\gamma}$ region in 0–10% centrality events.

6 Systematic uncertainties

The primary sources of systematic uncertainty can be grouped into three major categories: the measurement of p_T^{jet} ; the selection of the photon and measurement of p_T^γ ; the modelling and subtraction of the combinatoric background; and the unfolding procedure. For each variation described below, the entire analysis is repeated including the background correction steps and unfolding. The differences between the resulting $x_{J\gamma}$ values and the nominal ones are taken as an estimate of the uncertainty from each source.

A standard set of uncertainties in the jet p_T scale and resolution, following the strategy described in Ref. [57] and commonly used for measurements in 2015 Pb+Pb and pp data [54, 58], are used in this analysis. The impact of the uncertainties is evaluated by modifying the response matrix according to the given variations in the reconstructed jet p_T . These include uncertainties in the p_T scale derived from *in situ* studies of the calorimeter response [47, 59], an uncertainty in the resolution derived using data-driven techniques [60], and uncertainties in both which result from a small relative energy-scale difference between the heavy-ion jet reconstruction procedure and that used in $\sqrt{s} = 13$ TeV pp collisions [53]. All of the above uncertainties apply equally to jets in pp and Pb+Pb events. A separate, centrality-dependent uncertainty is included in 0–60% Pb+Pb collisions. This uncertainty accounts for a possible modification of the jet response after energy loss and is evaluated through *in situ* comparisons of the charged-particle track-jet and calorimeter-jet p_T values in data and simulation. More details are provided in Refs. [54, 57]. No additional uncertainty is included for 60–80% centrality events.

Uncertainties in the photon purity estimate are determined by varying the non-tight identification and isolation criteria used to select hadron background candidates and by considering a possible non-factorisation of the hadron background along the axes used in the double-sideband procedure. The sensitivity to the modelling of photon shower shapes in simulation is evaluated by removing the data-driven corrections to these quantities [50]. Finally, the photon p_T scale and resolution uncertainties are described in detail in Ref. [51], and their impact is evaluated by applying them as variations to the response matrices used in unfolding.

Modelling- or unfolding-related systematic uncertainties arise from several sources. The estimate of the combinatoric photon–jet rate in the data-overlay simulation is sensitive to the requirement on the minimum p_T of a generator-level jet in the classification of a given reconstructed jet as a combinatoric jet, as opposed to a photon-correlated jet. To provide one estimate of the sensitivity to this threshold, it is varied in the range 20 ± 10 GeV. To assess the sensitivity to the choice of prior, the unfolding is repeated using the alternative priors which are systematically closer to and farther from the original PYTHIA prior. The sensitivity to statistical limitations of the simulation samples is determined through pseudo-experiments, resampling entries in the response matrices according to their uncertainty. Finally, the analysis is repeated using the SHERPA simulation to perform the corrections and unfolding, since this generator provides a different description of photon–jet production topologies.

Figure 2 summarises the systematic uncertainties in each category, as well as the total uncertainty, for the lowest- p_T^γ interval in pp and 0–10% Pb+Pb events. The jet-related uncertainties are generally the dominant ones, except in more central events and lower- p_T^γ intervals, where the unfolding and modelling uncertainties become co-dominant.

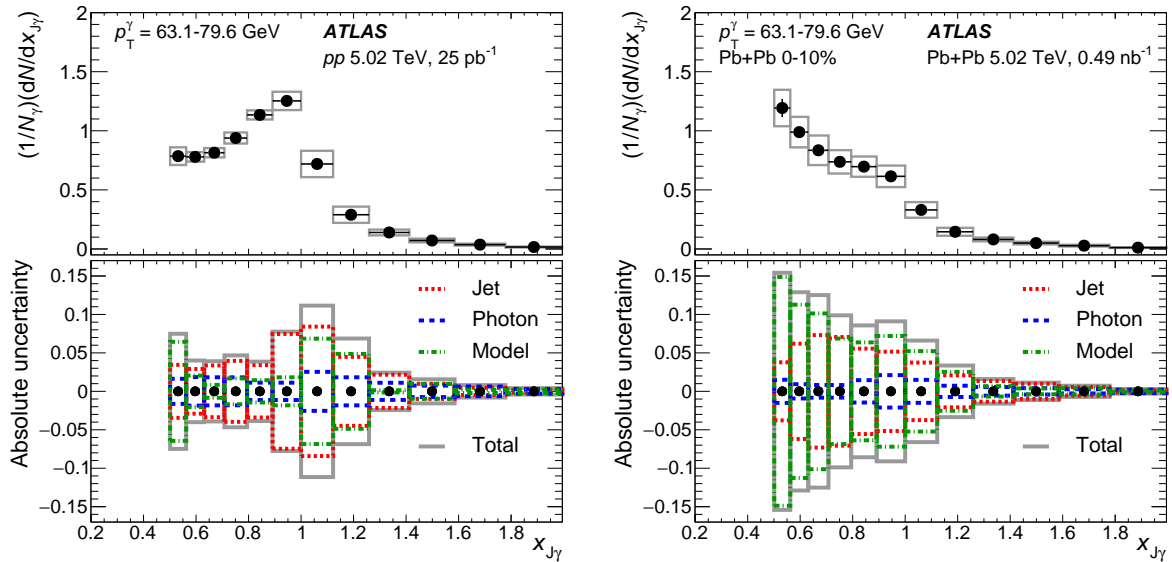


Figure 2: Unfolded distributions and summary of systematic uncertainties in the per-photon jet-yield measurement for $p_T^\gamma = 63.1\text{--}79.6 \text{ GeV}$ in (left) pp events and (right) 0–10% centrality Pb+Pb events. Top panels show the photon–jet p_T -balance $x_{J\gamma}$ distributions and total uncertainties, while the bottom panels show the absolute uncertainties from jet-related, photon-related, and modelling or unfolding sources, as well as the total uncertainty.

As an additional check on the features in the unfolded $x_{J\gamma}$ distributions observed in data, the analysis was repeated with two modifications which change the signal photon–jet definition. First, the photon–jet $\Delta\phi$ requirement was changed from $> 7\pi/8$ to $> 3\pi/4$. With this alteration, the correlated jet yield changes only by a small amount, while the combinatoric background, which is constant in $\Delta\phi$, doubles. Second, the analysis was repeated, but selecting only the leading (highest- p_T) jet in the event if it fell within the $\Delta\phi$ window. In this case, the combinatoric background contribution is no longer purely additive and the inefficiency when a higher- p_T uncorrelated jet is selected instead of the photon-correlated jet must be accounted for, similar to Ref. [12]. In both cases, the distributions in Pb+Pb exhibit a qualitatively similar modification pattern compared to the main results as a function of $x_{J\gamma}$.

7 Results

The unfolded $(1/N_\gamma)(dN/dx_{J\gamma})$ distributions in pp collisions are shown for each p_T^γ interval in Figure 3. The distributions are reported for all $x_{J\gamma}$ bins where the jet minimum p_T requirement is fully efficient. Also shown are the corresponding generator-level distributions from the PYTHIA, SHERPA and HERWIG samples. Each generator describes the data fairly well, with HERWIG generally overpredicting the yield at large- $x_{J\gamma}$ and SHERPA showing the best agreement over the full $x_{J\gamma}$ range.

The unfolded $(1/N_\gamma)(dN/dx_{J\gamma})$ distributions in Pb+Pb collisions are presented in Figures 4 through 7, with each figure representing a different p_T^γ interval. Since the results are fully corrected, they may be directly compared with the analogous $x_{J\gamma}$ distributions in pp collisions, which are reproduced in each panel for convenience.

For all p_T^γ intervals, the $x_{J\gamma}$ distributions in Pb+Pb collisions evolve smoothly with centrality. For peripheral collisions with centrality 50–80%, they are similar to those measured in pp collisions. However, in increasingly more central collisions, the distributions become progressively more modified. For the $p_T^\gamma < 100$ GeV intervals shown in Figures 4 and 5, the $x_{J\gamma}$ distributions in the most central 0–10% events are so strongly modified that they decrease monotonically over the measured $x_{J\gamma}$ range and no peak is observed. For the $p_T^\gamma > 100$ GeV region shown in Figure 6, the $x_{J\gamma}$ distributions retain a peak at or near $x_{J\gamma} \approx 0.9$ even in the most central collisions. However, the magnitude of the peak is lower and significantly wider than the sharp peak in pp events. In both cases, the jet yield at small $x_{J\gamma}$ is systematically higher than that in pp collisions, by up to a factor of two. In less central events, a peak-like structure develops at the same position as the maximum in pp events, near $x_{J\gamma} \approx 0.9$. For the lowest- p_T^γ interval, this occurs only for 50–80% centrality events, while in the highest two p_T^γ intervals the distribution in 0–10% events is consistent with a local peak.

As another way of characterising how the modified $x_{J\gamma}$ distributions depend on centrality and p_T^γ , Figure 8 presents their mean value, $\langle x_{J\gamma} \rangle$, and integral, R^γ , with both values calculated in the region $x_{J\gamma} > 0.5$. These quantities are shown as a function of the mean number of participating nucleons N_{part} in the corresponding centrality selection, and are plotted for the first three p_T^γ intervals where they have small statistical uncertainties. When measured in the region $x_{J\gamma} > 0.5$, the value of $\langle x_{J\gamma} \rangle$ in pp collisions is observed to be ≈ 0.89 for all p_T^γ intervals. Simulation studies show that, at generator level, the jet yield at $x_{J\gamma} > 0.5$ corresponds to only the leading (highest- p_T) photon-correlated jet in each event. Thus, $\langle x_{J\gamma} \rangle$ can be interpreted as a conditional per-jet fractional energy loss, and R^γ can be interpreted as the fraction of photons with a leading jet above $x_{J\gamma} = 0.5$. In pp collisions, R^γ ranges from 0.65 to 0.75 in the three p_T^γ intervals shown, which is below unity due to the jet selection criteria ($\Delta\phi > 7\pi/8$, $|\eta| < 2.8$).

In Pb+Pb events, $\langle x_{J\gamma} \rangle$ decreases monotonically from the value in pp collisions as the collisions become more central. In the most central collisions, it is below the pp value by 0.04–0.06, depending on the p_T^γ interval, while in peripheral collisions it reaches a value which is statistically compatible with that in pp events. The R^γ value also decreases monotonically as the collisions become more central, reflecting the overall shift of the $x_{J\gamma}$ value of leading jets below $x_{J\gamma} = 0.5$. At low p_T^γ in central Pb+Pb collisions, R^γ reaches the value of 0.5, which is only $\approx 75\%$ of its value in pp collisions.

The results are compared with the following theoretical predictions which include Monte Carlo generators and analytical calculations of jet energy loss: (1) a pQCD calculation which includes Sudakov resummation to describe the vacuum distributions and energy loss in Pb+Pb collisions as described in the BDMPS-Z formalism [26], (2) a perturbative calculation within the framework of soft-collinear effective field theory with Glauber gluons (SCET_G) in the soft gluon emission (energy-loss) limit [27], (3) the JEWEL Monte Carlo event generator which simulates QCD jet evolution in heavy-ion collisions and includes energy-loss effects from radiative and elastic scattering processes [28], and (4) the Hybrid Strong/Weak Coupling model [29] which combines initial production using PYTHIA with a parameterisation of energy loss derived from holographic methods, and includes back-reaction effects.

Figures 9 and 10 compare a selection of the measured $x_{J\gamma}$ distributions with the results of these theoretical predictions, where possible. Before testing the description of energy-loss effects in Pb+Pb events, the predicted $x_{J\gamma}$ distributions are compared with pp data in Figure 9. The Hybrid model and JEWEL, which use PYTHIA for the photon-jet production in vacuum, give a good description of pp events over the measured $x_{J\gamma}$ range in both p_T^γ intervals shown. The BDMPS-Z and SCET_G perturbative calculations capture the general features but predict distributions that are more and less peaked, respectively, than those in data.

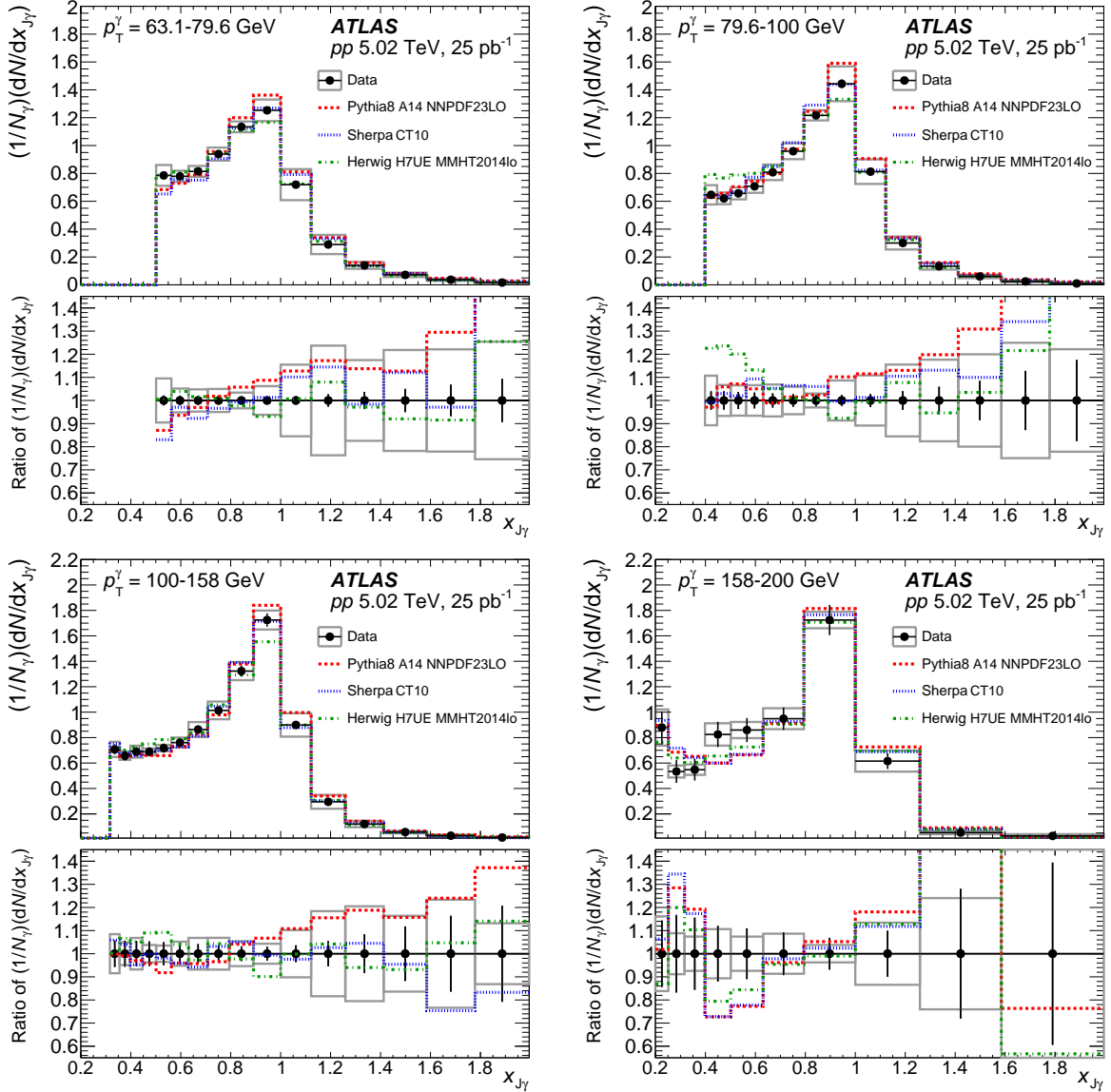


Figure 3: Photon–jet p_T -balance distributions $(1/N_\gamma)(dN/dx_{J\gamma})$ in pp collisions, each panel showing a different photon- p_T interval. The unfolded results are compared with the particle-level distributions from three Monte Carlo event generators. Bottom panels show the ratios of the generators to the pp data. Total systematic uncertainties are shown as boxes, while statistical uncertainties are shown as vertical bars.

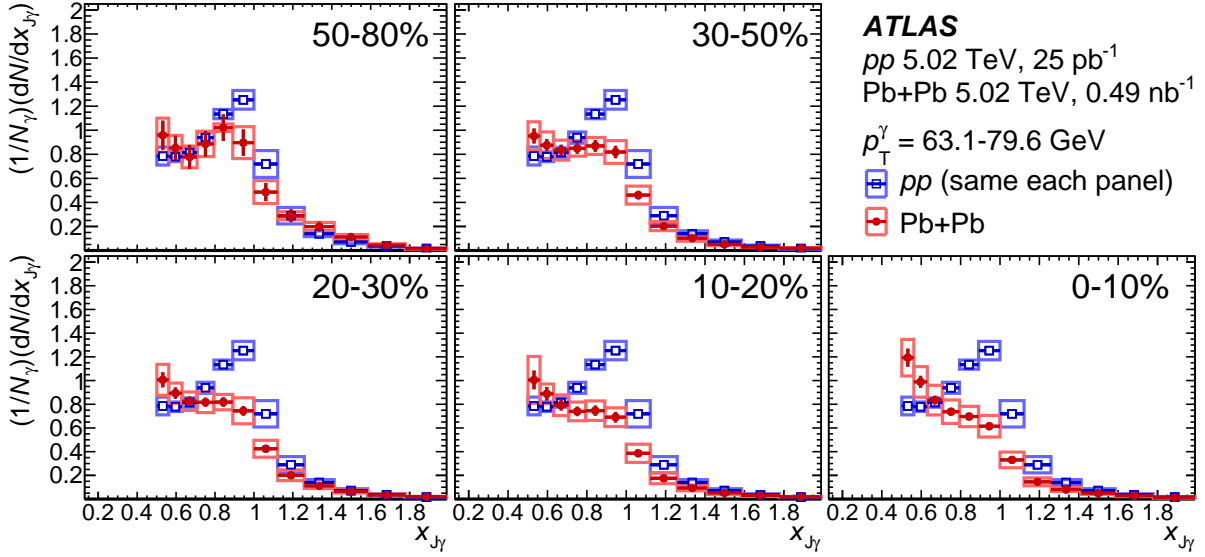


Figure 4: Photon–jet p_T -balance distributions $(1/N_\gamma)(dN/dx_{J\gamma})$ in Pb+Pb events (red circles) with each panel showing a different centrality selection compared to that in pp events (blue squares). These panels show results for $p_T^\gamma = 63.1\text{--}79.6$ GeV. Total systematic uncertainties are shown as boxes, while statistical uncertainties are shown as vertical bars.

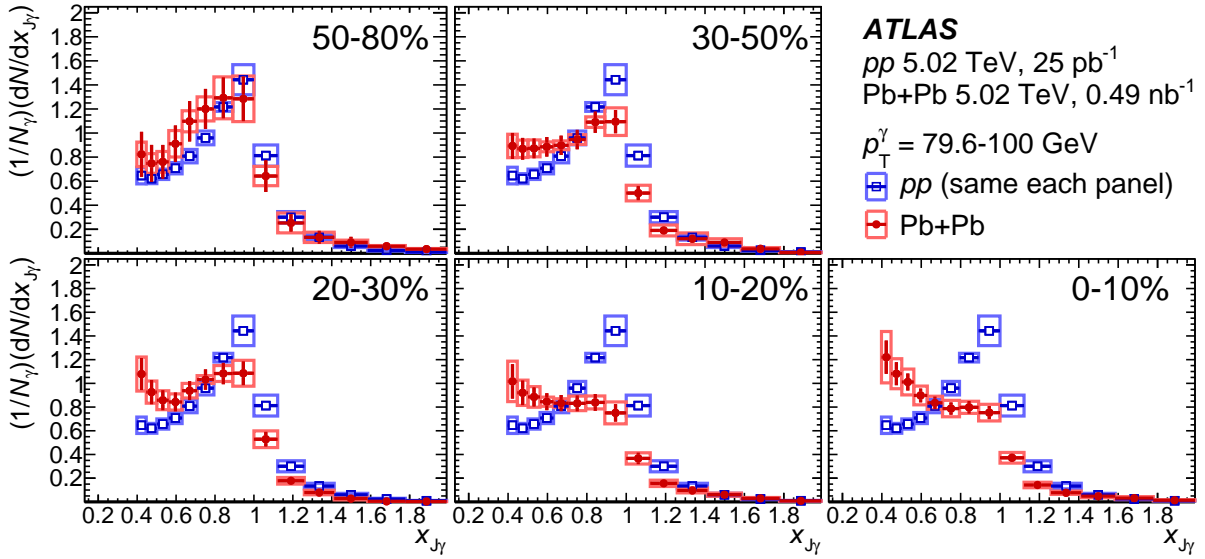


Figure 5: Photon–jet p_T -balance distributions $(1/N_\gamma)(dN/dx_{J\gamma})$ in Pb+Pb events (red circles) with each panel showing a different centrality selection compared to that in pp events (blue squares). These panels show results for $p_T^\gamma = 79.6\text{--}100$ GeV. Total systematic uncertainties are shown as boxes, while statistical uncertainties are shown as vertical bars.

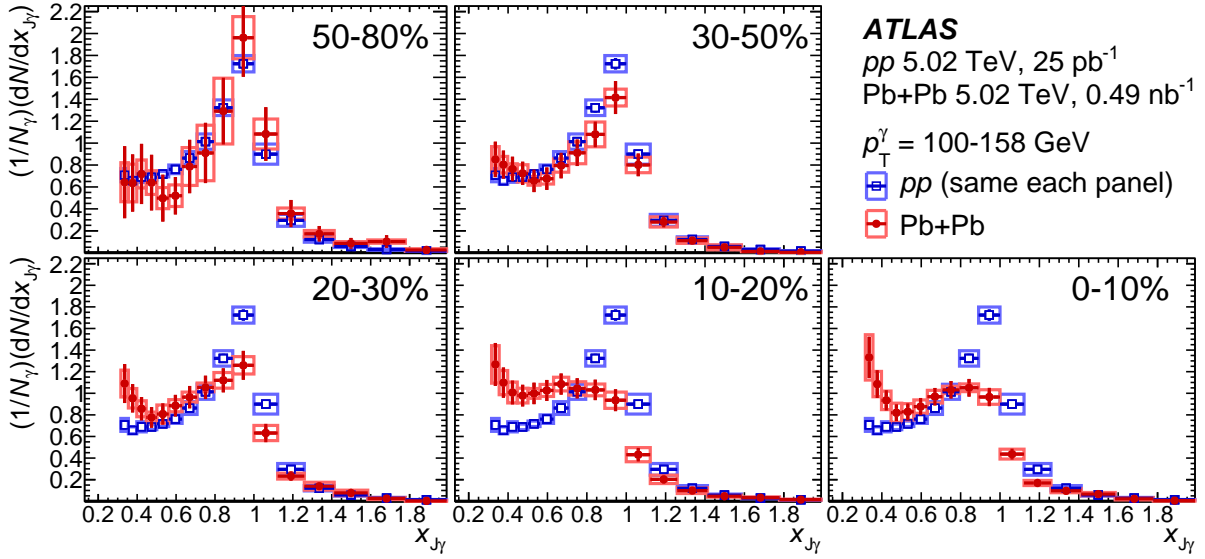


Figure 6: Photon-jet p_T -balance distributions $(1/N_\gamma)(dN/dx_{J\gamma})$ in Pb+Pb events (red circles) with each panel showing a different centrality selection compared to that in pp events (blue squares). These panels show results for $p_T^\gamma = 100\text{--}158 GeV. Total systematic uncertainties are shown as boxes, while statistical uncertainties are shown as vertical bars.$

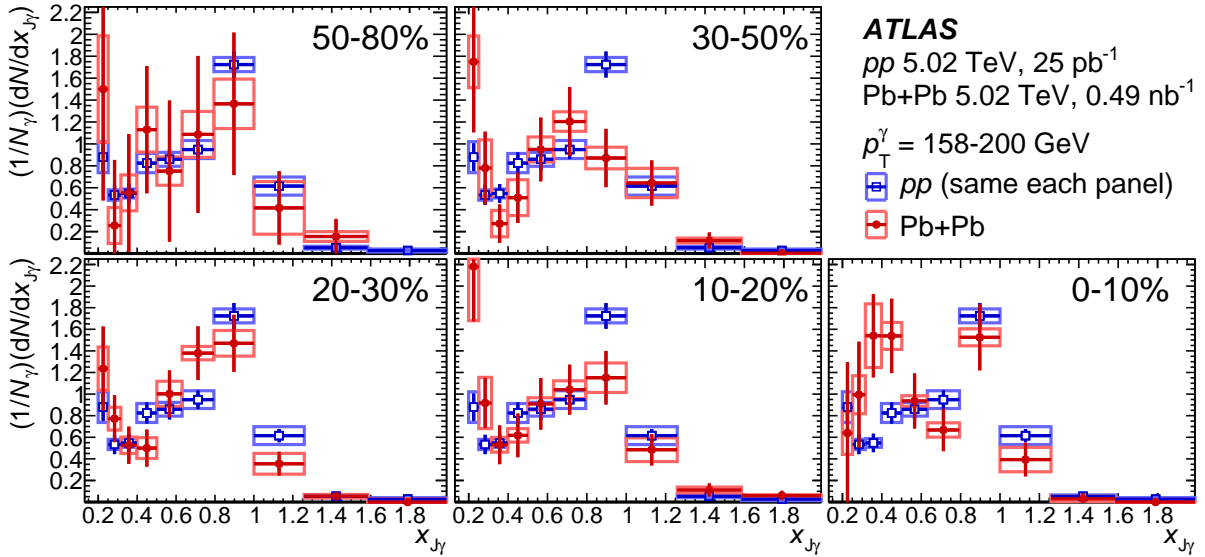


Figure 7: Photon-jet p_T -balance distributions $(1/N_\gamma)(dN/dx_{J\gamma})$ in Pb+Pb events (red circles) with each panel showing a different centrality selection compared to that in pp events (blue squares). These panels show results for $p_T^\gamma = 158\text{--}200$ GeV. Total systematic uncertainties are shown as boxes, while statistical uncertainties are shown as vertical bars.

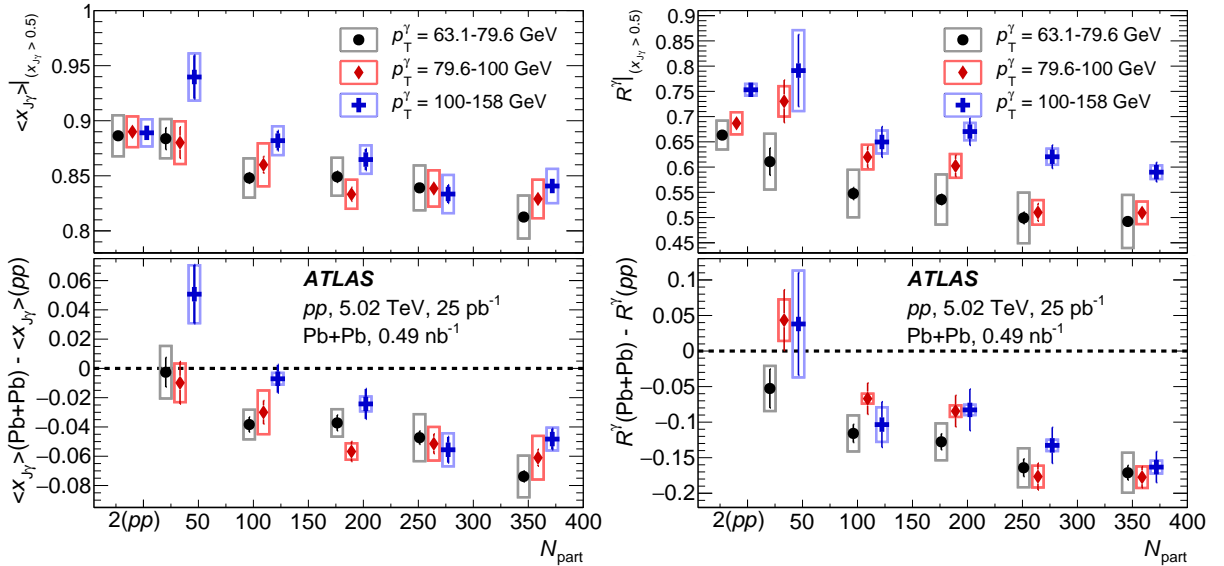


Figure 8: Summary of (left) the mean jet-to-photon p_T ratio $\langle x_{J\gamma} \rangle$ and (right) the total per-photon jet yield R^γ , calculated in the region $x_{J\gamma} > 0.5$. The values are presented as a function of the mean number of participating nucleons N_{part} in top panels. Each colour and symbol represents a different p_T^γ interval, where the lowest and highest intervals are displaced horizontally for clarity. The points plotted at $N_{\text{part}} = 2$ correspond to pp collisions. The bottom panels show the difference between the Pb+Pb centrality selection and pp collisions. Boxes show the total systematic uncertainty while the vertical bars represent statistical uncertainties.

In Pb+Pb events with low p_T^γ , shown in the left panel of Figure 10, the JEWEL, Hybrid, and SCET_G models successfully capture several key features of the $x_{J\gamma}$ distribution, including the absence of a visible peak, and the monotonically increasing behaviour with decreasing $x_{J\gamma}$. The BDMPS-Z model predicts a suppression of the yield near $x_{J\gamma} \approx 0.9$ relative to what is predicted in pp events, consistent with the trend in data. However, it underestimates the yield at low $x_{J\gamma}$ in both pp and Pb+Pb collisions. In the higher- p_T^γ interval, the Hybrid model and JEWEL successfully describe the reappearance of a localised peak near $x_{J\gamma} \approx 0.9$. However, none of the models considered here describe the increase of the jet yield at $x_{J\gamma} < 0.5$ above that observed in pp events. Additional comparisons between these data and theoretical calculations which are differential in both p_T^γ and centrality will further constrain the description of the strongly coupled medium in these models.

8 Conclusion

This Letter presents a study of photon–jet transverse momentum correlations for photons with $63.1 < p_T^\gamma < 200$ GeV in Pb+Pb collisions at $\sqrt{s_{\text{NN}}} = 5.02$ TeV and pp collisions at $\sqrt{s} = 5.02$ TeV. The data were recorded with the ATLAS detector at the LHC and correspond to integrated luminosities of 0.49 nb^{-1} and 25 pb^{-1} , respectively. The data are corrected for the presence of combinatoric photon–jet pairs and of dijet pairs where one of the jets is misidentified as a photon. The measured quantities in data are fully corrected for detector effects and reported at the particle level. Per-photon distributions of the jet-to-photon p_T ratio, $x_{J\gamma} = p_T^{\text{jet}} / p_T^\gamma$, are measured for pairs with an azimuthally balanced configuration, $\Delta\phi > 7\pi/8$. In pp

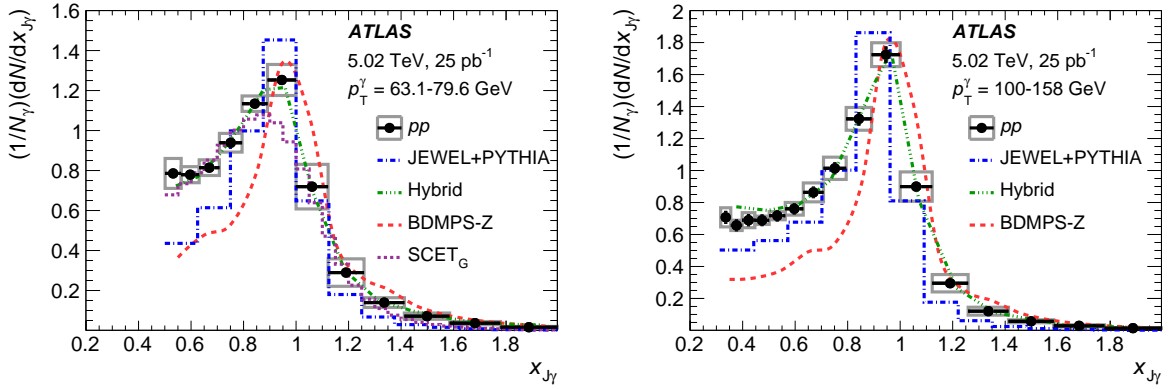


Figure 9: Photon–jet p_T -balance distributions $(1/N_\gamma)(dN/dx_{J\gamma})$ in pp collisions for (left) $p_T^\gamma = 63.1\text{--}79.6 \text{ GeV}$ and (right) $p_T^\gamma = 100\text{--}158 \text{ GeV}$. The unfolded results are compared with the theoretical calculations shown as dashed coloured lines (see text). Total systematic uncertainties are shown as boxes, while statistical uncertainties are shown as vertical bars.

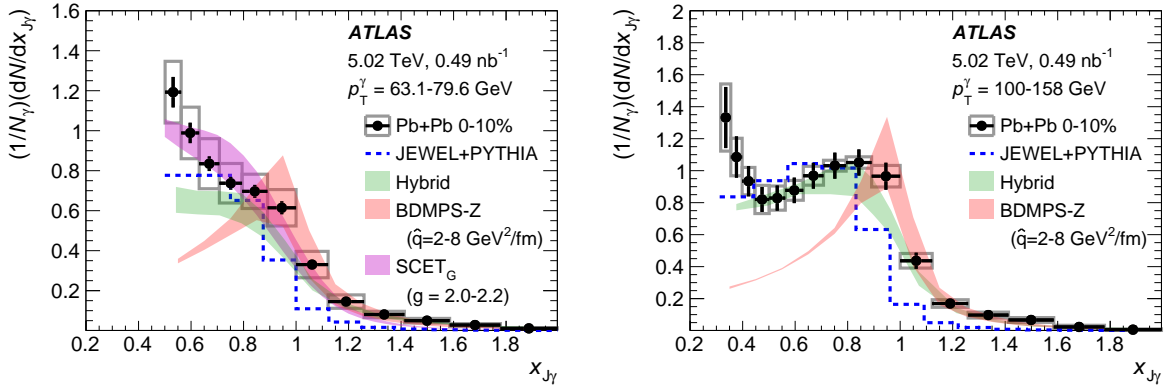


Figure 10: Photon–jet p_T -balance distributions $(1/N_\gamma)(dN/dx_{J\gamma})$ in 0–10% Pb+Pb collisions for (left) $p_T^\gamma = 63.1\text{--}79.6 \text{ GeV}$ and (right) $p_T^\gamma = 100\text{--}158 \text{ GeV}$. The unfolded results are compared with the theoretical calculations shown as dashed coloured lines denoting central values or coloured bands which correspond to a range of theoretical parameters (see text). Total systematic uncertainties are shown as boxes, while statistical uncertainties are shown as vertical bars.

events, the data are well reproduced by event generators or models that depend on them, but are not fully described in detail by approaches based on perturbative calculations.

In Pb+Pb collisions, $x_{J\gamma}$ distributions are observed to have a significantly modified total yield and shape compared with those in pp collisions. These modifications have a smooth onset as a function of Pb+Pb event centrality and p_T^γ . In peripheral collisions at high p_T^γ , the distributions in Pb+Pb are statistically compatible with those in pp . In the most central Pb+Pb events at low p_T^γ , the yield decreases monotonically with increasing $x_{J\gamma}$ over the measured range, in strong contrast to the sharply peaked distributions in pp events. However, in less central events or in higher- p_T^γ intervals, the $x_{J\gamma}$ distributions retain a peak-like excess at an $x_{J\gamma}$ value similar to that in pp collisions but with a smaller per-photon yield. This last observation suggests that the amount of energy lost by jets in single events has a broad distribution, with

a small but significant population of jets retaining a pp -like p_T correlation with the photon because they do not lose an appreciable amount of energy.

These results are sensitive to how partons initially produced opposite to a high- p_T photon lose energy in their interactions with the hot nuclear medium. Taken together with other measurements of single-jet and dijet production, the data provide new, complementary information about how energy loss in the strongly coupled medium varies with the initial parton flavour and p_T .

Acknowledgements

We thank CERN for the very successful operation of the LHC, as well as the support staff from our institutions without whom ATLAS could not be operated efficiently.

We acknowledge the support of ANPCyT, Argentina; YerPhI, Armenia; ARC, Australia; BMWFW and FWF, Austria; ANAS, Azerbaijan; SSTC, Belarus; CNPq and FAPESP, Brazil; NSERC, NRC and CFI, Canada; CERN; CONICYT, Chile; CAS, MOST and NSFC, China; COLCIENCIAS, Colombia; MSMT CR, MPO CR and VSC CR, Czech Republic; DNRF and DNSRC, Denmark; IN2P3-CNRS, CEA-DRF/IRFU, France; SRNSFG, Georgia; BMBF, HGF, and MPG, Germany; GSRT, Greece; RGC, Hong Kong SAR, China; ISF and Benoziyo Center, Israel; INFN, Italy; MEXT and JSPS, Japan; CNRST, Morocco; NWO, Netherlands; RCN, Norway; MNiSW and NCN, Poland; FCT, Portugal; MNE/IFA, Romania; MES of Russia and NRC KI, Russian Federation; JINR; MESTD, Serbia; MSSR, Slovakia; ARRS and MIZŠ, Slovenia; DST/NRF, South Africa; MINECO, Spain; SRC and Wallenberg Foundation, Sweden; SERI, SNSF and Cantons of Bern and Geneva, Switzerland; MOST, Taiwan; TAEK, Turkey; STFC, United Kingdom; DOE and NSF, United States of America. In addition, individual groups and members have received support from BCKDF, CANARIE, CRC and Compute Canada, Canada; COST, ERC, ERDF, Horizon 2020, and Marie Skłodowska-Curie Actions, European Union; Investissements d’Avenir Labex and Idex, ANR, France; DFG and AvH Foundation, Germany; Herakleitos, Thales and Aristeia programmes co-financed by EU-ESF and the Greek NSRF, Greece; BSF-NSF and GIF, Israel; CERCA Programme Generalitat de Catalunya, Spain; The Royal Society and Leverhulme Trust, United Kingdom.

The crucial computing support from all WLCG partners is acknowledged gratefully, in particular from CERN, the ATLAS Tier-1 facilities at TRIUMF (Canada), NDGF (Denmark, Norway, Sweden), CC-IN2P3 (France), KIT/GridKA (Germany), INFN-CNAF (Italy), NL-T1 (Netherlands), PIC (Spain), ASGC (Taiwan), RAL (UK) and BNL (USA), the Tier-2 facilities worldwide and large non-WLCG resource providers. Major contributors of computing resources are listed in Ref. [61].

References

- [1] X.-N. Wang, Z. Huang and I. Sarcevic, *Jet Quenching in the Direction Opposite to a Tagged Photon in High-Energy Heavy-Ion Collisions*, *Phys. Rev. Lett.* **77** (1996) 231, arXiv: [hep-ph/9605213](#).
- [2] X.-N. Wang and Z. Huang, *Medium-induced parton energy loss in $\gamma + \text{jet}$ events of high-energy heavy-ion collisions*, *Phys. Rev. C* **55** (1997) 3047, arXiv: [hep-ph/9701227](#).
- [3] G.-Y. Qin, J. Ruppert, C. Gale, S. Jeon and G. D. Moore, *Jet energy loss, photon production, and photon-hadron correlations at energies available at the BNL Relativistic Heavy Ion Collider (RHIC)*, *Phys. Rev. C* **80** (2009) 054909, arXiv: [0906.3280 \[hep-ph\]](#).
- [4] T. Renk, *γ -hadron correlations as a tool to trace the flow of energy lost from hard partons in heavy-ion collisions*, *Phys. Rev. C* **80** (2009) 014901, arXiv: [0904.3806 \[hep-ph\]](#).
- [5] G.-Y. Qin, *Parton shower evolution in medium and nuclear modification of photon-tagged jets in Pb+Pb collisions at the LHC*, *Eur. Phys. J. C* **74** (2014) 2959, arXiv: [1210.6610 \[hep-ph\]](#).
- [6] X.-N. Wang and Y. Zhu, *Medium Modification of γ -jets in High-energy Heavy-ion Collisions*, *Phys. Rev. Lett.* **111** (2013) 062301, arXiv: [1302.5874 \[hep-ph\]](#).
- [7] W. Dai, I. Vitev and B.-W. Zhang, *Momentum Imbalance of Isolated Photon-Tagged Jet Production at RHIC and LHC*, *Phys. Rev. Lett.* **110** (2013) 142001, arXiv: [1207.5177 \[hep-ph\]](#).
- [8] PHENIX Collaboration, *Measurement of Direct Photons in Au+Au Collisions at $\sqrt{s_{NN}} = 200$ GeV*, *Phys. Rev. Lett.* **109** (2012) 152302, arXiv: [1205.5759 \[nucl-ex\]](#).
- [9] ATLAS Collaboration, *Centrality, rapidity and transverse momentum dependence of isolated prompt photon production in lead–lead collisions at $\sqrt{s_{NN}} = 2.76$ TeV measured with the ATLAS detector*, *Phys. Rev. C* **93** (2016) 034914, arXiv: [1506.08552 \[hep-ex\]](#).
- [10] F. Arleo, K. J. Eskola, H. Paukkunen and C. A. Salgado, *Inclusive prompt photon production in nuclear collisions at RHIC and LHC*, *JHEP* **04** (2011) 055, arXiv: [1103.1471 \[hep-ph\]](#).
- [11] ATLAS Collaboration, *Observation of a Centrality-Dependent Dijet Asymmetry in Lead–Lead Collisions at $\sqrt{s_{NN}} = 2.76$ TeV with the ATLAS Detector at the LHC*, *Phys. Rev. Lett.* **105** (2010) 252303, arXiv: [1011.6182 \[hep-ex\]](#).
- [12] ATLAS Collaboration, *Measurement of jet p_T correlations in Pb+Pb and pp collisions at $\sqrt{s_{NN}} = 2.76$ TeV with the ATLAS detector*, *Phys. Lett. B* **774** (2017) 379, arXiv: [1706.09363 \[hep-ex\]](#).
- [13] CMS Collaboration, *Observation and studies of jet quenching in PbPb collisions at $\sqrt{s_{NN}} = 2.76$ TeV*, *Phys. Rev. C* **84** (2011) 024906, arXiv: [1102.1957 \[nucl-ex\]](#).
- [14] ATLAS Collaboration, *Measurement of the jet radius and transverse momentum dependence of inclusive jet suppression in lead–lead collisions at $\sqrt{s_{NN}} = 2.76$ TeV with the ATLAS detector*, *Phys. Lett. B* **719** (2013) 220, arXiv: [1208.1967 \[hep-ex\]](#).

- [15] ATLAS Collaboration, *Measurements of the Nuclear Modification Factor for Jets in Pb+Pb Collisions at $\sqrt{s_{NN}} = 2.76$ TeV with the ATLAS Detector*, *Phys. Rev. Lett.* **114** (2015) 072302, arXiv: [1411.2357 \[hep-ex\]](#).
- [16] CMS Collaboration, *Jet momentum dependence of jet quenching in PbPb collisions at $\sqrt{s_{NN}} = 2.76$ TeV*, *Phys. Lett. B* **712** (2012) 176, arXiv: [1202.5022 \[nucl-ex\]](#).
- [17] ATLAS Collaboration, *Measurement of charged-particle spectra in Pb+Pb collisions at $\sqrt{s_{NN}} = 2.76$ TeV with the ATLAS detector at the LHC*, *JHEP* **09** (2015) 050, arXiv: [1504.04337 \[hep-ex\]](#).
- [18] CMS Collaboration, *Charged-particle nuclear modification factors in PbPb and pPb collisions at $\sqrt{s_{NN}} = 5.02$ TeV*, *JHEP* **04** (2017) 039, arXiv: [1611.01664 \[hep-ex\]](#).
- [19] ALICE Collaboration, *Transverse momentum spectra and nuclear modification factors of charged particles in pp, p-Pb and Pb-Pb collisions at the LHC*, (2018), arXiv: [1802.09145 \[nucl-ex\]](#).
- [20] PHENIX Collaboration, *Photon-Hadron Jet Correlations in p+p and Au+Au Collisions at $\sqrt{s_{NN}} = 200$ GeV*, *Phys. Rev. C* **80** (2009) 024908, arXiv: [0903.3399 \[nucl-ex\]](#).
- [21] PHENIX Collaboration, *Medium modification of jet fragmentation in Au + Au collisions at $\sqrt{s_{NN}} = 200$ GeV measured in direct photon-hadron correlations*, *Phys. Rev. Lett.* **111** (2013) 032301, arXiv: [1212.3323 \[nucl-ex\]](#).
- [22] STAR Collaboration, *Jet-like correlations with direct-photon and neutral-pion Triggers at $\sqrt{s_{NN}} = 200$ GeV*, *Phys. Lett. B* **760** (2016) 689, arXiv: [1604.01117 \[nucl-ex\]](#).
- [23] CMS Collaboration, *Studies of jet quenching using isolated-photon+jet correlations in PbPb and pp collisions at $\sqrt{s_{NN}} = 2.76$ TeV*, *Phys. Lett. B* **718** (2013) 773, arXiv: [1205.0206 \[nucl-ex\]](#).
- [24] CMS Collaboration, *Study of jet quenching with isolated-photon+jet correlations in PbPb and pp collisions at $\sqrt{s_{NN}} = 5.02$ TeV*, *Phys. Lett. B* **785** (2018) 14, arXiv: [1711.09738 \[nucl-ex\]](#).
- [25] ATLAS Collaboration, *Measurement of jet fragmentation in Pb+Pb and pp collisions at $\sqrt{s_{NN}} = 2.76$ TeV with the ATLAS detector at the LHC*, *Eur. Phys. J. C* **77** (2017) 379, arXiv: [1702.00674 \[hep-ex\]](#).
- [26] L. Chen et al., *Study of Isolated-photon and Jet Momentum Imbalance in pp and PbPb collisions*, *Nucl. Phys.* **B933** (2018) 306, arXiv: [1803.10533 \[hep-ph\]](#).
- [27] Z.-B. Kang, I. Vitev and H. Xing, *Vector-boson-tagged jet production in heavy ion collisions at energies available at the CERN Large Hadron Collider*, *Phys. Rev. C* **96** (2017) 014912, arXiv: [1702.07276 \[hep-ph\]](#).
- [28] R. Kunnawalkam Elayavalli and K. C. Zapp, *Simulating V+jet processes in heavy ion collisions with JEWEL*, *Eur. Phys. J. C* **76** (2016) 695, arXiv: [1608.03099 \[hep-ph\]](#).
- [29] J. Casalderrey-Solana, D. C. Gulhan, J. G. Milhano, D. Pablos and K. Rajagopal, *Predictions for boson-jet observables and fragmentation function ratios from a hybrid strong/weak coupling model for jet quenching*, *JHEP* **03** (2016) 053, arXiv: [1508.00815 \[hep-ph\]](#).

- [30] ATLAS Collaboration, *The ATLAS Experiment at the CERN Large Hadron Collider*, JINST **3** (2008) S08003.
- [31] ATLAS Collaboration, *Performance of the ATLAS trigger system in 2015*, Eur. Phys. J. C **77** (2017) 317, arXiv: [1611.09661 \[hep-ex\]](#).
- [32] ATLAS Collaboration, *Measurement of longitudinal flow de-correlations in Pb+Pb collisions at $\sqrt{s_{NN}} = 2.76$ and 5.02 TeV with the ATLAS detector*, Eur. Phys. J. C **78** (2018) 142, arXiv: [1709.02301 \[nucl-ex\]](#).
- [33] ATLAS Collaboration, *Measurement of the pseudorapidity and transverse momentum dependence of the elliptic flow of charged particles in lead–lead collisions at $\sqrt{s_{NN}} = 2.76$ TeV with the ATLAS detector*, Phys. Lett. B **707** (2012) 330, arXiv: [1108.6018 \[hep-ex\]](#).
- [34] M. L. Miller, K. Reygers, S. J. Sanders and P. Steinberg, *Glauber modeling in high energy nuclear collisions*, Ann. Rev. Nucl. Part. Sci. **57** (2007) 205, arXiv: [nucl-ex/0701025 \[nucl-ex\]](#).
- [35] ATLAS Collaboration, *Prompt and non-prompt J/ψ and $\psi(2S)$ suppression at high transverse momentum in 5.02 TeV Pb+Pb collisions with the ATLAS experiment*, Eur. Phys. J. C **78** (2018) 762, arXiv: [1805.04077 \[nucl-ex\]](#).
- [36] S. Agostinelli et al., *GEANT4: a simulation toolkit*, Nucl. Instrum. Meth. A **506** (2003) 250.
- [37] ATLAS Collaboration, *The ATLAS Simulation Infrastructure*, Eur. Phys. J. C **70** (2010) 823, arXiv: [1005.4568 \[physics.ins-det\]](#).
- [38] T. Sjöstrand, S. Mrenna and P. Z. Skands, *A brief introduction to PYTHIA 8.1*, Comput. Phys. Commun. **178** (2008) 852, arXiv: [0710.3820 \[hep-ph\]](#).
- [39] R. D. Ball et al., *Parton distributions with LHC data*, Nucl. Phys. B **867** (2013) 244, arXiv: [1207.1303 \[hep-ph\]](#).
- [40] ATLAS Collaboration, *ATLAS Pythia 8 tunes to 7 TeV data*, ATL-PHYS-PUB-2014-021, 2014, URL: <https://cds.cern.ch/record/1966419>.
- [41] T. Gleisberg et al., *Event generation with SHERPA 1.1*, JHEP **02** (2009) 007, arXiv: [0811.4622 \[hep-ph\]](#).
- [42] H.-L. Lai et al., *New parton distributions for collider physics*, Phys. Rev. D **82** (2010) 074024, arXiv: [1007.2241 \[hep-ph\]](#).
- [43] J. Bellm et al., *Herwig 7.0/Herwig++ 3.0 release note*, Eur. Phys. J. C **76** (2016) 196, arXiv: [1512.01178 \[hep-ph\]](#).
- [44] L. A. Harland-Lang, A. D. Martin, P. Motylinski and R. S. Thorne, *Parton distributions in the LHC era: MMHT 2014 PDFs*, Eur. Phys. J. C **75** (2015) 204, arXiv: [1412.3989 \[hep-ph\]](#).
- [45] M. Cacciari, G. P. Salam and G. Soyez, *The anti- k_t jet clustering algorithm*, JHEP **04** (2008) 063, arXiv: [0802.1189 \[hep-ph\]](#).
- [46] M. Cacciari, G. P. Salam and G. Soyez, *FastJet user manual*, Eur. Phys. J. C **72** (2012) 1896, arXiv: [1111.6097 \[hep-ph\]](#).
- [47] ATLAS Collaboration, *Jet energy measurement with the ATLAS detector in proton–proton collisions at $\sqrt{s} = 7$ TeV*, Eur. Phys. J. C **73** (2013) 2304, arXiv: [1112.6426 \[hep-ex\]](#).

- [48] ATLAS Collaboration, *Measurement of the inclusive isolated prompt photon cross section in pp collisions at $\sqrt{s} = 8$ TeV with the ATLAS detector*, *JHEP* **08** (2016) 005, arXiv: [1605.03495 \[hep-ex\]](#).
- [49] ATLAS Collaboration, *Measurement of the cross section for inclusive isolated-photon production in pp collisions at $\sqrt{s} = 13$ TeV using the ATLAS detector*, *Phys. Lett. B* **770** (2017) 473, arXiv: [1701.06882 \[hep-ex\]](#).
- [50] ATLAS Collaboration, *Photon identification in 2015 ATLAS data*, ATL-PHYS-PUB-2016-014, 2016, URL: <https://cds.cern.ch/record/2203125>.
- [51] ATLAS Collaboration, *Electron and photon energy calibration with the ATLAS detector using data collected in 2015 at $\sqrt{s} = 13$ TeV*, ATL-PHYS-PUB-2016-015, 2016, URL: <https://cds.cern.ch/record/2203514>.
- [52] ATLAS Collaboration, *Centrality and rapidity dependence of inclusive jet production in $\sqrt{s_{NN}} = 5.02$ TeV proton-lead collisions with the ATLAS detector*, *Phys. Lett. B* **748** (2015) 392, arXiv: [1412.4092 \[hep-ex\]](#).
- [53] ATLAS Collaboration, *Jet energy scale measurements and their systematic uncertainties in proton–proton collisions at $\sqrt{s} = 13$ TeV with the ATLAS detector*, *Phys. Rev. D* **96** (2017) 072002, arXiv: [1703.09665 \[hep-ex\]](#).
- [54] ATLAS Collaboration, *Measurement of the nuclear modification factor for inclusive jets in Pb+Pb collisions at $\sqrt{s_{NN}} = 5.02$ TeV with the ATLAS detector*, (2018), arXiv: [1805.05635 \[nucl-ex\]](#).
- [55] G. D'Agostini, *A multidimensional unfolding method based on Bayes' theorem*, *Nucl. Instrum. Meth. A* **362** (1995) 487.
- [56] T. Adye, *Unfolding algorithms and tests using RooUnfold*, (2011), arXiv: [1105.1160 \[physics.data-an\]](#).
- [57] ATLAS Collaboration, *Jet energy scale and its uncertainty for jets reconstructed using the ATLAS heavy ion jet algorithm*, ATLAS-CONF-2015-016, 2015, URL: <https://cds.cern.ch/record/2008677>.
- [58] ATLAS Collaboration, *Measurement of jet fragmentation in Pb+Pb and pp collisions at $\sqrt{s_{NN}} = 5.02$ TeV with the ATLAS detector*, *Phys. Rev. C* **98** (2018) 024908, arXiv: [1805.05424 \[nucl-ex\]](#).
- [59] ATLAS Collaboration, *Jet Calibration and Systematic Uncertainties for Jets Reconstructed in the ATLAS Detector at $\sqrt{s} = 13$ TeV*, ATL-PHYS-PUB-2015-015, 2015, URL: <https://cds.cern.ch/record/2037613>.
- [60] ATLAS Collaboration, *Data-driven determination of the energy scale and resolution of jets reconstructed in the ATLAS calorimeters using dijet and multijet events at $\sqrt{s} = 8$ TeV*, ATLAS-CONF-2015-017, 2015, URL: <https://cds.cern.ch/record/2008678>.
- [61] ATLAS Collaboration, *ATLAS Computing Acknowledgements 2016–2017*, ATL-GEN-PUB-2016-002, URL: <https://cds.cern.ch/record/2202407>.

The ATLAS Collaboration

M. Aaboud^{34d}, G. Aad⁹⁹, B. Abbott¹²⁴, O. Abdinov^{13,*}, B. Abelos¹²⁸, D.K. Abhayasinghe⁹¹, S.H. Abidi¹⁶⁴, O.S. AbouZeid³⁹, N.L. Abraham¹⁵³, H. Abramowicz¹⁵⁸, H. Abreu¹⁵⁷, Y. Abulaiti⁶, B.S. Acharya^{64a,64b,n}, S. Adachi¹⁶⁰, L. Adamczyk^{81a}, J. Adelman¹¹⁹, M. Adersberger¹¹², A. Adiguzel^{12c}, T. Adye¹⁴¹, A.A. Affolder¹⁴³, Y. Afik¹⁵⁷, C. Agheorghiesei^{27c}, J.A. Aguilar-Saavedra^{136f,136a}, F. Ahmadov^{77,ad}, G. Aielli^{71a,71b}, S. Akatsuka⁸³, T.P.A. Åkesson⁹⁴, E. Akilli⁵², A.V. Akimov¹⁰⁸, G.L. Alberghi^{23b,23a}, J. Albert¹⁷³, P. Albicocco⁴⁹, M.J. Alconada Verzini⁸⁶, S. Alderweireldt¹¹⁷, M. Aleksa³⁵, I.N. Aleksandrov⁷⁷, C. Alexa^{27b}, T. Alexopoulos¹⁰, M. Alhroob¹²⁴, B. Ali¹³⁸, G. Alimonti^{66a}, J. Alison³⁶, S.P. Alkire¹⁴⁵, C. Allaire¹²⁸, B.M.M. Allbrooke¹⁵³, B.W. Allen¹²⁷, P.P. Allport²¹, A. Aloisio^{67a,67b}, A. Alonso³⁹, F. Alonso⁸⁶, C. Alpigiani¹⁴⁵, A.A. Alshehri⁵⁵, M.I. Alstaty⁹⁹, B. Alvarez Gonzalez³⁵, D. Álvarez Piqueras¹⁷¹, M.G. Alvaggi^{67a,67b}, B.T. Amadio¹⁸, Y. Amaral Coutinho^{78b}, L. Ambroz¹³¹, C. Amelung²⁶, D. Amidei¹⁰³, S.P. Amor Dos Santos^{136a,136c}, S. Amoroso⁴⁴, C.S. Amrouche⁵², C. Anastopoulos¹⁴⁶, L.S. Ancu⁵², N. Andari¹⁴², T. Andeen¹¹, C.F. Anders^{59b}, J.K. Anders²⁰, K.J. Anderson³⁶, A. Andreazza^{66a,66b}, V. Andrei^{59a}, C.R. Anelli¹⁷³, S. Angelidakis³⁷, I. Angelozzi¹¹⁸, A. Angerami³⁸, A.V. Anisenkov^{120b,120a}, A. Annovi^{69a}, C. Antel^{59a}, M.T. Anthony¹⁴⁶, M. Antonelli⁴⁹, D.J.A. Antrim¹⁶⁸, F. Anulli^{70a}, M. Aoki⁷⁹, J.A. Aparisi Pozo¹⁷¹, L. Aperio Bella³⁵, G. Arabidze¹⁰⁴, J.P. Araque^{136a}, V. Araujo Ferraz^{78b}, R. Araujo Pereira^{78b}, A.T.H. Arce⁴⁷, R.E. Ardell⁹¹, F.A. Arduh⁸⁶, J-F. Arguin¹⁰⁷, S. Argyropoulos⁷⁵, A.J. Armbruster³⁵, L.J. Armitage⁹⁰, A. Armstrong¹⁶⁸, O. Arnaez¹⁶⁴, H. Arnold¹¹⁸, M. Arratia³¹, O. Arslan²⁴, A. Artamonov^{109,*}, G. Artoni¹³¹, S. Artz⁹⁷, S. Asai¹⁶⁰, N. Asbah⁵⁷, A. Ashkenazi¹⁵⁸, E.M. Asimakopoulou¹⁶⁹, L. Asquith¹⁵³, K. Assamagan²⁹, R. Astalos^{28a}, R.J. Atkin^{32a}, M. Atkinson¹⁷⁰, N.B. Atlay¹⁴⁸, K. Augsten¹³⁸, G. Avolio³⁵, R. Avramidou^{58a}, M.K. Ayoub^{15a}, G. Azuelos^{107,ap}, A.E. Baas^{59a}, M.J. Baca²¹, H. Bachacou¹⁴², K. Bachas^{65a,65b}, M. Backes¹³¹, P. Bagnaia^{70a,70b}, M. Bahmani⁸², H. Bahrasemani¹⁴⁹, A.J. Bailey¹⁷¹, J.T. Baines¹⁴¹, M. Bajic³⁹, C. Bakalis¹⁰, O.K. Baker¹⁸⁰, P.J. Bakker¹¹⁸, D. Bakshi Gupta⁹³, E.M. Baldin^{120b,120a}, P. Balek¹⁷⁷, F. Balli¹⁴², W.K. Balunas¹³³, J. Balz⁹⁷, E. Banas⁸², A. Bandyopadhyay²⁴, S. Banerjee^{178,j}, A.A.E. Bannoura¹⁷⁹, L. Barak¹⁵⁸, W.M. Barbe³⁷, E.L. Barberio¹⁰², D. Barberis^{53b,53a}, M. Barbero⁹⁹, T. Barillari¹¹³, M-S. Barisits³⁵, J. Barkeloo¹²⁷, T. Barklow¹⁵⁰, N. Barlow³¹, R. Barnea¹⁵⁷, S.L. Barnes^{58c}, B.M. Barnett¹⁴¹, R.M. Barnett¹⁸, Z. Barnovska-Blenessy^{58a}, A. Baroncelli^{72a}, G. Barone²⁶, A.J. Barr¹³¹, L. Barranco Navarro¹⁷¹, F. Barreiro⁹⁶, J. Barreiro Guimaraes da Costa^{15a}, R. Bartoldus¹⁵⁰, A.E. Barton⁸⁷, P. Bartos^{28a}, A. Basalaev¹³⁴, A. Bassalat¹²⁸, R.L. Bates⁵⁵, S.J. Batista¹⁶⁴, S. Batlamous^{34e}, J.R. Batley³¹, M. Battaglia¹⁴³, M. Bauce^{70a,70b}, F. Bauer¹⁴², K.T. Bauer¹⁶⁸, H.S. Bawa^{150,1}, J.B. Beacham¹²², T. Beau¹³², P.H. Beauchemin¹⁶⁷, P. Bechtle²⁴, H.C. Beck⁵¹, H.P. Beck^{20,p}, K. Becker⁵⁰, M. Becker⁹⁷, C. Becot⁴⁴, A. Beddall^{12d}, A.J. Beddall^{12a}, V.A. Bednyakov⁷⁷, M. Bedognetti¹¹⁸, C.P. Bee¹⁵², T.A. Beermann³⁵, M. Begalli^{78b}, M. Begel²⁹, A. Behera¹⁵², J.K. Behr⁴⁴, A.S. Bell⁹², G. Bella¹⁵⁸, L. Bellagamba^{23b}, A. Bellerive³³, M. Bellomo¹⁵⁷, P. Bellos⁹, K. Belotskiy¹¹⁰, N.L. Belyaev¹¹⁰, O. Benary^{158,*}, D. Benchekroun^{34a}, M. Bender¹¹², N. Benekos¹⁰, Y. Benhammou¹⁵⁸, E. Benhar Noccioli¹⁸⁰, J. Benitez⁷⁵, D.P. Benjamin⁴⁷, M. Benoit⁵², J.R. Bensinger²⁶, S. Bentvelsen¹¹⁸, L. Beresford¹³¹, M. Beretta⁴⁹, D. Berge⁴⁴, E. Bergeaas Kuutmann¹⁶⁹, N. Berger⁵, L.J. Bergsten²⁶, J. Beringer¹⁸, S. Berlendis⁷, N.R. Bernard¹⁰⁰, G. Bernardi¹³², C. Bernius¹⁵⁰, F.U. Bernlochner²⁴, T. Berry⁹¹, P. Berta⁹⁷, C. Bertella^{15a}, G. Bertoli^{43a,43b}, I.A. Bertram⁸⁷, G.J. Besjes³⁹, O. Bessidskaia Bylund¹⁷⁹, M. Bessner⁴⁴, N. Besson¹⁴², A. Bethani⁹⁸, S. Bethke¹¹³, A. Betti²⁴, A.J. Bevan⁹⁰, J. Beyer¹¹³, R.M.B. Bianchi¹³⁵, O. Biebel¹¹², D. Biedermann¹⁹, R. Bielski³⁵, K. Bierwagen⁹⁷, N.V. Biesuz^{69a,69b}, M. Biglietti^{72a}, T.R.V. Billoud¹⁰⁷, M. Bindi⁵¹, A. Bingul^{12d}, C. Bini^{70a,70b}, S. Biondi^{23b,23a}, M. Birman¹⁷⁷, T. Bisanz⁵¹, J.P. Biswal¹⁵⁸, C. Bittrich⁴⁶,

D.M. Bjergaard⁴⁷, J.E. Black¹⁵⁰, K.M. Black²⁵, T. Blazek^{28a}, I. Bloch⁴⁴, C. Blocker²⁶, A. Blue⁵⁵, U. Blumenschein⁹⁰, Dr. Blunier^{144a}, G.J. Bobbink¹¹⁸, V.S. Bobrovnikov^{120b,120a}, S.S. Bocchetta⁹⁴, A. Bocci⁴⁷, D. Boerner¹⁷⁹, D. Bogavac¹¹², A.G. Bogdanchikov^{120b,120a}, C. Bohm^{43a}, V. Boisvert⁹¹, P. Bokan^{169,w}, T. Bold^{81a}, A.S. Boldyrev¹¹¹, A.E. Bolz^{59b}, M. Bomben¹³², M. Bona⁹⁰, J.S. Bonilla¹²⁷, M. Boonekamp¹⁴², A. Borisov¹⁴⁰, G. Borissov⁸⁷, J. Bortfeldt³⁵, D. Bortolotto¹³¹, V. Bortolotto^{71a,71b}, D. Boscherini^{23b}, M. Bosman¹⁴, J.D. Bossio Sola³⁰, K. Bouaouda^{34a}, J. Boudreau¹³⁵, E.V. Bouhova-Thacker⁸⁷, D. Boumediene³⁷, C. Bourdarios¹²⁸, S.K. Boutle⁵⁵, A. Boveia¹²², J. Boyd³⁵, D. Boye^{32b}, I.R. Boyko⁷⁷, A.J. Bozson⁹¹, J. Bracinik²¹, N. Brahimi⁹⁹, A. Brandt⁸, G. Brandt¹⁷⁹, O. Brandt^{59a}, F. Braren⁴⁴, U. Bratzler¹⁶¹, B. Brau¹⁰⁰, J.E. Brau¹²⁷, W.D. Breaden Madden⁵⁵, K. Brendlinger⁴⁴, L. Brenner⁴⁴, R. Brenner¹⁶⁹, S. Bressler¹⁷⁷, B. Brickwedde⁹⁷, D.L. Briglin²¹, D. Britton⁵⁵, D. Britzger^{59b}, I. Brock²⁴, R. Brock¹⁰⁴, G. Brooijmans³⁸, T. Brooks⁹¹, W.K. Brooks^{144b}, E. Brost¹¹⁹, J.H. Broughton²¹, P.A. Bruckman de Renstrom⁸², D. Bruncko^{28b}, A. Bruni^{23b}, G. Bruni^{23b}, L.S. Bruni¹¹⁸, S. Bruno^{71a,71b}, B.H. Brunt³¹, M. Bruschi^{23b}, N. Bruscino¹³⁵, P. Bryant³⁶, L. Bryngemark⁴⁴, T. Buanes¹⁷, Q. Buat³⁵, P. Buchholz¹⁴⁸, A.G. Buckley⁵⁵, I.A. Budagov⁷⁷, F. Buehrer⁵⁰, M.K. Bugge¹³⁰, O. Bulekov¹¹⁰, D. Bullock⁸, T.J. Burch¹¹⁹, S. Burdin⁸⁸, C.D. Burgard¹¹⁸, A.M. Burger⁵, B. Burghgrave¹¹⁹, K. Burka⁸², S. Burke¹⁴¹, I. Burmeister⁴⁵, J.T.P. Burr¹³¹, D. Büscher⁵⁰, V. Büscher⁹⁷, E. Buschmann⁵¹, P. Bussey⁵⁵, J.M. Butler²⁵, C.M. Buttar⁵⁵, J.M. Butterworth⁹², P. Butti³⁵, W. Buttinger³⁵, A. Buzatu¹⁵⁵, A.R. Buzykaev^{120b,120a}, G. Cabras^{23b,23a}, S. Cabrera Urbán¹⁷¹, D. Caforio¹³⁸, H. Cat¹⁷⁰, V.M.M. Cairo², O. Cakir^{4a}, N. Calace⁵², P. Calafiura¹⁸, A. Calandri⁹⁹, G. Calderini¹³², P. Calfayan⁶³, G. Callea^{40b,40a}, L.P. Caloba^{78b}, S. Calvente Lopez⁹⁶, D. Calvet³⁷, S. Calvet³⁷, T.P. Calvet¹⁵², M. Calvetti^{69a,69b}, R. Camacho Toro¹³², S. Camarda³⁵, P. Camarri^{71a,71b}, D. Cameron¹³⁰, R. Caminal Armadans¹⁰⁰, C. Camincher³⁵, S. Campana³⁵, M. Campanelli⁹², A. Camplani³⁹, A. Campoverde¹⁴⁸, V. Canale^{67a,67b}, M. Cano Bret^{58c}, J. Cantero¹²⁵, T. Cao¹⁵⁸, Y. Cao¹⁷⁰, M.D.M. Capeans Garrido³⁵, I. Caprini^{27b}, M. Caprini^{27b}, M. Capua^{40b,40a}, R.M. Carbone³⁸, R. Cardarelli^{71a}, F.C. Cardillo¹⁴⁶, I. Carli¹³⁹, T. Carli³⁵, G. Carlino^{67a}, B.T. Carlson¹³⁵, L. Carminati^{66a,66b}, R.M.D. Carney^{43a,43b}, S. Caron¹¹⁷, E. Carquin^{144b}, S. Carrá^{66a,66b}, G.D. Carrillo-Montoya³⁵, D. Casadei^{32b}, M.P. Casado^{14,f}, A.F. Casha¹⁶⁴, D.W. Casper¹⁶⁸, R. Castelijn¹¹⁸, F.L. Castillo¹⁷¹, V. Castillo Gimenez¹⁷¹, N.F. Castro^{136a,136e}, A. Catinaccio³⁵, J.R. Catmore¹³⁰, A. Cattai³⁵, J. Caudron²⁴, V. Cavalieri²⁹, E. Cavallaro¹⁴, D. Cavalli^{66a}, M. Cavalli-Sforza¹⁴, V. Cavasinni^{69a,69b}, E. Celebi^{12b}, F. Ceradini^{72a,72b}, L. Cerdá Alberich¹⁷¹, A.S. Cerqueira^{78a}, A. Cerri¹⁵³, L. Cerrito^{71a,71b}, F. Cerutti¹⁸, A. Cervelli^{23b,23a}, S.A. Cetin^{12b}, A. Chafaq^{34a}, D. Chakraborty¹¹⁹, S.K. Chan⁵⁷, W.S. Chan¹¹⁸, Y.L. Chan^{61a}, J.D. Chapman³¹, B. Chargeishvili^{156b}, D.G. Charlton²¹, C.C. Chau³³, C.A. Chavez Barajas¹⁵³, S. Che¹²², A. Chegwidden¹⁰⁴, S. Chekanov⁶, S.V. Chekulaev^{165a}, G.A. Chelkov^{77,ao}, M.A. Chelstowska³⁵, C. Chen^{58a}, C.H. Chen⁷⁶, H. Chen²⁹, J. Chen^{58a}, J. Chen³⁸, S. Chen¹³³, S.J. Chen^{15b}, X. Chen^{15c,an}, Y. Chen⁸⁰, Y-H. Chen⁴⁴, H.C. Cheng¹⁰³, H.J. Cheng^{15d}, A. Cheplakov⁷⁷, E. Cheremushkina¹⁴⁰, R. Cherkaoui El Moursli^{34e}, E. Cheu⁷, K. Cheung⁶², L. Chevalier¹⁴², V. Chiarella⁴⁹, G. Chiarelli^{69a}, G. Chiodini^{65a}, A.S. Chisholm³⁵, A. Chitan^{27b}, I. Chiu¹⁶⁰, Y.H. Chiu¹⁷³, M.V. Chizhov⁷⁷, K. Choi⁶³, A.R. Chomont¹²⁸, S. Chouridou¹⁵⁹, Y.S. Chow¹¹⁸, V. Christodoulou⁹², M.C. Chu^{61a}, J. Chudoba¹³⁷, A.J. Chuinard¹⁰¹, J.J. Chwastowski⁸², L. Chytka¹²⁶, D. Cinca⁴⁵, V. Cindro⁸⁹, I.A. Cioara²⁴, A. Ciocio¹⁸, F. Cirotto^{67a,67b}, Z.H. Citron¹⁷⁷, M. Citterio^{66a}, A. Clark⁵², M.R. Clark³⁸, P.J. Clark⁴⁸, C. Clement^{43a,43b}, Y. Coadou⁹⁹, M. Cobal^{64a,64c}, A. Coccaro^{53b,53a}, J. Cochran⁷⁶, H. Cohen¹⁵⁸, A.E.C. Coimbra¹⁷⁷, L. Colasurdo¹¹⁷, B. Cole³⁸, A.P. Colijn¹¹⁸, J. Collot⁵⁶, P. Conde Muñoz^{136a,136b}, E. Coniavitis⁵⁰, S.H. Connell^{32b}, I.A. Connelly⁹⁸, S. Constantinescu^{27b}, F. Conventi^{67a,aq}, A.M. Cooper-Sarkar¹³¹, F. Cormier¹⁷², K.J.R. Cormier¹⁶⁴, M. Corradi^{70a,70b}, E.E. Corrigan⁹⁴, F. Corriveau^{101,ab}, A. Cortes-Gonzalez³⁵, M.J. Costa¹⁷¹, D. Costanzo¹⁴⁶, G. Cottin³¹, G. Cowan⁹¹, B.E. Cox⁹⁸, J. Crane⁹⁸, K. Cranmer¹²¹, S.J. Crawley⁵⁵, R.A. Creager¹³³, G. Cree³³, S. Crépé-Renaudin⁵⁶, F. Crescioli¹³²,

M. Cristinziani²⁴, V. Croft¹²¹, G. Crosetti^{40b,40a}, A. Cueto⁹⁶, T. Cuhadar Donszelmann¹⁴⁶,
 A.R. Cukierman¹⁵⁰, J. Cúth⁹⁷, S. Czekierda⁸², P. Czodrowski³⁵,
 M.J. Da Cunha Sargedas De Sousa^{58b,136b}, C. Da Via⁹⁸, W. Dabrowski^{81a}, T. Dado^{28a,w}, S. Dahbi^{34e},
 T. Dai¹⁰³, F. Dallaire¹⁰⁷, C. Dallapiccola¹⁰⁰, M. Dam³⁹, G. D'amen^{23b,23a}, J. Damp⁹⁷, J.R. Dandoy¹³³,
 M.F. Daneri³⁰, N.P. Dang^{178,j}, N.D Dann⁹⁸, M. Danninger¹⁷², V. Dao³⁵, G. Darbo^{53b}, S. Darmora⁸,
 O. Dartsi⁵, A. Dattagupta¹²⁷, T. Daubney⁴⁴, S. D'Auria⁵⁵, W. Davey²⁴, C. David⁴⁴, T. Davidek¹³⁹,
 D.R. Davis⁴⁷, E. Dawe¹⁰², I. Dawson¹⁴⁶, K. De⁸, R. De Asmundis^{67a}, A. De Benedetti¹²⁴,
 M. De Beurs¹¹⁸, S. De Castro^{23b,23a}, S. De Cecco^{70a,70b}, N. De Groot¹¹⁷, P. de Jong¹¹⁸, H. De la Torre¹⁰⁴,
 F. De Lorenzi⁷⁶, A. De Maria^{51,r}, D. De Pedis^{70a}, A. De Salvo^{70a}, U. De Sanctis^{71a,71b},
 M. De Santis^{71a,71b}, A. De Santo¹⁵³, K. De Vasconcelos Corga⁹⁹, J.B. De Vivie De Regie¹²⁸,
 C. Debenedetti¹⁴³, D.V. Dedovich⁷⁷, N. Dehghanian³, M. Del Gaudio^{40b,40a}, J. Del Peso⁹⁶,
 Y. Delabat Diaz⁴⁴, D. Delgove¹²⁸, F. Deliot¹⁴², C.M. Delitzsch⁷, M. Della Pietra^{67a,67b}, D. Della Volpe⁵²,
 A. Dell'Acqua³⁵, L. Dell'Asta²⁵, M. Delmastro⁵, C. Delporte¹²⁸, P.A. Delsart⁵⁶, D.A. DeMarco¹⁶⁴,
 S. Demers¹⁸⁰, M. Demichev⁷⁷, S.P. Denisov¹⁴⁰, D. Denysiuk¹¹⁸, L. D'Eramo¹³², D. Derendarz⁸²,
 J.E. Derkaoui^{34d}, F. Derue¹³², P. Dervan⁸⁸, K. Desch²⁴, C. Deterre⁴⁴, K. Dette¹⁶⁴, M.R. Devesa³⁰,
 P.O. Deviveiros³⁵, A. Dewhurst¹⁴¹, S. Dhaliwal²⁶, F.A. Di Bello⁵², A. Di Ciaccio^{71a,71b}, L. Di Ciaccio⁵,
 W.K. Di Clemente¹³³, C. Di Donato^{67a,67b}, A. Di Girolamo³⁵, B. Di Micco^{72a,72b}, R. Di Nardo¹⁰⁰,
 K.F. Di Petrillo⁵⁷, R. Di Sipio¹⁶⁴, D. Di Valentino³³, C. Diaconu⁹⁹, M. Diamond¹⁶⁴, F.A. Dias³⁹,
 T. Dias Do Vale^{136a}, M.A. Diaz^{144a}, J. Dickinson¹⁸, E.B. Diehl¹⁰³, J. Dietrich¹⁹, S. Díez Cornell⁴⁴,
 A. Dimitrievska¹⁸, J. Dingfelder²⁴, F. Dittus³⁵, F. Djama⁹⁹, T. Djobava^{156b}, J.I. Djuvsland^{59a},
 M.A.B. Do Vale^{78c}, M. Dobre^{27b}, D. Dodsworth²⁶, C. Doglioni⁹⁴, J. Dolejsi¹³⁹, Z. Dolezal¹³⁹,
 M. Donadelli^{78d}, J. Donini³⁷, A. D'onofrio⁹⁰, M. D'Onofrio⁸⁸, J. Dopke¹⁴¹, A. Doria^{67a}, M.T. Dova⁸⁶,
 A.T. Doyle⁵⁵, E. Drechsler⁵¹, E. Dreyer¹⁴⁹, T. Dreyer⁵¹, Y. Du^{58b}, J. Duarte-Campderros¹⁵⁸,
 F. Dubinin¹⁰⁸, M. Dubovsky^{28a}, A. Dubreuil⁵², E. Duchovni¹⁷⁷, G. Duckeck¹¹², A. Ducourthial¹³²,
 O.A. Ducu^{107,v}, D. Duda¹¹³, A. Dudarev³⁵, A.C. Dudder⁹⁷, E.M. Duffield¹⁸, L. Duflot¹²⁸,
 M. Dührssen³⁵, C. Dülsen¹⁷⁹, M. Dumancic¹⁷⁷, A.E. Dumitriu^{27b,d}, A.K. Duncan⁵⁵, M. Dunford^{59a},
 A. Duperrin⁹⁹, H. Duran Yildiz^{4a}, M. Düren⁵⁴, A. Durglishvili^{156b}, D. Duschinger⁴⁶, B. Dutta⁴⁴,
 D. Duvnjak¹, M. Dyndal⁴⁴, S. Dysch⁹⁸, B.S. Dziedzic⁸², C. Eckardt⁴⁴, K.M. Ecker¹¹³, R.C. Edgar¹⁰³,
 T. Eifert³⁵, G. Eigen¹⁷, K. Einsweiler¹⁸, T. Ekelof¹⁶⁹, M. El Kacimi^{34c}, R. El Kosseifi⁹⁹, V. Ellajosyula⁹⁹,
 M. Ellert¹⁶⁹, F. Ellinghaus¹⁷⁹, A.A. Elliot⁹⁰, N. Ellis³⁵, J. Elmsheuser²⁹, M. Elsing³⁵, D. Emeliyanov¹⁴¹,
 Y. Enari¹⁶⁰, J.S. Ennis¹⁷⁵, M.B. Epland⁴⁷, J. Erdmann⁴⁵, A. Ereditato²⁰, S. Errede¹⁷⁰, M. Escalier¹²⁸,
 C. Escobar¹⁷¹, O. Estrada Pastor¹⁷¹, A.I. Etienne¹⁴², E. Etzion¹⁵⁸, H. Evans⁶³, A. Ezhilov¹³⁴,
 M. Ezzi^{34e}, F. Fabbri⁵⁵, L. Fabbri^{23b,23a}, V. Fabiani¹¹⁷, G. Facini⁹², R.M. Faisca Rodrigues Pereira^{136a},
 R.M. Fakhrutdinov¹⁴⁰, S. Falciano^{70a}, P.J. Falke⁵, S. Falke⁵, J. Faltova¹³⁹, Y. Fang^{15a}, M. Fanti^{66a,66b},
 A. Farbin⁸, A. Farilla^{72a}, E.M. Farina^{68a,68b}, T. Farooque¹⁰⁴, S. Farrell¹⁸, S.M. Farrington¹⁷⁵,
 P. Farthouat³⁵, F. Fassi^{34e}, P. Fassnacht³⁵, D. Fassouliotis⁹, M. Fucci Giannelli⁴⁸, A. Favareto^{53b,53a},
 W.J. Fawcett³¹, L. Fayard¹²⁸, O.L. Fedin^{134,o}, W. Fedorko¹⁷², M. Feickert⁴¹, S. Feigl¹³⁰, L. Feligioni⁹⁹,
 C. Feng^{58b}, E.J. Feng³⁵, M. Feng⁴⁷, M.J. Fenton⁵⁵, A.B. Fenyuk¹⁴⁰, L. Feremenga⁸, J. Ferrando⁴⁴,
 A. Ferrari¹⁶⁹, P. Ferrari¹¹⁸, R. Ferrari^{68a}, D.E. Ferreira de Lima^{59b}, A. Ferrer¹⁷¹, D. Ferrere⁵²,
 C. Ferretti¹⁰³, F. Fiedler⁹⁷, A. Filipčič⁸⁹, F. Filthaut¹¹⁷, K.D. Finelli²⁵, M.C.N. Fiolhais^{136a,136c,a},
 L. Fiorini¹⁷¹, C. Fischer¹⁴, W.C. Fisher¹⁰⁴, N. Flaschel⁴⁴, I. Fleck¹⁴⁸, P. Fleischmann¹⁰³,
 R.R.M. Fletcher¹³³, T. Flick¹⁷⁹, B.M. Flierl¹¹², L.M. Flores¹³³, L.R. Flores Castillo^{61a},
 F.M. Follega^{73a,73b}, N. Fomin¹⁷, G.T. Forcolin⁹⁸, A. Formica¹⁴², F.A. Förster¹⁴, A.C. Forti⁹⁸,
 A.G. Foster²¹, D. Fournier¹²⁸, H. Fox⁸⁷, S. Fracchia¹⁴⁶, P. Francavilla^{69a,69b}, M. Franchini^{23b,23a},
 S. Franchino^{59a}, D. Francis³⁵, L. Franconi¹³⁰, M. Franklin⁵⁷, M. Frate¹⁶⁸, M. Fraternali^{68a,68b},
 A.N. Fray⁹⁰, D. Freeborn⁹², S.M. Fressard-Batraneanu³⁵, B. Freund¹⁰⁷, W.S. Freund^{78b}, D.C. Frizzell¹²⁴,
 D. Froidevaux³⁵, J.A. Frost¹³¹, C. Fukunaga¹⁶¹, E. Fullana Torregrosa¹⁷¹, T. Fusayasu¹¹⁴, J. Fuster¹⁷¹,

O. Gabizon¹⁵⁷, A. Gabrielli^{23b,23a}, A. Gabrielli¹⁸, G.P. Gach^{81a}, S. Gadatsch⁵², P. Gadow¹¹³,
 G. Gagliardi^{53b,53a}, L.G. Gagnon¹⁰⁷, C. Galea^{27b}, B. Galhardo^{136a,136c}, E.J. Gallas¹³¹, B.J. Gallop¹⁴¹,
 P. Gallus¹³⁸, G. Galster³⁹, R. Gamboa Goni⁹⁰, K.K. Gan¹²², S. Ganguly¹⁷⁷, J. Gao^{58a}, Y. Gao⁸⁸,
 Y.S. Gao^{150,1}, C. García¹⁷¹, J.E. García Navarro¹⁷¹, J.A. García Pascual^{15a}, M. Garcia-Sciveres¹⁸,
 R.W. Gardner³⁶, N. Garelli¹⁵⁰, V. Garonne¹³⁰, K. Gasnikova⁴⁴, A. Gaudiello^{53b,53a}, G. Gaudio^{68a},
 I.L. Gavrilenko¹⁰⁸, A. Gavrilyuk¹⁰⁹, C. Gay¹⁷², G. Gaycken²⁴, E.N. Gazis¹⁰, C.N.P. Gee¹⁴¹, J. Geisen⁵¹,
 M. Geisen⁹⁷, M.P. Geisler^{59a}, K. Gellerstedt^{43a,43b}, C. Gemme^{53b}, M.H. Genest⁵⁶, C. Geng¹⁰³,
 S. Gentile^{70a,70b}, S. George⁹¹, D. Gerbaudo¹⁴, G. Gessner⁴⁵, S. Ghasemi¹⁴⁸, M. Ghasemi Bostanabad¹⁷³,
 M. Ghneimat²⁴, B. Giacobbe^{23b}, S. Giagu^{70a,70b}, N. Giangiacomi^{23b,23a}, P. Giannetti^{69a},
 A. Giannini^{67a,67b}, S.M. Gibson⁹¹, M. Gignac¹⁴³, D. Gillberg³³, G. Gilles¹⁷⁹, D.M. Gingrich^{3,ap},
 M.P. Giordani^{64a,64c}, F.M. Giorgi^{23b}, P.F. Giraud¹⁴², P. Giromini⁵⁷, G. Giugliarelli^{64a,64c}, D. Giugni^{66a},
 F. Giuli¹³¹, M. Giulini^{59b}, S. Gkaitatzis¹⁵⁹, I. Gkialas^{9,i}, E.L. Gkougkousis¹⁴, P. Gkountoumis¹⁰,
 L.K. Gladilin¹¹¹, C. Glasman⁹⁶, J. Glatzer¹⁴, P.C.F. Glaysher⁴⁴, A. Glazov⁴⁴, M. Goblirsch-Kolb²⁶,
 J. Godlewski⁸², S. Goldfarb¹⁰², T. Golling⁵², D. Golubkov¹⁴⁰, A. Gomes^{136a,136b,136d},
 R. Goncalves Gama^{78a}, R. Gonçalo^{136a}, G. Gonella⁵⁰, L. Gonella²¹, A. Gongadze⁷⁷, F. Gonnella²¹,
 J.L. Gonski⁵⁷, S. González de la Hoz¹⁷¹, S. Gonzalez-Sevilla⁵², L. Goossens³⁵, P.A. Gorbounov¹⁰⁹,
 H.A. Gordon²⁹, B. Gorini³⁵, E. Gorini^{65a,65b}, A. Gorišek⁸⁹, A.T. Goshaw⁴⁷, C. Gössling⁴⁵,
 M.I. Gostkin⁷⁷, C.A. Gottardo²⁴, C.R. Goudet¹²⁸, D. Goujdami^{34c}, A.G. Goussiou¹⁴⁵, N. Govender^{32b,b},
 C. Goy⁵, E. Gozani¹⁵⁷, I. Grabowska-Bold^{81a}, P.O.J. Gradin¹⁶⁹, E.C. Graham⁸⁸, J. Gramling¹⁶⁸,
 E. Gramstad¹³⁰, S. Grancagnolo¹⁹, V. Gratchev¹³⁴, P.M. Gravila^{27f}, F.G. Gravili^{65a,65b}, C. Gray⁵⁵,
 H.M. Gray¹⁸, Z.D. Greenwood^{93,ag}, C. Grefe²⁴, K. Gregersen⁹⁴, I.M. Gregor⁴⁴, P. Grenier¹⁵⁰,
 K. Grevtsov⁴⁴, N.A. Grieser¹²⁴, J. Griffiths⁸, A.A. Grillo¹⁴³, K. Grimm¹⁵⁰, S. Grinstein^{14,x}, Ph. Gris³⁷,
 J.-F. Grivaz¹²⁸, S. Groh⁹⁷, E. Gross¹⁷⁷, J. Grosse-Knetter⁵¹, G.C. Grossi⁹³, Z.J. Grout⁹², C. Grud¹⁰³,
 A. Grummer¹¹⁶, L. Guan¹⁰³, W. Guan¹⁷⁸, J. Guenther³⁵, A. Guerguichon¹²⁸, F. Guescini^{165a},
 D. Guest¹⁶⁸, R. Gugel⁵⁰, B. Gui¹²², T. Guillemin⁵, S. Guindon³⁵, U. Gul⁵⁵, C. Gumpert³⁵, J. Guo^{58c},
 W. Guo¹⁰³, Y. Guo^{58a,q}, Z. Guo⁹⁹, R. Gupta⁴¹, S. Gurbuz^{12c}, G. Gustavino¹²⁴, B.J. Gutelman¹⁵⁷,
 P. Gutierrez¹²⁴, C. Gutschow⁹², C. Guyot¹⁴², M.P. Guzik^{81a}, C. Gwenlan¹³¹, C.B. Gwilliam⁸⁸,
 A. Haas¹²¹, C. Haber¹⁸, H.K. Hadavand⁸, N. Haddad^{34e}, A. Hadef^{58a}, S. Hageböck²⁴, M. Hagihara¹⁶⁶,
 H. Hakobyan^{181,*}, M. Haleem¹⁷⁴, J. Haley¹²⁵, G. Halladjian¹⁰⁴, G.D. Hallewell⁹⁹, K. Hamacher¹⁷⁹,
 P. Hamal¹²⁶, K. Hamano¹⁷³, A. Hamilton^{32a}, G.N. Hamity¹⁴⁶, K. Han^{58a,af}, L. Han^{58a}, S. Han^{15d},
 K. Hanagaki^{79,t}, M. Hance¹⁴³, D.M. Handl¹¹², B. Haney¹³³, R. Hankache¹³², P. Hanke^{59a}, E. Hansen⁹⁴,
 J.B. Hansen³⁹, J.D. Hansen³⁹, M.C. Hansen²⁴, P.H. Hansen³⁹, K. Hara¹⁶⁶, A.S. Hard¹⁷⁸, T. Harenberg¹⁷⁹,
 S. Harkusha¹⁰⁵, P.F. Harrison¹⁷⁵, N.M. Hartmann¹¹², Y. Hasegawa¹⁴⁷, A. Hasib⁴⁸, S. Hassani¹⁴²,
 S. Haug²⁰, R. Hauser¹⁰⁴, L. Hauswald⁴⁶, L.B. Havener³⁸, M. Havranek¹³⁸, C.M. Hawkes²¹,
 R.J. Hawkings³⁵, D. Hayden¹⁰⁴, C. Hayes¹⁵², C.P. Hays¹³¹, J.M. Hays⁹⁰, H.S. Hayward⁸⁸,
 S.J. Haywood¹⁴¹, M.P. Heath⁴⁸, V. Hedberg⁹⁴, L. Heelan⁸, S. Heer²⁴, K.K. Heidegger⁵⁰, J. Heilman³³,
 S. Heim⁴⁴, T. Heim¹⁸, B. Heinemann^{44,ak}, J.J. Heinrich¹¹², L. Heinrich¹²¹, C. Heinz⁵⁴, J. Hejbal¹³⁷,
 L. Helary³⁵, A. Held¹⁷², S. Hellesund¹³⁰, S. Hellman^{43a,43b}, C. Helsens³⁵, R.C.W. Henderson⁸⁷,
 Y. Heng¹⁷⁸, S. Henkelmann¹⁷², A.M. Henriques Correia³⁵, G.H. Herbert¹⁹, H. Herde²⁶, V. Herget¹⁷⁴,
 Y. Hernández Jiménez^{32c}, H. Herr⁹⁷, M.G. Herrmann¹¹², G. Herten⁵⁰, R. Hertenberger¹¹², L. Hervas³⁵,
 T.C. Herwig¹³³, G.G. Hesketh⁹², N.P. Hessey^{165a}, J.W. Hetherly⁴¹, S. Higashino⁷⁹,
 E. Higón-Rodríguez¹⁷¹, K. Hildebrand³⁶, E. Hill¹⁷³, J.C. Hill³¹, K.K. Hill²⁹, K.H. Hiller⁴⁴, S.J. Hillier²¹,
 M. Hils⁴⁶, I. Hinchliffe¹⁸, M. Hirose¹²⁹, D. Hirschbuehl¹⁷⁹, B. Hiti⁸⁹, O. Hladík¹³⁷, D.R. Hlaluku^{32c},
 X. Hoad⁴⁸, J. Hobbs¹⁵², N. Hod^{165a}, M.C. Hodgkinson¹⁴⁶, A. Hoecker³⁵, M.R. Hoeferkamp¹¹⁶,
 F. Hoenig¹¹², D. Hohn²⁴, D. Hohov¹²⁸, T.R. Holmes³⁶, M. Holzbock¹¹², M. Homann⁴⁵, S. Honda¹⁶⁶,
 T. Honda⁷⁹, T.M. Hong¹³⁵, A. Hönlle¹¹³, B.H. Hooberman¹⁷⁰, W.H. Hopkins¹²⁷, Y. Horii¹¹⁵, P. Horn⁴⁶,
 A.J. Horton¹⁴⁹, L.A. Horyn³⁶, J-Y. Hostachy⁵⁶, A. Hostiuc¹⁴⁵, S. Hou¹⁵⁵, A. Hoummada^{34a},

J. Howarth⁹⁸, J. Hoya⁸⁶, M. Hrabovsky¹²⁶, J. Hrdinka³⁵, I. Hristova¹⁹, J. Hrvnac¹²⁸, A. Hrynevich¹⁰⁶, T. Hrynová⁵, P.J. Hsu⁶², S.-C. Hsu¹⁴⁵, Q. Hu²⁹, S. Hu^{58c}, Y. Huang^{15a}, Z. Hubacek¹³⁸, F. Hubaut⁹⁹, M. Huebner²⁴, F. Huegging²⁴, T.B. Huffman¹³¹, E.W. Hughes³⁸, M. Huhtinen³⁵, R.F.H. Hunter³³, P. Huo¹⁵², A.M. Hupe³³, N. Huseynov^{77,ad}, J. Huston¹⁰⁴, J. Huth⁵⁷, R. Hyneman¹⁰³, G. Iacobucci⁵², G. Iakovidis²⁹, I. Ibragimov¹⁴⁸, L. Iconomidou-Fayard¹²⁸, Z. Idrissi^{34e}, P. Iengo³⁵, R. Ignazzi³⁹, O. Igonkina^{118,z}, R. Iguchi¹⁶⁰, T. Iizawa⁵², Y. Ikegami⁷⁹, M. Ikeno⁷⁹, D. Iliadis¹⁵⁹, N. Illic¹⁵⁰, F. Iltzsche⁴⁶, G. Introzzi^{68a,68b}, M. Iodice^{72a}, K. Iordanidou³⁸, V. Ippolito^{70a,70b}, M.F. Isaacson¹⁶⁹, N. Ishijima¹²⁹, M. Ishino¹⁶⁰, M. Ishitsuka¹⁶², W. Islam¹²⁵, C. Issever¹³¹, S. Istin¹⁵⁷, F. Ito¹⁶⁶, J.M. Iturbe Ponce^{61a}, R. Iuppa^{73a,73b}, A. Ivina¹⁷⁷, H. Iwasaki⁷⁹, J.M. Izen⁴², V. Izzo^{67a}, P. Jacka¹³⁷, P. Jackson¹, R.M. Jacobs²⁴, V. Jain², G. Jäkel¹⁷⁹, K.B. Jakobi⁹⁷, K. Jakobs⁵⁰, S. Jakobsen⁷⁴, T. Jakoubek¹³⁷, D.O. Jamin¹²⁵, D.K. Jana⁹³, R. Jansky⁵², J. Janssen²⁴, M. Janus⁵¹, P.A. Janus^{81a}, G. Jarlskog⁹⁴, N. Javadov^{77,ad}, T. Javůrek³⁵, M. Javurkova⁵⁰, F. Jeanneau¹⁴², L. Jeanty¹⁸, J. Jejelava^{156a,ae}, A. Jelinskas¹⁷⁵, P. Jenni^{50,c}, J. Jeong⁴⁴, S. Jézéquel⁵, H. Ji¹⁷⁸, J. Jia¹⁵², H. Jiang⁷⁶, Y. Jiang^{58a}, Z. Jiang¹⁵⁰, S. Jiggins⁵⁰, F.A. Jimenez Morales³⁷, J. Jimenez Pena¹⁷¹, S. Jin^{15b}, A. Jinaru^{27b}, O. Jinnouchi¹⁶², H. Jivan^{32c}, P. Johansson¹⁴⁶, K.A. Johns⁷, C.A. Johnson⁶³, W.J. Johnson¹⁴⁵, K. Jon-And^{43a,43b}, R.W.L. Jones⁸⁷, S.D. Jones¹⁵³, S. Jones⁷, T.J. Jones⁸⁸, J. Jongmanns^{59a}, P.M. Jorge^{136a,136b}, J. Jovicevic^{165a}, X. Ju¹⁸, J.J. Junggeburth¹¹³, A. Juste Rozas^{14,x}, A. Kaczmarska⁸², M. Kado¹²⁸, H. Kagan¹²², M. Kagan¹⁵⁰, T. Kaji¹⁷⁶, E. Kajomovitz¹⁵⁷, C.W. Kalderon⁹⁴, A. Kaluza⁹⁷, S. Kama⁴¹, A. Kamenshchikov¹⁴⁰, L. Kanjir⁸⁹, Y. Kano¹⁶⁰, V.A. Kantserov¹¹⁰, J. Kanzaki⁷⁹, B. Kaplan¹²¹, L.S. Kaplan¹⁷⁸, D. Kar^{32c}, M.J. Kareem^{165b}, E. Karentzos¹⁰, S.N. Karpov⁷⁷, Z.M. Karpova⁷⁷, V. Kartvelishvili⁸⁷, A.N. Karyukhin¹⁴⁰, L. Kashif¹⁷⁸, R.D. Kass¹²², A. Kastanas¹⁵¹, Y. Kataoka¹⁶⁰, C. Kato^{58d,58c}, J. Katzy⁴⁴, K. Kawade⁸⁰, K. Kawagoe⁸⁵, T. Kawamoto¹⁶⁰, G. Kawamura⁵¹, E.F. Kay⁸⁸, V.F. Kazanin^{120b,120a}, R. Keeler¹⁷³, R. Kehoe⁴¹, J.S. Keller³³, E. Kellermann⁹⁴, J.J. Kempster²¹, J. Kendrick²¹, O. Kepka¹³⁷, S. Kersten¹⁷⁹, B.P. Kerševan⁸⁹, R.A. Keyes¹⁰¹, M. Khader¹⁷⁰, F. Khalil-Zada¹³, A. Khanov¹²⁵, A.G. Kharlamov^{120b,120a}, T. Kharlamova^{120b,120a}, E.E. Khoda¹⁷², A. Khodinov¹⁶³, T.J. Khoo⁵², E. Khramov⁷⁷, J. Khubua^{156b}, S. Kido⁸⁰, M. Kiehn⁵², C.R. Kilby⁹¹, Y.K. Kim³⁶, N. Kimura^{64a,64c}, O.M. Kind¹⁹, B.T. King⁸⁸, D. Kirchmeier⁴⁶, J. Kirk¹⁴¹, A.E. Kiryunin¹¹³, T. Kishimoto¹⁶⁰, D. Kisielewska^{81a}, V. Kitali⁴⁴, O. Kivernyk⁵, E. Kladiva^{28b}, T. Klapdor-Kleingrothaus⁵⁰, M.H. Klein¹⁰³, M. Klein⁸⁸, U. Klein⁸⁸, K. Kleinknecht⁹⁷, P. Klimek¹¹⁹, A. Klimentov²⁹, R. Klingenberg^{45,*}, T. Klingl²⁴, T. Klioutchnikova³⁵, F.F. Klitzner¹¹², P. Kluit¹¹⁸, S. Kluth¹¹³, E. Kneringer⁷⁴, E.B.F.G. Knoops⁹⁹, A. Knue⁵⁰, A. Kobayashi¹⁶⁰, D. Kobayashi⁸⁵, T. Kobayashi¹⁶⁰, M. Kobel⁴⁶, M. Kocian¹⁵⁰, P. Kodys¹³⁹, P.T. Koenig²⁴, T. Koffman³³, E. Koffeman¹¹⁸, N.M. Köhler¹¹³, T. Koi¹⁵⁰, M. Kolb^{59b}, I. Koletsou⁵, T. Kondo⁷⁹, N. Kondrashova^{58c}, K. Köneke⁵⁰, A.C. König¹¹⁷, T. Kono⁷⁹, R. Konoplich^{121,ah}, V. Konstantinides⁹², N. Konstantinidis⁹², B. Konya⁹⁴, R. Kopeliansky⁶³, S. Koperny^{81a}, K. Korcyl⁸², K. Kordas¹⁵⁹, G. Koren¹⁵⁸, A. Korn⁹², I. Korolkov¹⁴, E.V. Korolkova¹⁴⁶, N. Korotkova¹¹¹, O. Kortner¹¹³, S. Kortner¹¹³, T. Kosek¹³⁹, V.V. Kostyukhin²⁴, A. Kotwal⁴⁷, A. Koulouris¹⁰, A. Kourkoumeli-Charalampidi^{68a,68b}, C. Kourkoumelis⁹, E. Kourlitis¹⁴⁶, V. Kouskoura²⁹, A.B. Kowalewska⁸², R. Kowalewski¹⁷³, T.Z. Kowalski^{81a}, C. Kozakai¹⁶⁰, W. Kozanecki¹⁴², A.S. Kozhin¹⁴⁰, V.A. Kramarenko¹¹¹, G. Kramberger⁸⁹, D. Krasnopal'tsev^{58a}, M.W. Krasny¹³², A. Krasznahorkay³⁵, D. Krauss¹¹³, J.A. Kremer^{81a}, J. Kretzschmar⁸⁸, P. Krieger¹⁶⁴, K. Krizka¹⁸, K. Kroeninger⁴⁵, H. Kroha¹¹³, J. Kroll¹³⁷, J. Kroll¹³³, J. Krstic¹⁶, U. Kruchonak⁷⁷, H. Krüger²⁴, N. Krumnack⁷⁶, M.C. Kruse⁴⁷, T. Kubota¹⁰², S. Kuday^{4b}, J.T. Kuechler¹⁷⁹, S. Kuehn³⁵, A. Kugel^{59a}, F. Kuger¹⁷⁴, T. Kuhl⁴⁴, V. Kukhtin⁷⁷, R. Kukla⁹⁹, Y. Kulchitsky¹⁰⁵, S. Kuleshov^{144b}, Y.P. Kulinich¹⁷⁰, M. Kuna⁵⁶, T. Kunigo⁸³, A. Kupco¹³⁷, T. Kupfer⁴⁵, O. Kuprash¹⁵⁸, H. Kurashige⁸⁰, L.L. Kurchaninov^{165a}, Y.A. Kurochkin¹⁰⁵, M.G. Kurth^{15d}, E.S. Kuwertz³⁵, M. Kuze¹⁶², J. Kvita¹²⁶, T. Kwan¹⁰¹, A. La Rosa¹¹³, J.L. La Rosa Navarro^{78d}, L. La Rotonda^{40b,40a}, F. La Ruffa^{40b,40a}, C. Lacasta¹⁷¹, F. Lacava^{70a,70b}, J. Lacey⁴⁴, D.P.J. Lack⁹⁸, H. Lacker¹⁹, D. Lacour¹³², E. Ladygin⁷⁷,

R. Lafaye⁵, B. Laforge¹³², T. Lagouri^{32c}, S. Lai⁵¹, S. Lammers⁶³, W. Lampl⁷, E. Lançon²⁹,
 U. Landgraf⁵⁰, M.P.J. Landon⁹⁰, M.C. Lanfermann⁵², V.S. Lang⁴⁴, J.C. Lange¹⁴, R.J. Langenberg³⁵,
 A.J. Lankford¹⁶⁸, F. Lanni²⁹, K. Lantzsch²⁴, A. Lanza^{68a}, A. Lapertosa^{53b,53a}, S. Laplace¹³²,
 J.F. Laporte¹⁴², T. Lari^{66a}, F. Lasagni Manghi^{23b,23a}, M. Lassnig³⁵, T.S. Lau^{61a}, A. Laudrain¹²⁸,
 M. Lavorgna^{67a,67b}, A.T. Law¹⁴³, P. Laycock⁸⁸, M. Lazzaroni^{66a,66b}, B. Le¹⁰², O. Le Dertz¹³²,
 E. Le Guirriec⁹⁹, E.P. Le Quilleuc¹⁴², M. LeBlanc⁷, T. LeCompte⁶, F. Ledroit-Guillon⁵⁶, C.A. Lee²⁹,
 G.R. Lee^{144a}, L. Lee⁵⁷, S.C. Lee¹⁵⁵, B. Lefebvre¹⁰¹, M. Lefebvre¹⁷³, F. Legger¹¹², C. Leggett¹⁸,
 K. Lehmann¹⁴⁹, N. Lehmann¹⁷⁹, G. Lehmann Miotto³⁵, W.A. Leight⁴⁴, A. Leisos^{159,u}, M.A.L. Leite^{78d},
 R. Leitner¹³⁹, D. Lellouch¹⁷⁷, B. Lemmer⁵¹, K.J.C. Leney⁹², T. Lenz²⁴, B. Lenzi³⁵, R. Leone⁷,
 S. Leone^{69a}, C. Leonidopoulos⁴⁸, G. Lerner¹⁵³, C. Leroy¹⁰⁷, R. Les¹⁶⁴, A.A.J. Lesage¹⁴², C.G. Lester³¹,
 M. Levchenko¹³⁴, J. Levêque⁵, D. Levin¹⁰³, L.J. Levinson¹⁷⁷, D. Lewis⁹⁰, B. Li¹⁰³, C-Q. Li^{58a}, H. Li^{58b},
 L. Li^{58c}, Q. Li^{15d}, Q.Y. Li^{58a}, S. Li^{58d,58c}, X. Li^{58c}, Y. Li¹⁴⁸, Z. Liang^{15a}, B. Liberti^{71a}, A. Liblong¹⁶⁴,
 K. Lie^{61c}, S. Liem¹¹⁸, A. Limosani¹⁵⁴, C.Y. Lin³¹, K. Lin¹⁰⁴, T.H. Lin⁹⁷, R.A. Linck⁶³, J.H. Lindon²¹,
 B.E. Lindquist¹⁵², A.L. Lioni⁵², E. Lipeles¹³³, A. Lipniacka¹⁷, M. Lisovyi^{59b}, T.M. Liss^{170,am},
 A. Lister¹⁷², A.M. Litke¹⁴³, J.D. Little⁸, B. Liu⁷⁶, B.L. Liu⁶, H.B. Liu²⁹, H. Liu¹⁰³, J.B. Liu^{58a},
 J.K.K. Liu¹³¹, K. Liu¹³², M. Liu^{58a}, P. Liu¹⁸, Y. Liu^{15a}, Y.L. Liu^{58a}, Y.W. Liu^{58a}, M. Livan^{68a,68b},
 A. Lleres⁵⁶, J. Llorente Merino^{15a}, S.L. Lloyd⁹⁰, C.Y. Lo^{61b}, F. Lo Sterzo⁴¹, E.M. Lobodzinska⁴⁴,
 P. Loch⁷, A. Loesle⁵⁰, T. Lohse¹⁹, K. Lohwasser¹⁴⁶, M. Lokajicek¹³⁷, B.A. Long²⁵, J.D. Long¹⁷⁰,
 R.E. Long⁸⁷, L. Longo^{65a,65b}, K.A.Looper¹²², J.A. Lopez^{144b}, I. Lopez Paz¹⁴, A. Lopez Solis¹⁴⁶,
 J. Lorenz¹¹², N. Lorenzo Martinez⁵, M. Losada²², P.J. Lösel¹¹², X. Lou⁴⁴, X. Lou^{15a}, A. Lounis¹²⁸,
 J. Love⁶, P.A. Love⁸⁷, J.J. Lozano Bahilo¹⁷¹, H. Lu^{61a}, M. Lu^{58a}, N. Lu¹⁰³, Y.J. Lu⁶², H.J. Lubatti¹⁴⁵,
 C. Luci^{70a,70b}, A. Lucotte⁵⁶, C. Luedtke⁵⁰, F. Luehring⁶³, I. Luise¹³², L. Luminari^{70a}, B. Lund-Jensen¹⁵¹,
 M.S. Lutz¹⁰⁰, P.M. Luzi¹³², D. Lynn²⁹, R. Lysak¹³⁷, E. Lytken⁹⁴, F. Lyu^{15a}, V. Lyubushkin⁷⁷, H. Ma²⁹,
 L.L. Ma^{58b}, Y. Ma^{58b}, G. Maccarrone⁴⁹, A. Macchiolo¹¹³, C.M. Macdonald¹⁴⁶,
 J. Machado Miguens^{133,136b}, D. Madaffari¹⁷¹, R. Madar³⁷, W.F. Mader⁴⁶, A. Madsen⁴⁴, N. Madysa⁴⁶,
 J. Maeda⁸⁰, K. Maekawa¹⁶⁰, S. Maeland¹⁷, T. Maeno²⁹, A.S. Maevskiy¹¹¹, V. Magerl⁵⁰,
 C. Maidantchik^{78b}, T. Maier¹¹², A. Maio^{136a,136b,136d}, O. Majersky^{28a}, S. Majewski¹²⁷, Y. Makida⁷⁹,
 N. Makovec¹²⁸, B. Malaescu¹³², Pa. Malecki⁸², V.P. Maleev¹³⁴, F. Malek⁵⁶, U. Mallik⁷⁵, D. Malon⁶,
 C. Malone³¹, S. Maltezos¹⁰, S. Malyukov³⁵, J. Mamuzic¹⁷¹, G. Mancini⁴⁹, I. Mandic⁸⁹, J. Maneira^{136a},
 L. Manhaes de Andrade Filho^{78a}, J. Manjarres Ramos⁴⁶, K.H. Mankinen⁹⁴, A. Mann¹¹², A. Manousos⁷⁴,
 B. Mansoulie¹⁴², J.D. Mansour^{15a}, M. Mantoani⁵¹, S. Manzoni^{66a,66b}, G. Marceca³⁰, L. March⁵²,
 L. Marchese¹³¹, G. Marchiori¹³², M. Marcisovsky¹³⁷, C.A. Marin Tobon³⁵, M. Marjanovic³⁷,
 D.E. Marley¹⁰³, F. Marroquim^{78b}, Z. Marshall¹⁸, M.U.F Martensson¹⁶⁹, S. Marti-Garcia¹⁷¹,
 C.B. Martin¹²², T.A. Martin¹⁷⁵, V.J. Martin⁴⁸, B. Martin dit Latour¹⁷, M. Martinez^{14,x},
 V.I. Martinez Outschoorn¹⁰⁰, S. Martin-Haugh¹⁴¹, V.S. Martoiu^{27b}, A.C. Martyniuk⁹², A. Marzin³⁵,
 L. Masetti⁹⁷, T. Mashimo¹⁶⁰, R. Mashinistov¹⁰⁸, J. Masik⁹⁸, A.L. Maslennikov^{120b,120a}, L.H. Mason¹⁰²,
 L. Massa^{71a,71b}, P. Massarotti^{67a,67b}, P. Mastrandrea⁵, A. Mastroberardino^{40b,40a}, T. Masubuchi¹⁶⁰,
 P. Mättig¹⁷⁹, J. Maurer^{27b}, B. Maček⁸⁹, S.J. Maxfield⁸⁸, D.A. Maximov^{120b,120a}, R. Mazini¹⁵⁵,
 I. Maznas¹⁵⁹, S.M. Mazza¹⁴³, N.C. Mc Fadden¹¹⁶, G. Mc Goldrick¹⁶⁴, S.P. Mc Kee¹⁰³, A. McCarn¹⁰³,
 T.G. McCarthy¹¹³, L.I. McClymont⁹², E.F. McDonald¹⁰², J.A. Mcfayden³⁵, G. Mchedlidze⁵¹,
 M.A. McKay⁴¹, K.D. McLean¹⁷³, S.J. McMahon¹⁴¹, P.C. McNamara¹⁰², C.J. McNicol¹⁷⁵,
 R.A. McPherson^{173,ab}, J.E. Mdhluli^{32c}, Z.A. Meadows¹⁰⁰, S. Meehan¹⁴⁵, T. Megy⁵⁰, S. Mehlhase¹¹²,
 A. Mehta⁸⁸, T. Meideck⁵⁶, B. Meirose⁴², D. Melini^{171,g}, B.R. Mellado Garcia^{32c}, J.D. Mellenthin⁵¹,
 M. Melo^{28a}, F. Meloni⁴⁴, A. Melzer²⁴, S.B. Menary⁹⁸, E.D. Mendes Gouveia^{136a}, L. Meng⁸⁸,
 X.T. Meng¹⁰³, A. Mengarelli^{23b,23a}, S. Menke¹¹³, E. Meoni^{40b,40a}, S. Mergelmeyer¹⁹, C. Merlassino²⁰,
 P. Mermod⁵², L. Merola^{67a,67b}, C. Meroni^{66a}, F.S. Merritt³⁶, A. Messina^{70a,70b}, J. Metcalfe⁶,
 A.S. Mete¹⁶⁸, C. Meyer¹³³, J. Meyer¹⁵⁷, J-P. Meyer¹⁴², H. Meyer Zu Theenhausen^{59a}, F. Miano¹⁵³,

R.P. Middleton¹⁴¹, L. Mijovic⁴⁸, G. Mikenberg¹⁷⁷, M. Mikestikova¹³⁷, M. Mikuž⁸⁹, M. Milesi¹⁰²,
 A. Milic¹⁶⁴, D.A. Millar⁹⁰, D.W. Miller³⁶, A. Milov¹⁷⁷, D.A. Milstead^{43a,43b}, A.A. Minaenko¹⁴⁰,
 M. Miñano Moya¹⁷¹, I.A. Minashvili^{156b}, A.I. Mincer¹²¹, B. Mindur^{81a}, M. Mineev⁷⁷, Y. Minegishi¹⁶⁰,
 Y. Ming¹⁷⁸, L.M. Mir¹⁴, A. Mirto^{65a,65b}, K.P. Mistry¹³³, T. Mitani¹⁷⁶, J. Mitrevski¹¹², V.A. Mitsou¹⁷¹,
 A. Miucci²⁰, P.S. Miyagawa¹⁴⁶, A. Mizukami⁷⁹, J.U. Mjörnmark⁹⁴, T. Mkrtchyan¹⁸¹, M. Mlynarikova¹³⁹,
 T. Moa^{43a,43b}, K. Mochizuki¹⁰⁷, P. Mogg⁵⁰, S. Mohapatra³⁸, S. Molander^{43a,43b}, R. Moles-Valls²⁴,
 M.C. Mondragon¹⁰⁴, K. Mönig⁴⁴, J. Monk³⁹, E. Monnier⁹⁹, A. Montalbano¹⁴⁹, J. Montejo Berlingen³⁵,
 F. Monticelli⁸⁶, S. Monzani^{66a}, N. Morange¹²⁸, D. Moreno²², M. Moreno Llácer³⁵, P. Morettini^{53b},
 M. Morgenstern¹¹⁸, S. Morgenstern⁴⁶, D. Mori¹⁴⁹, M. Morii⁵⁷, M. Morinaga¹⁷⁶, V. Morisbak¹³⁰,
 A.K. Morley³⁵, G. Mornacchi³⁵, A.P. Morris⁹², J.D. Morris⁹⁰, L. Morvaj¹⁵², P. Moschovakos¹⁰,
 M. Mosidze^{156b}, H.J. Moss¹⁴⁶, J. Moss^{150,m}, K. Motohashi¹⁶², R. Mount¹⁵⁰, E. Mountricha³⁵,
 E.J.W. Moyse¹⁰⁰, S. Muanza⁹⁹, F. Mueller¹¹³, J. Mueller¹³⁵, R.S.P. Mueller¹¹², D. Muenstermann⁸⁷,
 G.A. Mullier²⁰, F.J. Munoz Sanchez⁹⁸, P. Murin^{28b}, W.J. Murray^{175,141}, A. Murrone^{66a,66b},
 M. Muškinja⁸⁹, C. Mwewa^{32a}, A.G. Myagkov^{140,ai}, J. Myers¹²⁷, M. Myska¹³⁸, B.P. Nachman¹⁸,
 O. Nackenhorst⁴⁵, K. Nagai¹³¹, K. Nagano⁷⁹, Y. Nagasaka⁶⁰, M. Nagel⁵⁰, E. Nagy⁹⁹, A.M. Nairz³⁵,
 Y. Nakahama¹¹⁵, K. Nakamura⁷⁹, T. Nakamura¹⁶⁰, I. Nakano¹²³, H. Nanjo¹²⁹, F. Napolitano^{59a},
 R.F. Naranjo Garcia⁴⁴, R. Narayan¹¹, D.I. Narrias Villar^{59a}, I. Naryshkin¹³⁴, T. Naumann⁴⁴,
 G. Navarro²², R. Nayyar⁷, H.A. Neal¹⁰³, P.Y. Nechaeva¹⁰⁸, T.J. Neep¹⁴², A. Negri^{68a,68b}, M. Negrini^{23b},
 S. Nektarijevic¹¹⁷, C. Nellist⁵¹, M.E. Nelson¹³¹, S. Nemecek¹³⁷, P. Nemethy¹²¹, M. Nessi^{35,e},
 M.S. Neubauer¹⁷⁰, M. Neumann¹⁷⁹, P.R. Newman²¹, T.Y. Ng^{61c}, Y.S. Ng¹⁹, H.D.N. Nguyen⁹⁹,
 T. Nguyen Manh¹⁰⁷, E. Nibigira³⁷, R.B. Nickerson¹³¹, R. Nicolaïdou¹⁴², J. Nielsen¹⁴³, N. Nikiforou¹¹,
 V. Nikolaenko^{140,ai}, I. Nikolic-Audit¹³², K. Nikolopoulos²¹, P. Nilsson²⁹, Y. Ninomiya⁷⁹, A. Nisati^{70a},
 N. Nishu^{58c}, R. Nisius¹¹³, I. Nitsche⁴⁵, T. Nitta¹⁷⁶, T. Nobe¹⁶⁰, Y. Noguchi⁸³, M. Nomachi¹²⁹,
 I. Nomidis¹³², M.A. Nomura²⁹, T. Nooney⁹⁰, M. Nordberg³⁵, N. Norjoharuddeen¹³¹, T. Novak⁸⁹,
 O. Novgorodova⁴⁶, R. Novotny¹³⁸, L. Nozka¹²⁶, K. Ntekas¹⁶⁸, E. Nurse⁹², F. Nuti¹⁰², F.G. Oakham^{33,ap},
 H. Oberlack¹¹³, T. Obermann²⁴, J. Ocariz¹³², A. Ochi⁸⁰, I. Ochoa³⁸, J.P. Ochoa-Ricoux^{144a},
 K. O'Connor²⁶, S. Oda⁸⁵, S. Odaka⁷⁹, S. Oerdekk⁵¹, A. Oh⁹⁸, S.H. Oh⁴⁷, C.C. Ohm¹⁵¹, H. Oide^{53b,53a},
 M.L. Ojeda¹⁶⁴, H. Okawa¹⁶⁶, Y. Okazaki⁸³, Y. Okumura¹⁶⁰, T. Okuyama⁷⁹, A. Olariu^{27b},
 L.F. Oleiro Seabra^{136a}, S.A. Olivares Pino^{144a}, D. Oliveira Damazio²⁹, J.L. Oliver¹, M.J.R. Olsson³⁶,
 A. Olszewski⁸², J. Olszowska⁸², D.C. O'Neil¹⁴⁹, A. Onofre^{136a,136e}, K. Onogi¹¹⁵, P.U.E. Onyisi¹¹,
 H. Oppen¹³⁰, M.J. Oreglia³⁶, Y. Oren¹⁵⁸, D. Orestano^{72a,72b}, E.C. Orgill⁹⁸, N. Orlando^{61b},
 A.A. O'Rourke⁴⁴, R.S. Orr¹⁶⁴, B. Osculati^{53b,53a,*}, V. O'Shea⁵⁵, R. Ospanov^{58a}, G. Otero y Garzon³⁰,
 H. Otomo⁸⁵, M. Ouchrif^{34d}, F. Ould-Saada¹³⁰, A. Ouraou¹⁴², Q. Ouyang^{15a}, M. Owen⁵⁵, R.E. Owen²¹,
 V.E. Ozcan^{12c}, N. Ozturk⁸, J. Pacalt¹²⁶, H.A. Pacey³¹, K. Pachal¹⁴⁹, A. Pacheco Pages¹⁴,
 L. Pacheco Rodriguez¹⁴², C. Padilla Aranda¹⁴, S. Pagan Griso¹⁸, M. Paganini¹⁸⁰, G. Palacino⁶³,
 S. Palazzo^{40b,40a}, S. Palestini³⁵, M. Palka^{81b}, D. Pallin³⁷, I. Panagoulias¹⁰, C.E. Pandini³⁵,
 J.G. Panduro Vazquez⁹¹, P. Pani³⁵, G. Panizzo^{64a,64c}, L. Paolozzi⁵², T.D. Papadopoulou¹⁰,
 K. Papageorgiou^{9,i}, A. Paramonov⁶, D. Paredes Hernandez^{61b}, S.R. Paredes Saenz¹³¹, B. Parida^{58c},
 A.J. Parker⁸⁷, K.A. Parker⁴⁴, M.A. Parker³¹, F. Parodi^{53b,53a}, J.A. Parsons³⁸, U. Parzefall⁵⁰,
 V.R. Pascuzzi¹⁶⁴, J.M.P. Pasner¹⁴³, E. Pasqualucci^{70a}, S. Passaggio^{53b}, F. Pastore⁹¹, P. Pasuwan^{43a,43b},
 S. Pataria⁹⁷, J.R. Pater⁹⁸, A. Pathak^{178,j}, T. Pauly³⁵, B. Pearson¹¹³, M. Pedersen¹³⁰, L. Pedraza Diaz¹¹⁷,
 R. Pedro^{136a,136b}, S.V. Peleganchuk^{120b,120a}, O. Penc¹³⁷, C. Peng^{15d}, H. Peng^{58a}, B.S. Peralva^{78a},
 M.M. Perego¹⁴², A.P. Pereira Peixoto^{136a}, D.V. Perekiltsa²⁹, F. Peri¹⁹, L. Perini^{66a,66b}, H. Pernegger³⁵,
 S. Perrella^{67a,67b}, V.D. Peshekhanov^{77,*}, K. Peters⁴⁴, R.F.Y. Peters⁹⁸, B.A. Petersen³⁵, T.C. Petersen³⁹,
 E. Petit⁵⁶, A. Petridis¹, C. Petridou¹⁵⁹, P. Petroff¹²⁸, M. Petrov¹³¹, F. Petrucci^{72a,72b}, M. Pettee¹⁸⁰,
 N.E. Pettersson¹⁰⁰, A. Peyaud¹⁴², R. Pezoa^{144b}, T. Pham¹⁰², F.H. Phillips¹⁰⁴, P.W. Phillips¹⁴¹,
 G. Piacquadio¹⁵², E. Pianori¹⁸, A. Picazio¹⁰⁰, M.A. Pickering¹³¹, R.H. Pickles⁹⁸, R. Piegai³⁰,

J.E. Pilcher³⁶, A.D. Pilkington⁹⁸, M. Pinamonti^{71a,71b}, J.L. Pinfold³, M. Pitt¹⁷⁷, M-A. Pleier²⁹,
 V. Pleskot¹³⁹, E. Plotnikova⁷⁷, D. Pluth⁷⁶, P. Podberezko^{120b,120a}, R. Poettgen⁹⁴, R. Poggi⁵²,
 L. Poggioli¹²⁸, I. Pogrebnyak¹⁰⁴, D. Pohl²⁴, I. Pokharel⁵¹, G. Polesello^{68a}, A. Poley¹⁸,
 A. Pollicchio^{70a,70b}, R. Polifka³⁵, A. Polini^{23b}, C.S. Pollard⁴⁴, V. Polychronakos²⁹, D. Ponomarenko¹¹⁰,
 L. Pontecorvo^{70a}, G.A. Popeneciu^{27d}, D.M. Portillo Quintero¹³², S. Pospisil¹³⁸, K. Potamianos⁴⁴,
 I.N. Potrap⁷⁷, C.J. Potter³¹, H. Potti¹¹, T. Poulsen⁹⁴, J. Poveda³⁵, T.D. Powell¹⁴⁶,
 M.E. Pozo Astigarraga³⁵, P. Pralavorio⁹⁹, S. Prell⁷⁶, D. Price⁹⁸, M. Primavera^{65a}, S. Prince¹⁰¹,
 N. Proklova¹¹⁰, K. Prokofiev^{61c}, F. Prokoshin^{144b}, S. Protopopescu²⁹, J. Proudfoot⁶, M. Przybycien^{81a},
 A. Puri¹⁷⁰, P. Puzo¹²⁸, J. Qian¹⁰³, Y. Qin⁹⁸, A. Quadri⁵¹, M. Queitsch-Maitland⁴⁴, A. Qureshi¹,
 P. Rados¹⁰², F. Ragusa^{66a,66b}, G. Rahal⁹⁵, J.A. Raine⁵², S. Rajagopalan²⁹, A. Ramirez Morales⁹⁰,
 T. Rashid¹²⁸, S. Raspopov⁵, M.G. Ratti^{66a,66b}, D.M. Rauch⁴⁴, F. Rauscher¹¹², S. Rave⁹⁷, B. Ravina¹⁴⁶,
 I. Ravinovich¹⁷⁷, J.H. Rawling⁹⁸, M. Raymond³⁵, A.L. Read¹³⁰, N.P. Readoff⁵⁶, M. Reale^{65a,65b},
 D.M. Rebuzzi^{68a,68b}, A. Redelbach¹⁷⁴, G. Redlinger²⁹, R. Reece¹⁴³, R.G. Reed^{32c}, K. Reeves⁴²,
 L. Rehnisch¹⁹, J. Reichert¹³³, A. Reiss⁹⁷, C. Rembser³⁵, H. Ren^{15d}, M. Rescigno^{70a}, S. Resconi^{66a},
 E.D. Ressegue¹³³, S. Rettie¹⁷², E. Reynolds²¹, O.L. Rezanova^{120b,120a}, P. Reznicek¹³⁹, E. Ricci^{73a,73b},
 R. Richter¹¹³, S. Richter⁹², E. Richter-Was^{81b}, O. Ricken²⁴, M. Ridel¹³², P. Rieck¹¹³, C.J. Riegel¹⁷⁹,
 O. Rifki⁴⁴, M. Rijssenbeek¹⁵², A. Rimoldi^{68a,68b}, M. Rimoldi²⁰, L. Rinaldi^{23b}, G. Ripellino¹⁵¹,
 B. Ristic⁸⁷, E. Ritsch³⁵, I. Riu¹⁴, J.C. Rivera Vergara^{144a}, F. Rizatdinova¹²⁵, E. Rizvi⁹⁰, C. Rizzi¹⁴,
 R.T. Roberts⁹⁸, S.H. Robertson^{101,ab}, D. Robinson³¹, J.E.M. Robinson⁴⁴, A. Robson⁵⁵, E. Rocco⁹⁷,
 C. Roda^{69a,69b}, Y. Rodina⁹⁹, S. Rodriguez Bosca¹⁷¹, A. Rodriguez Perez¹⁴, D. Rodriguez Rodriguez¹⁷¹,
 A.M. Rodriguez Vera^{165b}, S. Roe³⁵, C.S. Rogan⁵⁷, O. Røhne¹³⁰, R. Röhrlig¹¹³, C.P.A. Roland⁶³,
 J. Roloff⁵⁷, A. Romanouk¹¹⁰, M. Romano^{23b,23a}, N. Rompotis⁸⁸, M. Ronzani¹²¹, L. Roos¹³²,
 S. Rosati^{70a}, K. Rosbach⁵⁰, P. Rose¹⁴³, N-A. Rosien⁵¹, E. Rossi⁴⁴, E. Rossi^{67a,67b}, L.P. Rossi^{53b},
 L. Rossini^{66a,66b}, J.H.N. Rosten³¹, R. Rosten¹⁴, M. Rotaru^{27b}, J. Rothberg¹⁴⁵, D. Rousseau¹²⁸, D. Roy^{32c},
 A. Rozanov⁹⁹, Y. Rozen¹⁵⁷, X. Ruan^{32c}, F. Rubbo¹⁵⁰, F. Rühr⁵⁰, A. Ruiz-Martinez¹⁷¹, Z. Rurikova⁵⁰,
 N.A. Rusakovich⁷⁷, H.L. Russell¹⁰¹, J.P. Rutherford⁷, E.M. Rüttinger^{44,k}, Y.F. Ryabov¹³⁴, M. Rybar¹⁷⁰,
 G. Rybkin¹²⁸, S. Ryu⁶, A. Ryzhov¹⁴⁰, G.F. Rzehorzh⁵¹, P. Sabatini⁵¹, G. Sabato¹¹⁸, S. Sacerdoti¹²⁸,
 H.F-W. Sadrozinski¹⁴³, R. Sadykov⁷⁷, F. Safai Tehrani^{70a}, P. Saha¹¹⁹, M. Sahinsoy^{59a}, A. Sahu¹⁷⁹,
 M. Saimpert⁴⁴, M. Saito¹⁶⁰, T. Saito¹⁶⁰, H. Sakamoto¹⁶⁰, A. Sakharov^{121,ah}, D. Salamani⁵²,
 G. Salamanna^{72a,72b}, J.E. Salazar Loyola^{144b}, D. Salek¹¹⁸, P.H. Sales De Bruin¹⁶⁹, D. Salihagic¹¹³,
 A. Salnikov¹⁵⁰, J. Salt¹⁷¹, D. Salvatore^{40b,40a}, F. Salvatore¹⁵³, A. Salvucci^{61a,61b,61c}, A. Salzburger³⁵,
 J. Samarati³⁵, D. Sammel⁵⁰, D. Sampsonidis¹⁵⁹, D. Sampsonidou¹⁵⁹, J. Sánchez¹⁷¹,
 A. Sanchez Pineda^{64a,64c}, H. Sandaker¹³⁰, C.O. Sander⁴⁴, M. Sandhoff¹⁷⁹, C. Sandoval²²,
 D.P.C. Sankey¹⁴¹, M. Sannino^{53b,53a}, Y. Sano¹¹⁵, A. Sansoni⁴⁹, C. Santoni³⁷, H. Santos^{136a},
 I. Santoyo Castillo¹⁵³, A. Santra¹⁷¹, A. Sapronov⁷⁷, J.G. Saraiva^{136a,136d}, O. Sasaki⁷⁹, K. Sato¹⁶⁶,
 E. Sauvan⁵, P. Savard^{164,ap}, N. Savic¹¹³, R. Sawada¹⁶⁰, C. Sawyer¹⁴¹, L. Sawyer^{93,ag}, C. Sbarra^{23b},
 A. Sbrizzi^{23b,23a}, T. Scanlon⁹², J. Schaarschmidt¹⁴⁵, P. Schacht¹¹³, B.M. Schachtner¹¹², D. Schaefer³⁶,
 L. Schaefer¹³³, J. Schaeffer⁹⁷, S. Schaepe³⁵, U. Schäfer⁹⁷, A.C. Schaffer¹²⁸, D. Schaile¹¹²,
 R.D. Schamberger¹⁵², N. Scharnberg⁹⁸, V.A. Schegelsky¹³⁴, D. Scheirich¹³⁹, F. Schenck¹⁹,
 M. Schernau¹⁶⁸, C. Schiavi^{53b,53a}, S. Schier¹⁴³, L.K. Schildgen²⁴, Z.M. Schillaci²⁶, E.J. Schioppa³⁵,
 M. Schioppa^{40b,40a}, K.E. Schleicher⁵⁰, S. Schlenker³⁵, K.R. Schmidt-Sommerfeld¹¹³, K. Schmieden³⁵,
 C. Schmitt⁹⁷, S. Schmitt⁴⁴, S. Schmitz⁹⁷, J.C. Schmoekel⁴⁴, U. Schnoor⁵⁰, L. Schoeffel¹⁴²,
 A. Schoening^{59b}, E. Schopf²⁴, M. Schott⁹⁷, J.F.P. Schouwenberg¹¹⁷, J. Schovancova³⁵, S. Schramm⁵²,
 A. Schulte⁹⁷, H-C. Schultz-Coulon^{59a}, M. Schumacher⁵⁰, B.A. Schumm¹⁴³, Ph. Schune¹⁴²,
 A. Schwartzman¹⁵⁰, T.A. Schwarz¹⁰³, H. Schweiger⁹⁸, Ph. Schwemling¹⁴², R. Schwienhorst¹⁰⁴,
 A. Sciandra²⁴, G. Sciolla²⁶, M. Scornajenghi^{40b,40a}, F. Scuri^{69a}, F. Scutti¹⁰², L.M. Scyboz¹¹³,
 J. Searcy¹⁰³, C.D. Sebastiani^{70a,70b}, P. Seema²⁴, S.C. Seidel¹¹⁶, A. Seiden¹⁴³, T. Seiss³⁶, J.M. Seixas^{78b},

G. Sekhniadze^{67a}, K. Sekhon¹⁰³, S.J. Sekula⁴¹, N. Semprini-Cesari^{23b,23a}, S. Sen⁴⁷, S. Senkin³⁷,
 C. Serfon¹³⁰, L. Serin¹²⁸, L. Serkin^{64a,64b}, M. Sessa^{72a,72b}, H. Severini¹²⁴, F. Sforza¹⁶⁷, A. Sfyrla⁵²,
 E. Shabalina⁵¹, J.D. Shahinian¹⁴³, N.W. Shaikh^{43a,43b}, L.Y. Shan^{15a}, R. Shang¹⁷⁰, J.T. Shank²⁵,
 M. Shapiro¹⁸, A.S. Sharma¹, A. Sharma¹³¹, P.B. Shatalov¹⁰⁹, K. Shaw¹⁵³, S.M. Shaw⁹⁸,
 A. Shcherbakova¹³⁴, Y. Shen¹²⁴, N. Sherafati³³, A.D. Sherman²⁵, P. Sherwood⁹², L. Shi^{155,al},
 S. Shimizu⁷⁹, C.O. Shimmin¹⁸⁰, M. Shimojima¹¹⁴, I.P.J. Shipsey¹³¹, S. Shirabe⁸⁵, M. Shiyakova⁷⁷,
 J. Shlomi¹⁷⁷, A. Shmeleva¹⁰⁸, D. Shoaleh Saadi¹⁰⁷, M.J. Shochet³⁶, S. Shojaii¹⁰², D.R. Shope¹²⁴,
 S. Shrestha¹²², E. Shulga¹¹⁰, P. Sicho¹³⁷, A.M. Sickles¹⁷⁰, P.E. Sidebo¹⁵¹, E. Sideras Haddad^{32c},
 O. Sidiropoulou³⁵, A. Sidoti^{23b,23a}, F. Siegert⁴⁶, Dj. Sijacki¹⁶, J. Silva^{136a}, M. Silva Jr.¹⁷⁸,
 M.V. Silva Oliveira^{78a}, S.B. Silverstein^{43a}, L. Simic⁷⁷, S. Simion¹²⁸, E. Simioni⁹⁷, M. Simon⁹⁷,
 R. Simoniello⁹⁷, P. Sinervo¹⁶⁴, N.B. Sinev¹²⁷, M. Sioli^{23b,23a}, G. Siragusa¹⁷⁴, I. Siral¹⁰³,
 S.Yu. Sivoklokov¹¹¹, J. Sjölin^{43a,43b}, P. Skubic¹²⁴, M. Slater²¹, T. Slavicek¹³⁸, M. Slawinska⁸²,
 K. Sliwa¹⁶⁷, R. Slovak¹³⁹, V. Smakhtin¹⁷⁷, B.H. Smart⁵, J. Smiesko^{28a}, N. Smirnov¹¹⁰,
 S.Yu. Smirnov¹¹⁰, Y. Smirnov¹¹⁰, L.N. Smirnova¹¹¹, O. Smirnova⁹⁴, J.W. Smith⁵¹, M.N.K. Smith³⁸,
 M. Smizanska⁸⁷, K. Smolek¹³⁸, A. Smykiewicz⁸², A.A. Snesarev¹⁰⁸, I.M. Snyder¹²⁷, S. Snyder²⁹,
 R. Sobie^{173,ab}, A.M. Soffa¹⁶⁸, A. Soffer¹⁵⁸, A. Søgaard⁴⁸, D.A. Soh¹⁵⁵, G. Sokhrannyi⁸⁹,
 C.A. Solans Sanchez³⁵, M. Solar¹³⁸, E.Yu. Soldatov¹¹⁰, U. Soldevila¹⁷¹, A.A. Solodkov¹⁴⁰,
 A. Soloshenko⁷⁷, O.V. Solovyanov¹⁴⁰, V. Solovyev¹³⁴, P. Sommer¹⁴⁶, H. Son¹⁶⁷, W. Song¹⁴¹,
 W.Y. Song^{165b}, A. Sopczak¹³⁸, F. Sopkova^{28b}, D. Sosa^{59b}, C.L. Sotiropoulou^{69a,69b},
 S. Sottocornola^{68a,68b}, R. Soualah^{64a,64c,h}, A.M. Soukharev^{120b,120a}, D. South⁴⁴, B.C. Sowden⁹¹,
 S. Spagnolo^{65a,65b}, M. Spalla¹¹³, M. Spangenberg¹⁷⁵, F. Spanò⁹¹, D. Sperlich¹⁹, F. Spettel¹¹³,
 T.M. Spieker^{59a}, R. Spighi^{23b}, G. Spigo³⁵, L.A. Spiller¹⁰², D.P. Spiteri⁵⁵, M. Spousta¹³⁹,
 A. Stabile^{66a,66b}, R. Stamen^{59a}, S. Stamm¹⁹, E. Stanecka⁸², R.W. Stanek⁶, C. Stanescu^{72a},
 B. Stanislaus¹³¹, M.M. Stanitzki⁴⁴, B.S. Stapf¹¹⁸, S. Stapnes¹³⁰, E.A. Starchenko¹⁴⁰, G.H. Stark³⁶,
 J. Stark⁵⁶, S.H Stark³⁹, P. Staroba¹³⁷, P. Starovoitov^{59a}, S. Stärz³⁵, R. Staszewski⁸², M. Stegler⁴⁴,
 P. Steinberg²⁹, B. Stelzer¹⁴⁹, H.J. Stelzer³⁵, O. Stelzer-Chilton^{165a}, H. Stenzel⁵⁴, T.J. Stevenson⁹⁰,
 G.A. Stewart⁵⁵, M.C. Stockton¹²⁷, G. Stoica^{27b}, P. Stolte⁵¹, S. Stonjek¹¹³, A. Straessner⁴⁶,
 J. Strandberg¹⁵¹, S. Strandberg^{43a,43b}, M. Strauss¹²⁴, P. Strizenec^{28b}, R. Ströhmer¹⁷⁴, D.M. Strom¹²⁷,
 R. Stroynowski⁴¹, A. Strubig⁴⁸, S.A. Stucci²⁹, B. Stugu¹⁷, J. Stupak¹²⁴, N.A. Styles⁴⁴, D. Su¹⁵⁰, J. Su¹³⁵,
 S. Suchek^{59a}, Y. Sugaya¹²⁹, M. Suk¹³⁸, V.V. Sulin¹⁰⁸, D.M.S. Sultan⁵², S. Sultansoy^{4c}, T. Sumida⁸³,
 S. Sun¹⁰³, X. Sun³, K. Suruliz¹⁵³, C.J.E. Suster¹⁵⁴, M.R. Sutton¹⁵³, S. Suzuki⁷⁹, M. Svatos¹³⁷,
 M. Swiatlowski³⁶, S.P. Swift², A. Sydorenko⁹⁷, I. Sykora^{28a}, T. Sykora¹³⁹, D. Ta⁹⁷, K. Tackmann^{44,y},
 J. Taenzer¹⁵⁸, A. Taffard¹⁶⁸, R. Tafirout^{165a}, E. Tahirovic⁹⁰, N. Taiblum¹⁵⁸, H. Takai²⁹, R. Takashima⁸⁴,
 E.H. Takasugi¹¹³, K. Takeda⁸⁰, T. Takeshita¹⁴⁷, Y. Takubo⁷⁹, M. Talby⁹⁹, A.A. Talyshев^{120b,120a},
 J. Tanaka¹⁶⁰, M. Tanaka¹⁶², R. Tanaka¹²⁸, B.B. Tannenwald¹²², S. Tapia Araya^{144b}, S. Tapprogge⁹⁷,
 A. Tarek Abouelfadl Mohamed¹³², S. Tarem¹⁵⁷, G. Tarna^{27b,d}, G.F. Tartarelli^{66a}, P. Tas¹³⁹,
 M. Tasevsky¹³⁷, T. Tashiro⁸³, E. Tassi^{40b,40a}, A. Tavares Delgado^{136a,136b}, Y. Tayalati^{34e}, A.C. Taylor¹¹⁶,
 A.J. Taylor⁴⁸, G.N. Taylor¹⁰², P.T.E. Taylor¹⁰², W. Taylor^{165b}, A.S. Tee⁸⁷, P. Teixeira-Dias⁹¹,
 H. Ten Kate³⁵, P.K. Teng¹⁵⁵, J.J. Teoh¹¹⁸, F. Tepel¹⁷⁹, S. Terada⁷⁹, K. Terashi¹⁶⁰, J. Terron⁹⁶, S. Terzo¹⁴,
 M. Testa⁴⁹, R.J. Teuscher^{164,ab}, S.J. Thais¹⁸⁰, T. Theveneaux-Pelzer⁴⁴, F. Thiele³⁹, D.W. Thomas⁹¹,
 J.P. Thomas²¹, A.S. Thompson⁵⁵, P.D. Thompson²¹, L.A. Thomsen¹⁸⁰, E. Thomson¹³³, Y. Tian³⁸,
 R.E. Ticse Torres⁵¹, V.O. Tikhomirov^{108,aj}, Yu.A. Tikhonov^{120b,120a}, S. Timoshenko¹¹⁰, P. Tipton¹⁸⁰,
 S. Tisserant⁹⁹, K. Todome¹⁶², S. Todorova-Nova⁵, S. Todt⁴⁶, J. Tojo⁸⁵, S. Tokár^{28a}, K. Tokushuku⁷⁹,
 E. Tolley¹²², K.G. Tomiwa^{32c}, M. Tomoto¹¹⁵, L. Tompkins¹⁵⁰, K. Toms¹¹⁶, B. Tong⁵⁷, P. Tornambe⁵⁰,
 E. Torrence¹²⁷, H. Torres⁴⁶, E. Torró Pastor¹⁴⁵, C. Tosciri¹³¹, J. Toth^{99,aa}, F. Touchard⁹⁹, D.R. Tovey¹⁴⁶,
 C.J. Treado¹²¹, T. Trefzger¹⁷⁴, F. Tresoldi¹⁵³, A. Tricoli²⁹, I.M. Trigger^{165a}, S. Trincaz-Duvoid¹³²,
 M.F. Tripiana¹⁴, W. Trischuk¹⁶⁴, B. Trocmé⁵⁶, A. Trofymov¹²⁸, C. Troncon^{66a}, M. Trovatelli¹⁷³,

F. Trovato¹⁵³, L. Truong^{32b}, M. Trzebinski⁸², A. Trzupek⁸², F. Tsai⁴⁴, J.C-L. Tseng¹³¹, P.V. Tsiareshka¹⁰⁵, A. Tsirigotis¹⁵⁹, N. Tsirintanis⁹, V. Tsiskaridze¹⁵², E.G. Tskhadadze^{156a}, I.I. Tsukerman¹⁰⁹, V. Tsulaia¹⁸, S. Tsuno⁷⁹, D. Tsybychev^{152,163}, Y. Tu^{61b}, A. Tudorache^{27b}, V. Tudorache^{27b}, T.T. Tulbure^{27a}, A.N. Tuna⁵⁷, S. Turchikhin⁷⁷, D. Turgeman¹⁷⁷, I. Turk Cakir^{4b,s}, R. Turra^{66a}, P.M. Tuts³⁸, E. Tzovara⁹⁷, G. Ucchielli^{23b,23a}, I. Ueda⁷⁹, M. Ughetto^{43a,43b}, F. Ukegawa¹⁶⁶, G. Unal³⁵, A. Undrus²⁹, G. Unel¹⁶⁸, F.C. Ungaro¹⁰², Y. Unno⁷⁹, K. Uno¹⁶⁰, J. Urban^{28b}, P. Urquijo¹⁰², P. Urrejola⁹⁷, G. Usai⁸, J. Usui⁷⁹, L. Vacavant⁹⁹, V. Vacek¹³⁸, B. Vachon¹⁰¹, K.O.H. Vadla¹³⁰, A. Vaidya⁹², C. Valderanis¹¹², E. Valdes Santurio^{43a,43b}, M. Valente⁵², S. Valentineti^{23b,23a}, A. Valero¹⁷¹, L. Valéry⁴⁴, R.A. Vallance²¹, A. Vallier⁵, J.A. Valls Ferrer¹⁷¹, T.R. Van Daalen¹⁴, H. Van der Graaf¹¹⁸, P. Van Gemmeren⁶, J. Van Nieuwkoop¹⁴⁹, I. Van Vulpen¹¹⁸, M. Vanadia^{71a,71b}, W. Vandelli³⁵, A. Vaniachine¹⁶³, P. Vankov¹¹⁸, R. Vari^{70a}, E.W. Varnes⁷, C. Varni^{53b,53a}, T. Varol⁴¹, D. Varouchas¹²⁸, K.E. Varvell¹⁵⁴, G.A. Vasquez^{144b}, J.G. Vasquez¹⁸⁰, F. Vazeille³⁷, D. Vazquez Furelos¹⁴, T. Vazquez Schroeder¹⁰¹, J. Veatch⁵¹, V. Vecchio^{72a,72b}, L.M. Veloce¹⁶⁴, F. Veloso^{136a,136c}, S. Veneziano^{70a}, A. Ventura^{65a,65b}, M. Venturi¹⁷³, N. Venturi³⁵, V. Vercesi^{68a}, M. Verducci^{72a,72b}, C.M. Vergel Infante⁷⁶, C. Vergis²⁴, W. Verkerke¹¹⁸, A.T. Vermeulen¹¹⁸, J.C. Vermeulen¹¹⁸, M.C. Vetterli^{149,ap}, N. Viaux Maira^{144b}, M. Vicente Barreto Pinto⁵², I. Vichou^{170,*}, T. Vickey¹⁴⁶, O.E. Vickey Boeriu¹⁴⁶, G.H.A. Viehhauser¹³¹, S. Viel¹⁸, L. Vigani¹³¹, M. Villa^{23b,23a}, M. Villaplana Perez^{66a,66b}, E. Vilucchi⁴⁹, M.G. Vincter³³, V.B. Vinogradov⁷⁷, A. Vishwakarma⁴⁴, C. Vittori^{23b,23a}, I. Vivarelli¹⁵³, S. Vlachos¹⁰, M. Vogel¹⁷⁹, P. Vokac¹³⁸, G. Volpi¹⁴, S.E. Von Buddenbrock^{32c}, E. Von Toerne²⁴, V. Vorobel¹³⁹, K. Vorobev¹¹⁰, M. Vos¹⁷¹, J.H. Vossebeld⁸⁸, N. Vranjes¹⁶, M. Vranjes Milosavljevic¹⁶, V. Vrba¹³⁸, M. Vreeswijk¹¹⁸, T. Šfiligoj⁸⁹, R. Vuillermet³⁵, I. Vukotic³⁶, T. Ženiš^{28a}, L. Živković¹⁶, P. Wagner²⁴, W. Wagner¹⁷⁹, J. Wagner-Kuhr¹¹², H. Wahlberg⁸⁶, S. Wahrmund⁴⁶, K. Wakamiya⁸⁰, V.M. Walbrecht¹¹³, J. Walder⁸⁷, R. Walker¹¹², S.D. Walker⁹¹, W. Walkowiak¹⁴⁸, V. Wallangen^{43a,43b}, A.M. Wang⁵⁷, C. Wang^{58b,d}, F. Wang¹⁷⁸, H. Wang¹⁸, H. Wang³, J. Wang¹⁵⁴, J. Wang^{59b}, P. Wang⁴¹, Q. Wang¹²⁴, R.-J. Wang¹³², R. Wang^{58a}, R. Wang⁶, S.M. Wang¹⁵⁵, W.T. Wang^{58a}, W. Wang^{15b,ac}, W.X. Wang^{58a,ac}, Y. Wang^{58a}, Z. Wang^{58c}, C. Wanotayaroj⁴⁴, A. Warburton¹⁰¹, C.P. Ward³¹, D.R. Wardrope⁹², A. Washbrook⁴⁸, P.M. Watkins²¹, A.T. Watson²¹, M.F. Watson²¹, G. Watts¹⁴⁵, S. Watts⁹⁸, B.M. Waugh⁹², A.F. Webb¹¹, S. Webb⁹⁷, C. Weber¹⁸⁰, M.S. Weber²⁰, S.A. Weber³³, S.M. Weber^{59a}, A.R. Weidberg¹³¹, B. Weinert⁶³, J. Weingarten⁵¹, M. Weirich⁹⁷, C. Weiser⁵⁰, P.S. Wells³⁵, T. Wenaus²⁹, T. Wengler³⁵, S. Wenig³⁵, N. Wermes²⁴, M.D. Werner⁷⁶, P. Werner³⁵, M. Wessels^{59a}, T.D. Weston²⁰, K. Whalen¹²⁷, N.L. Whallon¹⁴⁵, A.M. Wharton⁸⁷, A.S. White¹⁰³, A. White⁸, M.J. White¹, R. White^{144b}, D. Whiteson¹⁶⁸, B.W. Whitmore⁸⁷, F.J. Wickens¹⁴¹, W. Wiedenmann¹⁷⁸, M. Wielers¹⁴¹, C. Wiglesworth³⁹, L.A.M. Wiik-Fuchs⁵⁰, A. Wildauer¹¹³, F. Wilk⁹⁸, H.G. Wilkens³⁵, L.J. Wilkins⁹¹, H.H. Williams¹³³, S. Williams³¹, C. Willis¹⁰⁴, S. Willocq¹⁰⁰, J.A. Wilson²¹, I. Wingerter-Seez⁵, E. Winkels¹⁵³, F. Winklmeier¹²⁷, O.J. Winston¹⁵³, B.T. Winter²⁴, M. Wittgen¹⁵⁰, M. Wobisch⁹³, A. Wolf⁹⁷, T.M.H. Wolf¹¹⁸, R. Wolff⁹⁹, M.W. Wolter⁸², H. Wolters^{136a,136c}, V.W.S. Wong¹⁷², N.L. Woods¹⁴³, S.D. Worm²¹, B.K. Wosiek⁸², K.W. Woźniak⁸², K. Wraith⁵⁵, M. Wu³⁶, S.L. Wu¹⁷⁸, X. Wu⁵², Y. Wu^{58a}, T.R. Wyatt⁹⁸, B.M. Wynne⁴⁸, S. Xella³⁹, Z. Xi¹⁰³, L. Xia¹⁷⁵, D. Xu^{15a}, H. Xu^{58a}, L. Xu²⁹, T. Xu¹⁴², W. Xu¹⁰³, B. Yabsley¹⁵⁴, S. Yacoob^{32a}, K. Yajima¹²⁹, D.P. Yallup⁹², D. Yamaguchi¹⁶², Y. Yamaguchi¹⁶², A. Yamamoto⁷⁹, T. Yamanaka¹⁶⁰, F. Yamane⁸⁰, M. Yamatani¹⁶⁰, T. Yamazaki¹⁶⁰, Y. Yamazaki⁸⁰, Z. Yan²⁵, H.J. Yang^{58c,58d}, H.T. Yang¹⁸, S. Yang⁷⁵, Y. Yang¹⁶⁰, Z. Yang¹⁷, W-M. Yao¹⁸, Y.C. Yap⁴⁴, Y. Yasu⁷⁹, E. Yatsenko^{58c,58d}, J. Ye⁴¹, S. Ye²⁹, I. Yeletskikh⁷⁷, E. Yigitbasi²⁵, E. Yildirim⁹⁷, K. Yorita¹⁷⁶, K. Yoshihara¹³³, C.J.S. Young³⁵, C. Young¹⁵⁰, J. Yu⁸, J. Yu⁷⁶, X. Yue^{59a}, S.P.Y. Yuen²⁴, B. Zabinski⁸², G. Zacharis¹⁰, E. Zaffaroni⁵², R. Zaidan¹⁴, A.M. Zaitsev^{140,ai}, T. Zakareishvili^{156b}, N. Zakharchuk⁴⁴, J. Zaliecas¹⁷, S. Zambito⁵⁷, D. Zanzi³⁵, D.R. Zaripovas⁵⁵, S.V. Zeißner⁴⁵, C. Zeitnitz¹⁷⁹, G. Zemaityte¹³¹, J.C. Zeng¹⁷⁰, Q. Zeng¹⁵⁰, O. Zenin¹⁴⁰, D. Zerwas¹²⁸, M. Zgubić¹³¹, D.F. Zhang^{58b}, D. Zhang¹⁰³, F. Zhang¹⁷⁸, G. Zhang^{58a}, H. Zhang^{15b}, J. Zhang⁶, L. Zhang^{15b},

L. Zhang^{58a}, M. Zhang¹⁷⁰, P. Zhang^{15b}, R. Zhang^{58a}, R. Zhang²⁴, X. Zhang^{58b}, Y. Zhang^{15d}, Z. Zhang¹²⁸, X. Zhao⁴¹, Y. Zhao^{58b,128,af}, Z. Zhao^{58a}, A. Zhemchugov⁷⁷, B. Zhou¹⁰³, C. Zhou¹⁷⁸, L. Zhou⁴¹, M.S. Zhou^{15d}, M. Zhou¹⁵², N. Zhou^{58c}, Y. Zhou⁷, C.G. Zhu^{58b}, H.L. Zhu^{58a}, H. Zhu^{15a}, J. Zhu¹⁰³, Y. Zhu^{58a}, X. Zhuang^{15a}, K. Zhukov¹⁰⁸, V. Zhulanov^{120b,120a}, A. Zibell¹⁷⁴, D. Ziemińska⁶³, N.I. Zimine⁷⁷, S. Zimmermann⁵⁰, Z. Zinonos¹¹³, M. Zinser⁹⁷, M. Ziolkowski¹⁴⁸, G. Zobernig¹⁷⁸, A. Zoccoli^{23b,23a}, K. Zoch⁵¹, T.G. Zorbas¹⁴⁶, R. Zou³⁶, M. Zur Nedden¹⁹, L. Zwalski³⁵.

¹Department of Physics, University of Adelaide, Adelaide; Australia.

²Physics Department, SUNY Albany, Albany NY; United States of America.

³Department of Physics, University of Alberta, Edmonton AB; Canada.

^{4(a)}Department of Physics, Ankara University, Ankara;^(b)Istanbul Aydin University, Istanbul;^(c)Division of Physics, TOBB University of Economics and Technology, Ankara; Turkey.

⁵LAPP, Université Grenoble Alpes, Université Savoie Mont Blanc, CNRS/IN2P3, Annecy; France.

⁶High Energy Physics Division, Argonne National Laboratory, Argonne IL; United States of America.

⁷Department of Physics, University of Arizona, Tucson AZ; United States of America.

⁸Department of Physics, University of Texas at Arlington, Arlington TX; United States of America.

⁹Physics Department, National and Kapodistrian University of Athens, Athens; Greece.

¹⁰Physics Department, National Technical University of Athens, Zografou; Greece.

¹¹Department of Physics, University of Texas at Austin, Austin TX; United States of America.

^{12(a)}Bahcesehir University, Faculty of Engineering and Natural Sciences, Istanbul;^(b)Istanbul Bilgi University, Faculty of Engineering and Natural Sciences, Istanbul;^(c)Department of Physics, Bogazici University, Istanbul;^(d)Department of Physics Engineering, Gaziantep University, Gaziantep; Turkey.

¹³Institute of Physics, Azerbaijan Academy of Sciences, Baku; Azerbaijan.

¹⁴Institut de Física d'Altes Energies (IFAE), Barcelona Institute of Science and Technology, Barcelona; Spain.

^{15(a)}Institute of High Energy Physics, Chinese Academy of Sciences, Beijing;^(b)Department of Physics, Nanjing University, Nanjing;^(c)Physics Department, Tsinghua University, Beijing;^(d)University of Chinese Academy of Science (UCAS), Beijing; China.

¹⁶Institute of Physics, University of Belgrade, Belgrade; Serbia.

¹⁷Department for Physics and Technology, University of Bergen, Bergen; Norway.

¹⁸Physics Division, Lawrence Berkeley National Laboratory and University of California, Berkeley CA; United States of America.

¹⁹Institut für Physik, Humboldt Universität zu Berlin, Berlin; Germany.

²⁰Albert Einstein Center for Fundamental Physics and Laboratory for High Energy Physics, University of Bern, Bern; Switzerland.

²¹School of Physics and Astronomy, University of Birmingham, Birmingham; United Kingdom.

²²Centro de Investigaciones, Universidad Antonio Nariño, Bogota; Colombia.

^{23(a)}Dipartimento di Fisica e Astronomia, Università di Bologna, Bologna;^(b)INFN Sezione di Bologna; Italy.

²⁴Physikalisches Institut, Universität Bonn, Bonn; Germany.

²⁵Department of Physics, Boston University, Boston MA; United States of America.

²⁶Department of Physics, Brandeis University, Waltham MA; United States of America.

^{27(a)}Transilvania University of Brasov, Brasov;^(b)Horia Hulubei National Institute of Physics and Nuclear Engineering, Bucharest;^(c)Department of Physics, Alexandru Ioan Cuza University of Iasi, Iasi;^(d)National Institute for Research and Development of Isotopic and Molecular Technologies, Physics Department, Cluj-Napoca;^(e)University Politehnica Bucharest, Bucharest;^(f)West University in Timisoara, Timisoara; Romania.

- ^{28(a)}Faculty of Mathematics, Physics and Informatics, Comenius University, Bratislava; ^(b)Department of Subnuclear Physics, Institute of Experimental Physics of the Slovak Academy of Sciences, Kosice; Slovak Republic.
- ²⁹Physics Department, Brookhaven National Laboratory, Upton NY; United States of America.
- ³⁰Departamento de Física, Universidad de Buenos Aires, Buenos Aires; Argentina.
- ³¹Cavendish Laboratory, University of Cambridge, Cambridge; United Kingdom.
- ^{32(a)}Department of Physics, University of Cape Town, Cape Town; ^(b)Department of Mechanical Engineering Science, University of Johannesburg, Johannesburg; ^(c)School of Physics, University of the Witwatersrand, Johannesburg; South Africa.
- ³³Department of Physics, Carleton University, Ottawa ON; Canada.
- ^{34(a)}Faculté des Sciences Ain Chock, Réseau Universitaire de Physique des Hautes Energies - Université Hassan II, Casablanca; ^(b)Centre National de l'Energie des Sciences Techniques Nucléaires (CNESTEN), Rabat; ^(c)Faculté des Sciences Semlalia, Université Cadi Ayyad, LPHEA-Marrakech; ^(d)Faculté des Sciences, Université Mohamed Premier and LPTPM, Oujda; ^(e)Faculté des sciences, Université Mohammed V, Rabat; Morocco.
- ³⁵CERN, Geneva; Switzerland.
- ³⁶Enrico Fermi Institute, University of Chicago, Chicago IL; United States of America.
- ³⁷LPC, Université Clermont Auvergne, CNRS/IN2P3, Clermont-Ferrand; France.
- ³⁸Nevis Laboratory, Columbia University, Irvington NY; United States of America.
- ³⁹Niels Bohr Institute, University of Copenhagen, Copenhagen; Denmark.
- ^{40(a)}Dipartimento di Fisica, Università della Calabria, Rende; ^(b)INFN Gruppo Collegato di Cosenza, Laboratori Nazionali di Frascati; Italy.
- ⁴¹Physics Department, Southern Methodist University, Dallas TX; United States of America.
- ⁴²Physics Department, University of Texas at Dallas, Richardson TX; United States of America.
- ^{43(a)}Department of Physics, Stockholm University; ^(b)Oskar Klein Centre, Stockholm; Sweden.
- ⁴⁴Deutsches Elektronen-Synchrotron DESY, Hamburg and Zeuthen; Germany.
- ⁴⁵Lehrstuhl für Experimentelle Physik IV, Technische Universität Dortmund, Dortmund; Germany.
- ⁴⁶Institut für Kern- und Teilchenphysik, Technische Universität Dresden, Dresden; Germany.
- ⁴⁷Department of Physics, Duke University, Durham NC; United States of America.
- ⁴⁸SUPA - School of Physics and Astronomy, University of Edinburgh, Edinburgh; United Kingdom.
- ⁴⁹INFN e Laboratori Nazionali di Frascati, Frascati; Italy.
- ⁵⁰Physikalisches Institut, Albert-Ludwigs-Universität Freiburg, Freiburg; Germany.
- ⁵¹II. Physikalisches Institut, Georg-August-Universität Göttingen, Göttingen; Germany.
- ⁵²Département de Physique Nucléaire et Corpusculaire, Université de Genève, Genève; Switzerland.
- ^{53(a)}Dipartimento di Fisica, Università di Genova, Genova; ^(b)INFN Sezione di Genova; Italy.
- ⁵⁴II. Physikalisch Institut, Justus-Liebig-Universität Giessen, Giessen; Germany.
- ⁵⁵SUPA - School of Physics and Astronomy, University of Glasgow, Glasgow; United Kingdom.
- ⁵⁶LPSC, Université Grenoble Alpes, CNRS/IN2P3, Grenoble INP, Grenoble; France.
- ⁵⁷Laboratory for Particle Physics and Cosmology, Harvard University, Cambridge MA; United States of America.
- ^{58(a)}Department of Modern Physics and State Key Laboratory of Particle Detection and Electronics, University of Science and Technology of China, Hefei; ^(b)Institute of Frontier and Interdisciplinary Science and Key Laboratory of Particle Physics and Particle Irradiation (MOE), Shandong University, Qingdao; ^(c)School of Physics and Astronomy, Shanghai Jiao Tong University, KLPPAC-MoE, SKLPPC, Shanghai; ^(d)Tsung-Dao Lee Institute, Shanghai; China.
- ^{59(a)}Kirchhoff-Institut für Physik, Ruprecht-Karls-Universität Heidelberg, Heidelberg; ^(b)Physikalisches Institut, Ruprecht-Karls-Universität Heidelberg, Heidelberg; Germany.

- ⁶⁰Faculty of Applied Information Science, Hiroshima Institute of Technology, Hiroshima; Japan.
- ^{61(a)}Department of Physics, Chinese University of Hong Kong, Shatin, N.T., Hong Kong;^(b)Department of Physics, University of Hong Kong, Hong Kong;^(c)Department of Physics and Institute for Advanced Study, Hong Kong University of Science and Technology, Clear Water Bay, Kowloon, Hong Kong; China.
- ⁶²Department of Physics, National Tsing Hua University, Hsinchu; Taiwan.
- ⁶³Department of Physics, Indiana University, Bloomington IN; United States of America.
- ^{64(a)}INFN Gruppo Collegato di Udine, Sezione di Trieste, Udine;^(b)ICTP, Trieste;^(c)Dipartimento di Chimica, Fisica e Ambiente, Università di Udine, Udine; Italy.
- ^{65(a)}INFN Sezione di Lecce;^(b)Dipartimento di Matematica e Fisica, Università del Salento, Lecce; Italy.
- ^{66(a)}INFN Sezione di Milano;^(b)Dipartimento di Fisica, Università di Milano, Milano; Italy.
- ^{67(a)}INFN Sezione di Napoli;^(b)Dipartimento di Fisica, Università di Napoli, Napoli; Italy.
- ^{68(a)}INFN Sezione di Pavia;^(b)Dipartimento di Fisica, Università di Pavia, Pavia; Italy.
- ^{69(a)}INFN Sezione di Pisa;^(b)Dipartimento di Fisica E. Fermi, Università di Pisa, Pisa; Italy.
- ^{70(a)}INFN Sezione di Roma;^(b)Dipartimento di Fisica, Sapienza Università di Roma, Roma; Italy.
- ^{71(a)}INFN Sezione di Roma Tor Vergata;^(b)Dipartimento di Fisica, Università di Roma Tor Vergata, Roma; Italy.
- ^{72(a)}INFN Sezione di Roma Tre;^(b)Dipartimento di Matematica e Fisica, Università Roma Tre, Roma; Italy.
- ^{73(a)}INFN-TIFPA;^(b)Università degli Studi di Trento, Trento; Italy.
- ⁷⁴Institut für Astro- und Teilchenphysik, Leopold-Franzens-Universität, Innsbruck; Austria.
- ⁷⁵University of Iowa, Iowa City IA; United States of America.
- ⁷⁶Department of Physics and Astronomy, Iowa State University, Ames IA; United States of America.
- ⁷⁷Joint Institute for Nuclear Research, Dubna; Russia.
- ^{78(a)}Departamento de Engenharia Elétrica, Universidade Federal de Juiz de Fora (UFJF), Juiz de Fora;^(b)Universidade Federal do Rio De Janeiro COPPE/EE/IF, Rio de Janeiro;^(c)Universidade Federal de São João del Rei (UFSJ), São João del Rei;^(d)Instituto de Física, Universidade de São Paulo, São Paulo; Brazil.
- ⁷⁹KEK, High Energy Accelerator Research Organization, Tsukuba; Japan.
- ⁸⁰Graduate School of Science, Kobe University, Kobe; Japan.
- ^{81(a)}AGH University of Science and Technology, Faculty of Physics and Applied Computer Science, Krakow;^(b)Marian Smoluchowski Institute of Physics, Jagiellonian University, Krakow; Poland.
- ⁸²Institute of Nuclear Physics Polish Academy of Sciences, Krakow; Poland.
- ⁸³Faculty of Science, Kyoto University, Kyoto; Japan.
- ⁸⁴Kyoto University of Education, Kyoto; Japan.
- ⁸⁵Research Center for Advanced Particle Physics and Department of Physics, Kyushu University, Fukuoka ; Japan.
- ⁸⁶Instituto de Física La Plata, Universidad Nacional de La Plata and CONICET, La Plata; Argentina.
- ⁸⁷Physics Department, Lancaster University, Lancaster; United Kingdom.
- ⁸⁸Oliver Lodge Laboratory, University of Liverpool, Liverpool; United Kingdom.
- ⁸⁹Department of Experimental Particle Physics, Jožef Stefan Institute and Department of Physics, University of Ljubljana, Ljubljana; Slovenia.
- ⁹⁰School of Physics and Astronomy, Queen Mary University of London, London; United Kingdom.
- ⁹¹Department of Physics, Royal Holloway University of London, Egham; United Kingdom.
- ⁹²Department of Physics and Astronomy, University College London, London; United Kingdom.
- ⁹³Louisiana Tech University, Ruston LA; United States of America.
- ⁹⁴Fysiska institutionen, Lunds universitet, Lund; Sweden.

- ⁹⁵Centre de Calcul de l’Institut National de Physique Nucléaire et de Physique des Particules (IN2P3), Villeurbanne; France.
- ⁹⁶Departamento de Física Teórica C-15 and CIAFF, Universidad Autónoma de Madrid, Madrid; Spain.
- ⁹⁷Institut für Physik, Universität Mainz, Mainz; Germany.
- ⁹⁸School of Physics and Astronomy, University of Manchester, Manchester; United Kingdom.
- ⁹⁹CPPM, Aix-Marseille Université, CNRS/IN2P3, Marseille; France.
- ¹⁰⁰Department of Physics, University of Massachusetts, Amherst MA; United States of America.
- ¹⁰¹Department of Physics, McGill University, Montreal QC; Canada.
- ¹⁰²School of Physics, University of Melbourne, Victoria; Australia.
- ¹⁰³Department of Physics, University of Michigan, Ann Arbor MI; United States of America.
- ¹⁰⁴Department of Physics and Astronomy, Michigan State University, East Lansing MI; United States of America.
- ¹⁰⁵B.I. Stepanov Institute of Physics, National Academy of Sciences of Belarus, Minsk; Belarus.
- ¹⁰⁶Research Institute for Nuclear Problems of Byelorussian State University, Minsk; Belarus.
- ¹⁰⁷Group of Particle Physics, University of Montreal, Montreal QC; Canada.
- ¹⁰⁸P.N. Lebedev Physical Institute of the Russian Academy of Sciences, Moscow; Russia.
- ¹⁰⁹Institute for Theoretical and Experimental Physics (ITEP), Moscow; Russia.
- ¹¹⁰National Research Nuclear University MEPhI, Moscow; Russia.
- ¹¹¹D.V. Skobeltsyn Institute of Nuclear Physics, M.V. Lomonosov Moscow State University, Moscow; Russia.
- ¹¹²Fakultät für Physik, Ludwig-Maximilians-Universität München, München; Germany.
- ¹¹³Max-Planck-Institut für Physik (Werner-Heisenberg-Institut), München; Germany.
- ¹¹⁴Nagasaki Institute of Applied Science, Nagasaki; Japan.
- ¹¹⁵Graduate School of Science and Kobayashi-Maskawa Institute, Nagoya University, Nagoya; Japan.
- ¹¹⁶Department of Physics and Astronomy, University of New Mexico, Albuquerque NM; United States of America.
- ¹¹⁷Institute for Mathematics, Astrophysics and Particle Physics, Radboud University Nijmegen/Nikhef, Nijmegen; Netherlands.
- ¹¹⁸Nikhef National Institute for Subatomic Physics and University of Amsterdam, Amsterdam; Netherlands.
- ¹¹⁹Department of Physics, Northern Illinois University, DeKalb IL; United States of America.
- ^{120^(a)}Budker Institute of Nuclear Physics, SB RAS, Novosibirsk;^(b)Novosibirsk State University Novosibirsk; Russia.
- ¹²¹Department of Physics, New York University, New York NY; United States of America.
- ¹²²Ohio State University, Columbus OH; United States of America.
- ¹²³Faculty of Science, Okayama University, Okayama; Japan.
- ¹²⁴Homer L. Dodge Department of Physics and Astronomy, University of Oklahoma, Norman OK; United States of America.
- ¹²⁵Department of Physics, Oklahoma State University, Stillwater OK; United States of America.
- ¹²⁶Palacký University, RCPTM, Joint Laboratory of Optics, Olomouc; Czech Republic.
- ¹²⁷Center for High Energy Physics, University of Oregon, Eugene OR; United States of America.
- ¹²⁸LAL, Université Paris-Sud, CNRS/IN2P3, Université Paris-Saclay, Orsay; France.
- ¹²⁹Graduate School of Science, Osaka University, Osaka; Japan.
- ¹³⁰Department of Physics, University of Oslo, Oslo; Norway.
- ¹³¹Department of Physics, Oxford University, Oxford; United Kingdom.
- ¹³²LPNHE, Sorbonne Université, Paris Diderot Sorbonne Paris Cité, CNRS/IN2P3, Paris; France.
- ¹³³Department of Physics, University of Pennsylvania, Philadelphia PA; United States of America.

- ¹³⁴Konstantinov Nuclear Physics Institute of National Research Centre "Kurchatov Institute", PNPI, St. Petersburg; Russia.
- ¹³⁵Department of Physics and Astronomy, University of Pittsburgh, Pittsburgh PA; United States of America.
- ^{136(a)}Laboratório de Instrumentação e Física Experimental de Partículas - LIP;^(b)Departamento de Física, Faculdade de Ciências, Universidade de Lisboa, Lisboa;^(c)Departamento de Física, Universidade de Coimbra, Coimbra;^(d)Centro de Física Nuclear da Universidade de Lisboa, Lisboa;^(e)Departamento de Física, Universidade do Minho, Braga;^(f)Departamento de Física Teorica y del Cosmos, Universidad de Granada, Granada (Spain);^(g)Dep Física and CEFITEC of Faculdade de Ciências e Tecnologia, Universidade Nova de Lisboa, Caparica; Portugal.
- ¹³⁷Institute of Physics, Academy of Sciences of the Czech Republic, Prague; Czech Republic.
- ¹³⁸Czech Technical University in Prague, Prague; Czech Republic.
- ¹³⁹Charles University, Faculty of Mathematics and Physics, Prague; Czech Republic.
- ¹⁴⁰State Research Center Institute for High Energy Physics, NRC KI, Protvino; Russia.
- ¹⁴¹Particle Physics Department, Rutherford Appleton Laboratory, Didcot; United Kingdom.
- ¹⁴²IRFU, CEA, Université Paris-Saclay, Gif-sur-Yvette; France.
- ¹⁴³Santa Cruz Institute for Particle Physics, University of California Santa Cruz, Santa Cruz CA; United States of America.
- ^{144(a)}Departamento de Física, Pontificia Universidad Católica de Chile, Santiago;^(b)Departamento de Física, Universidad Técnica Federico Santa María, Valparaíso; Chile.
- ¹⁴⁵Department of Physics, University of Washington, Seattle WA; United States of America.
- ¹⁴⁶Department of Physics and Astronomy, University of Sheffield, Sheffield; United Kingdom.
- ¹⁴⁷Department of Physics, Shinshu University, Nagano; Japan.
- ¹⁴⁸Department Physik, Universität Siegen, Siegen; Germany.
- ¹⁴⁹Department of Physics, Simon Fraser University, Burnaby BC; Canada.
- ¹⁵⁰SLAC National Accelerator Laboratory, Stanford CA; United States of America.
- ¹⁵¹Physics Department, Royal Institute of Technology, Stockholm; Sweden.
- ¹⁵²Departments of Physics and Astronomy, Stony Brook University, Stony Brook NY; United States of America.
- ¹⁵³Department of Physics and Astronomy, University of Sussex, Brighton; United Kingdom.
- ¹⁵⁴School of Physics, University of Sydney, Sydney; Australia.
- ¹⁵⁵Institute of Physics, Academia Sinica, Taipei; Taiwan.
- ^{156(a)}E. Andronikashvili Institute of Physics, Iv. Javakhishvili Tbilisi State University, Tbilisi;^(b)High Energy Physics Institute, Tbilisi State University, Tbilisi; Georgia.
- ¹⁵⁷Department of Physics, Technion, Israel Institute of Technology, Haifa; Israel.
- ¹⁵⁸Raymond and Beverly Sackler School of Physics and Astronomy, Tel Aviv University, Tel Aviv; Israel.
- ¹⁵⁹Department of Physics, Aristotle University of Thessaloniki, Thessaloniki; Greece.
- ¹⁶⁰International Center for Elementary Particle Physics and Department of Physics, University of Tokyo, Tokyo; Japan.
- ¹⁶¹Graduate School of Science and Technology, Tokyo Metropolitan University, Tokyo; Japan.
- ¹⁶²Department of Physics, Tokyo Institute of Technology, Tokyo; Japan.
- ¹⁶³Tomsk State University, Tomsk; Russia.
- ¹⁶⁴Department of Physics, University of Toronto, Toronto ON; Canada.
- ^{165(a)}TRIUMF, Vancouver BC;^(b)Department of Physics and Astronomy, York University, Toronto ON; Canada.
- ¹⁶⁶Division of Physics and Tomonaga Center for the History of the Universe, Faculty of Pure and Applied Sciences, University of Tsukuba, Tsukuba; Japan.

- ¹⁶⁷Department of Physics and Astronomy, Tufts University, Medford MA; United States of America.
- ¹⁶⁸Department of Physics and Astronomy, University of California Irvine, Irvine CA; United States of America.
- ¹⁶⁹Department of Physics and Astronomy, University of Uppsala, Uppsala; Sweden.
- ¹⁷⁰Department of Physics, University of Illinois, Urbana IL; United States of America.
- ¹⁷¹Instituto de Física Corpuscular (IFIC), Centro Mixto Universidad de Valencia - CSIC, Valencia; Spain.
- ¹⁷²Department of Physics, University of British Columbia, Vancouver BC; Canada.
- ¹⁷³Department of Physics and Astronomy, University of Victoria, Victoria BC; Canada.
- ¹⁷⁴Fakultät für Physik und Astronomie, Julius-Maximilians-Universität Würzburg, Würzburg; Germany.
- ¹⁷⁵Department of Physics, University of Warwick, Coventry; United Kingdom.
- ¹⁷⁶Waseda University, Tokyo; Japan.
- ¹⁷⁷Department of Particle Physics, Weizmann Institute of Science, Rehovot; Israel.
- ¹⁷⁸Department of Physics, University of Wisconsin, Madison WI; United States of America.
- ¹⁷⁹Fakultät für Mathematik und Naturwissenschaften, Fachgruppe Physik, Bergische Universität Wuppertal, Wuppertal; Germany.
- ¹⁸⁰Department of Physics, Yale University, New Haven CT; United States of America.
- ¹⁸¹Yerevan Physics Institute, Yerevan; Armenia.
- ^a Also at Borough of Manhattan Community College, City University of New York, NY; United States of America.
- ^b Also at Centre for High Performance Computing, CSIR Campus, Rosebank, Cape Town; South Africa.
- ^c Also at CERN, Geneva; Switzerland.
- ^d Also at CPPM, Aix-Marseille Université, CNRS/IN2P3, Marseille; France.
- ^e Also at Département de Physique Nucléaire et Corpusculaire, Université de Genève, Genève; Switzerland.
- ^f Also at Departament de Fisica de la Universitat Autònoma de Barcelona, Barcelona; Spain.
- ^g Also at Departamento de Física Teórica y del Cosmos, Universidad de Granada, Granada (Spain); Spain.
- ^h Also at Department of Applied Physics and Astronomy, University of Sharjah, Sharjah; United Arab Emirates.
- ⁱ Also at Department of Financial and Management Engineering, University of the Aegean, Chios; Greece.
- ^j Also at Department of Physics and Astronomy, University of Louisville, Louisville, KY; United States of America.
- ^k Also at Department of Physics and Astronomy, University of Sheffield, Sheffield; United Kingdom.
- ^l Also at Department of Physics, California State University, Fresno CA; United States of America.
- ^m Also at Department of Physics, California State University, Sacramento CA; United States of America.
- ⁿ Also at Department of Physics, King's College London, London; United Kingdom.
- ^o Also at Department of Physics, St. Petersburg State Polytechnical University, St. Petersburg; Russia.
- ^p Also at Department of Physics, University of Fribourg, Fribourg; Switzerland.
- ^q Also at Department of Physics, University of Michigan, Ann Arbor MI; United States of America.
- ^r Also at Dipartimento di Fisica E. Fermi, Università di Pisa, Pisa; Italy.
- ^s Also at Giresun University, Faculty of Engineering, Giresun; Turkey.
- ^t Also at Graduate School of Science, Osaka University, Osaka; Japan.
- ^u Also at Hellenic Open University, Patras; Greece.
- ^v Also at Horia Hulubei National Institute of Physics and Nuclear Engineering, Bucharest; Romania.
- ^w Also at II. Physikalisches Institut, Georg-August-Universität Göttingen, Göttingen; Germany.
- ^x Also at Institució Catalana de Recerca i Estudis Avancats, ICREA, Barcelona; Spain.

^y Also at Institut für Experimentalphysik, Universität Hamburg, Hamburg; Germany.

^z Also at Institute for Mathematics, Astrophysics and Particle Physics, Radboud University Nijmegen/Nikhef, Nijmegen; Netherlands.

^{aa} Also at Institute for Particle and Nuclear Physics, Wigner Research Centre for Physics, Budapest; Hungary.

^{ab} Also at Institute of Particle Physics (IPP); Canada.

^{ac} Also at Institute of Physics, Academia Sinica, Taipei; Taiwan.

^{ad} Also at Institute of Physics, Azerbaijan Academy of Sciences, Baku; Azerbaijan.

^{ae} Also at Institute of Theoretical Physics, Ilia State University, Tbilisi; Georgia.

^{af} Also at LAL, Université Paris-Sud, CNRS/IN2P3, Université Paris-Saclay, Orsay; France.

^{ag} Also at Louisiana Tech University, Ruston LA; United States of America.

^{ah} Also at Manhattan College, New York NY; United States of America.

^{ai} Also at Moscow Institute of Physics and Technology State University, Dolgoprudny; Russia.

^{aj} Also at National Research Nuclear University MEPhI, Moscow; Russia.

^{ak} Also at Physikalischs Institut, Albert-Ludwigs-Universität Freiburg, Freiburg; Germany.

^{al} Also at School of Physics, Sun Yat-sen University, Guangzhou; China.

^{am} Also at The City College of New York, New York NY; United States of America.

^{an} Also at The Collaborative Innovation Center of Quantum Matter (CICQM), Beijing; China.

^{ao} Also at Tomsk State University, Tomsk, and Moscow Institute of Physics and Technology State University, Dolgoprudny; Russia.

^{ap} Also at TRIUMF, Vancouver BC; Canada.

^{aq} Also at Universita di Napoli Parthenope, Napoli; Italy.

* Deceased